New fluorescent labels and probes for biological applications

Dissertation zur Erlangung des Doktorgrades

der Naturwissenschaften

(Dr. rer. nat.)

an der

naturwissenschaftlichen Fakultät IV

-Chemie und Pharmazie-

der Universität Regensburg

vorgelegt von

Martin Link

aus Laaber (Lkr. Regensburg)

März 2010

Diese Doktorarbeit entstand in der Zeit von Dezember 2006 bis Februar 2010 am Institut für Analytische Chemie, Chemo- und Biosensorik der Universität Regensburg.

Die Arbeit wurde angeleitet von Prof. Dr. Otto S. Wolfbeis.

Ein Gelehrter in seinem Laboratorium ist nicht nur ein Techniker, er steht auch vor den Naturgesetzen wie ein Kind vor der Märchenwelt

Marie Curie (1867-1934)

Acknowledgements

für Katja

Contents

Chapter 1

Introduction

1.1 Overview

Over the last 50 years fluorescence detection has become an important and powerful analytical tool which is firmly established in many areas of the scientific world, especially in biology and medicine. It is widely used in immunoassays, labeling of biomolecules with probes, fluorescent sensors for pH and ions, and other analytical procedures [1–3]. The success of this method asided versatility and simplicity, is based on the extremely low limit of detection (LOD) which typically ranges from μM to aM [4]. This is essential for the detection of low analyte concentrations which especially appear in biochemistry and cell analysis. In this case, conventional analytical techniques e.g. absorption spectroscopy has limited feasibility. Hence, fluorescent labels and probes have replaced many classical methods like staining reagents for proteins [5]. The developement started with compounds absorbing from the near-UV to the blue range and emitting between the violet and the green range of the electromagnetic spectrum. Dansyl chloride ($\lambda_{ex} = 340$ nm, $\lambda_{em} = 510$ nm, after reaction with an amine [6,7]) and fluorescein (λ_{ex} 493 nm, λ_{em} 519 nm [8]) are well known examples. Fluorescein in particular and its derivatives have been intensively used as protein labels (FITC) [9, 10] and pH probes [11].

In recent years, research has been engaged in the design of near infrared (NIR) probes and labels operating between 600 nm and 1000 nm. There are many advantages pertaining to this spectral region compared to the ultraviolet and visible part of the spectrum. The background signal caused by the intrinsic fluorescence of the analyte or its matrix and parts of the measurement setup, e.g. cuvetts, is decreased significantly. Furthermore, the high penetration of NIR radiation concerning skin and tissue in biological applications is another benefit of this region. Finally, the fluorophores can be excited with compact laser diodes as inexpensive and stable light sources [12]. In the future, the design of fluorescent molecules

with defined properties for specific applications constitutes a noteworthy synthetic challenge for the growing complexity of analytical purposes.

1.2 Motivation and Aim of Work

The demand of fluorescence based methods in analytical chemistry has increased during the last few years due to the undeniable advantages of this technique. Hence, intense research has been concentrated on new fluorescent labels for bio-molecules, stains for cells and tissues, probes and sensor systems for pH [13], metal ions [14] as well as for oxygen partial pressure [15]. This broad spectrum of applications entails to a need in fluorophores which differ in terms of functionality and spectral properties. Unfortunately, the number of commercially available labels and probes that are suitable for numerous analytical problems is limited. This causes a need for new and improved fluorescent compounds. In the last 15 years the development and the design of new fluorescent labels and probes has become an important part of the research activity at the Institute of Analytical Chemistry, Chemo- and Biosensors of the University of Regensburg. This research varies from covalent markers like the pyrilium dyes (the Py-dyes), a special form of color changing amino-reactive labels [16], to probes based on photoinduced electron transfer.

The synthesis, characterization and application of new fluorescent compounds for analytical problems are presented in this dissertation. One part of the work deals with labels, mainly amino-reactive, operating in the visible to the near in-frared part of the electromagnetic spectrum. The challenge of this work is to con-trive a synthetic pathway which is easy to follow for the design of small compounds with high molar absorbance and intensive color. The other part of the thesis deals with the development of fluorescent hydrogen peroxide probes based on the pho-toinduced electron transfer. The regeneration and the attachment to a polymeric support are additional criteria for the design of these compounds.

Chapter 2

New Fluorescent Labels

2.1 Background

Labeling involves the covalent modification of proteins, amino acids, DNA and other compounds of interest with reporter molecules. This method is a very powerful and important research tool in chemistry, medicine, and biology due to the fact that a large number of analytes can not be directly detected. Biomolecules like polypeptides or proteins show no or only an insufficient signal for qualitative or quantitative measurements, thus they represent a role model target for this technique. The answer to this problem is an adequate label generating a clear and easily detectable signal. The two most popular labeling methods include:

- radioactive labeling

- fluorescent labeling

The use of radioactive markers is one of the oldest techniques which bears the advantage of a nearly background free measurement. Therefore, the sensitivity of this method is very high resulting in a very low limit of detection. In general, one or more atoms of the label are exchanged by their radioactive isomers e.g. ^{1}H is replaced by ^{3}H. Figure 2.1 and figure 2.2 show two examples, the Bolton-Hunter reagent and the ^{3}H-succinimidylpropionate. Both are NHS-esters forming an amide bond with the amino group of the analyte [17, 18].

Nowadays, radioactive labeling is regarded as less advantageous as the handling of radioactive material affords full-fledged employees and the complex disposal of nuclear waste is required (for environmental reasons) thus rendering this method cost-intensive. Decay of the radioisotopes causes the signal to fade which is unfavorable compared to methods with a stable signal. Finally, this type of labeling is no longer able to keep with the miniaturization of the analytical systems. State
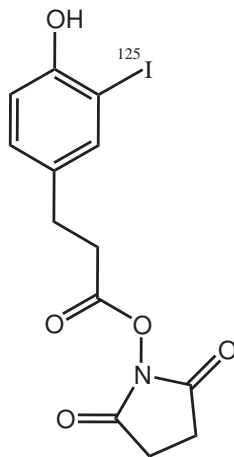
Figure 2.1: Structure of the Bolton-Hunter reagent [19]
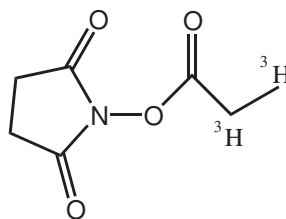
Figure 2.2: Structure of succinimidyl-propionate [20]

of the art is the lab-on-a-chip technology dealing with nano-liter scale reaction media [21]. The decrease of volume limits the concentration of the radioactive material. Hence, the complexity, measurement period as well as the cost for a quantitative measurement increase [22, 23].

The second technique is fluorescent labeling. A fluorescent dye is attached to the molecule of interest either through an electrostatic interaction or a covalent bond: the reactive group of the label will react with the functional group of the analyte [24]. Covalent labeling is preferable because of the higher selectivity of this method.

The importance of fluorescent dyes and markers rose significantly during the last years [25] bearing many advantageous thus causing shift away from radioactive tagging. The three most important arguments are:

1. Dealing with time-decreasing signals has become obsolete owing to the reversible character of the fluorescence process of excitation and emission.

2. The costs, both of purchase and deposal, can be reduced by applying fluorescent labels. This is important in high-throughput screening (HTS) [26], when a big quantity of analytes are measured.

3. Fluorescence labeling and detection is, besides its high sensitivity, a versatile technique: several parameter e.g. intensity, lifetime, polarisation, FRET and quenching behavior can be subjected to analysis as opposed to only one like absorbance in photometric detection for instance [27].

A lot of fluorophores with different absorption and emission wavelengths are commercially available. Fluorescein isothiocyanate (see figure 2.1) is a very com-

mon label in the visible range of the electromagnetic spectrum as well as Cy5 NHS-ester (see figure 2.4) in the near infrared part of the spectrum [28, 29]. Many international companies like "Invitrogen" (www.invitrogen.com) and "AttoTec" (www.atto-tec.com) offer a huge number of fluorescent dyes for different analytical applications [23].
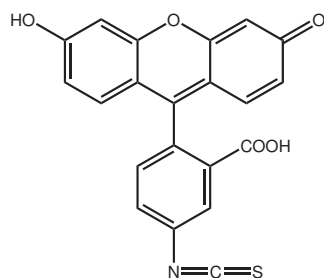
Figure 2.3: Structure of FITC   Figure 2.4: Structure of Cy5 NHS-ester
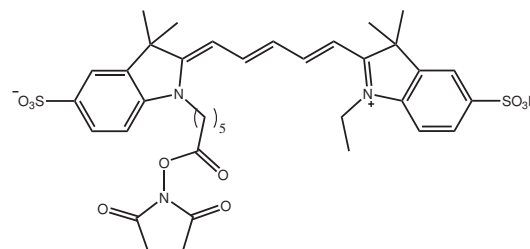
2.1.1 Classical labeling technologies

In general, fluorescent markers are attached covalently to the molecule of interest by reaction of a label with a functional group of the analyte. These functional groups normally consist of:

- amino groups (-NH$_2$) e.g. in amino acids as well as at the N-terminus of polypeptides or proteins

- thiol groups (-SH) at the side chain of sulfur-containing amino acids like cysteine

- carboxylic acid groups (-COOH) e.g. in amino acids (aspartic acid) as well as at the C-terminus of polypeptides or proteins

Hence, chemoselectivity is facilitated by a defined reaction of an appropriate label with one of these functionalities [30]. Typically, the amino-group serves as target for labeling experiments and various reagents have been designed for this moiety. **NHS-ester** for instance are prepared by the activation of a carboxylic group with N-hydroxysuccinimide and dicyclohexylcarbodiimide. These esters have high selectivity towards aliphatic amines and they are the most common reagents for labeling amino functionalities [31]. The best labeling condition in aqueous media is pH > 8.3 [32] because of the deprotonation of the amino group. At low labeling rates, these conditions are disadvantageous due to the hydrolization of the reagent in water. Another class of labels suitable for amino groups are the **isothiocyanates** which form thiourea bonds with the analyte. The reaction is preferably

performed in alkaline media and the isothiocyanates also tend to hydrolyze in water but at a much lower rate than NHS-esters. In this context, **sulfonyl halides** represent the last class of amino-reactive labels. These compounds generate, on account of their high reactivity in comparison to NHS-esters and isothiocyanates, very stable sulfonamide bonds. In comparision to the labels mentioned above, sulfonyl halides are less selective and moreover not stable in aqueous solvents due to their high reactivity [33]. Figure 2.5 shows the three labeling techniques in the order they are described above.

1a) Generation of NHS-ester
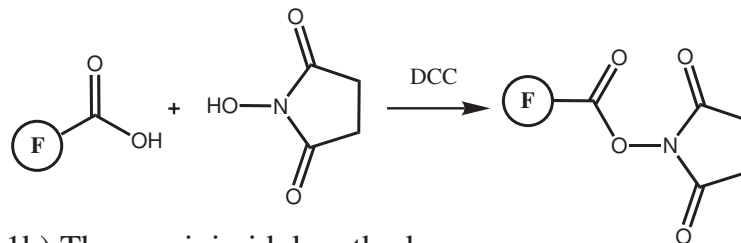
1b) The succinimidyl method
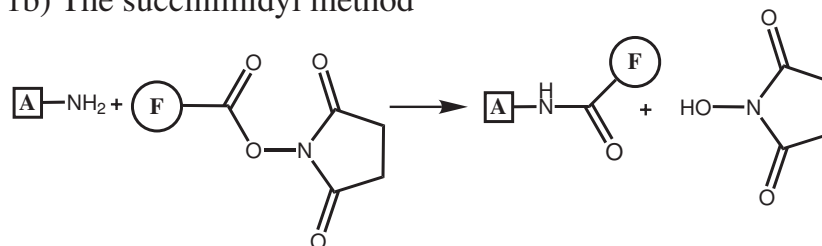
2) The isothiocyanate method
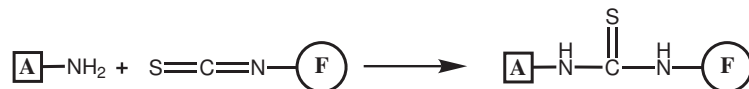
3) The sulfonyhalide method
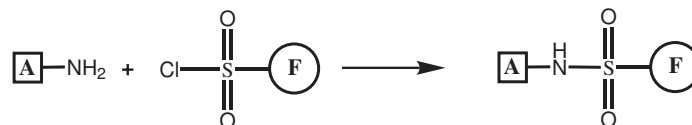
Figure 2.5: Summary of three most common labeling technologies for amino groups; A = analyte; F = fluorophore

2.1.2 "Click Chemistry" as new labeling technology

The concept of click chemistry was introduced and defined by Sharpless, Kolb and Finn in 2001 [34,35]. The concept of click chemistry applies only if a reaction meets the following criteria:

- modular

- wide in scope

- energetically favored

- specific

- very high yields

- generating only inoffensive byproducts which can be removed by nonchromatographic methods

Large efforts for the development of synthetic strategies for click chemistry have been made, since the definition of these criteria. As a result, complicated syntheses which normally require either complex apperatus or harsh experimental conditions can be simplified by following this concept. The most established method in this context is the copper-catalyzed Huisgen azide-alkyne cycloaddition (CuAAC) which is also known as the "click reaction" [36]. The synthetic route leading to a 1,2,3-triazole is shown in figure 2.6. It was presented in 2002 by Medal et al. who derived it from the Huisgen 1,3-dipolar cycloaddition by the addition of catalytic quantities of copper(I).
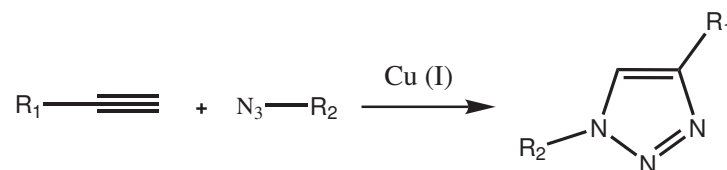
Figure 2.6: Scheme of the regioselective CuAAC leading to a 1,4 substituted 1,2,3-triazole

The catalyst is either added as a copper(I) salt like CuI or generated in situ from a water soluble salt e.g. $CuSO_4 \cdot 5\,H_2O$ and a reducing agent like ascorbic acid. The second method is normally preferred [37]. The copper(I) species accelerates the 1,3-dipolar cycloaddition and guarantees regioselectivity (1,4-product). The synthesis is of high yield and takes place at room temperature in both organic solvents and water [38, 39]. Thus CuAAC is perfectly suited for biological applications under

physiological conditions. Moreover, azide and alkyne functions can hardly be found in biological systems. This provides the opportunity for the chemoselective and bioorthogonal introduction of reporter molecules such as fluorescent labels. Kele et al. [40,41] provides a set of clickable fluorophores as well as different applications for click chemistry in biological contexts. Therefore, the label could either carry an alkyne or an azid moiety (figure 2.6, R_1 or R_2) whereas the biological material is functionalized with the corresponding counterpart.

One disadvantage of using the copper catalyzed cycloaddition in biological systems, however, is the toxicity of the transition metal. The answer is copper free clicking with cyclooctynes as alkyne species. The reactivity of this system relies on the geometrical deformation of the alkyne bond arising from ring strain. This ring strain is high enough to render a catalyst unnecessary [38,42].

2.2 Derivatives of 1,8-Naphthalimide as VIS-labels

Dyes operating in the visible part of the electromagnetic spectrum (450 nm - 750 nm) are intensely used as labels for biolgical material in medicine and biology. These markers are so popular that entire application systems have become commercially available for standard taggings. SigmaAldrich introduced the *Fluoro Tag^{TM} FITC conjugation kid* with fluorescein as a common visible chromophore. 1,8-naphthalimides of type **A** (shown in table 2.1) are another class of important daylight chromophores which have been studied extensively due to their photophysical properties [43]. They exhibit high chemo- and thermostability as well as high quantum yields [44,45]. Their polar structure enhances the water solubility of the dye reducing the risk of precipitation while working in aqueous media. This is essential in biological analysis [46,47]. In the past, the 1,8-naphthalimide structure has been used to synthesize laser dyes, molecular probes for pH or metal ion concentration and stains [43]. "Lucifer Yellow CH" for instance is a well known 4-amino-1,8-naphthalimide for intracellular staining [48]. In this section both the synthesis and the application of two amino-reactive labels, based on the 1,8-naphthalimide moiety are presented. Both dyes **1** and **4** are functionalized by the introduction of a C-6 linker carrying a carboxy group which can be activated (via its NHS-ester) to give the amino-reactive labels **2** and **5** (see table 2.1). The spectroscopic properties of the chromophores are mainly determined by the nitrogen atom in position 4. This entails an absorption in the blue part and an emission in the greenish yellow part of the elecromagnetic spectrum. The auxochrome group is represented by either an amino group (**1** and **2**) or a piperidyl moiety (**4** and **5**).
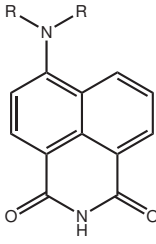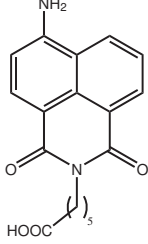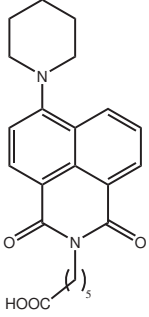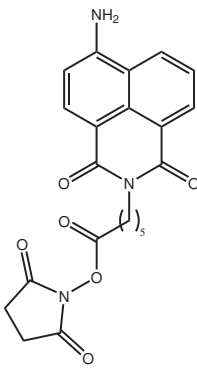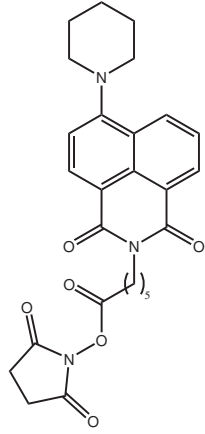
A	1	4	2	5

Table 2.1: Basic structure of the naphthalimide **A** (R = variable moieties), the free acids **1** and **4** as well as the amino-reactive labels **2** and **5**

2.2.1   Preparation of label 2

Label **2** is prepared in a two step synthesis (see figure 2.7) whereas the oxy-succinimidyl ester (often refered to as NHS-ester) is formed in-situ and used for tagging experiments without further purifications. The target chromophore **1** is synthesized by the reaction of 4-amino-1,8-naphthalic anhydride and 6-amino caproic acid in dry dimethylformamide (DMF) [49]. N,N-Diisopropyl-ethylamine is added as base and $Zn(OAc)_2$ as catalyst. Water is excluded by a 4-Å molecular sieve as described in [50]. Dye **1** is activated in-situ by converting it into its N-
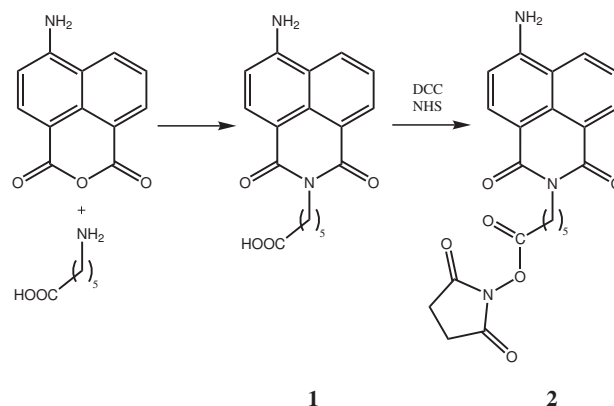
Figure 2.7: Synthetic pathway to label **2**

hydroxysuccinimidyl ester **2** using N-hydroxysuccinimide (NHS) and dicyclohexyl-carbodiimide (DCC) in dry dimethyl sulfoxide (DMSO) at room temperature [51]. This solution is used directly for labeling and can be stored at -18°C at least for one week.

2.2.2   Properties of label 2

Spectroscopic properties

The absorption and emission spectrum of label **2** are shown in figure 2.8. Its absorption in phosphate buffer solution of pH 7.0 peaks at 431 nm with a molar absorption coefficient of $6.9 \cdot 10^3 \ \frac{L}{mol \cdot cm}$. Solutions of **2** are strongly fluorescent, with an emission maximum at 550 nm and a fluorescence quantum yield of 0.1. The fluorophore is excited with a 375 nm picosecond laser. The large Stokes' shift of 119 nm facilitates the separation of excitation and emission. The photostability of **2** is tested by monitoring the absorbance at 431 nm during prolonged exposure of a 10 μM solution in phosphate buffer solution of pH 7 to daylight. No loss of absorbance can be observed over 20 days, whereas a parallel experiment with fluorescein resulted in an absorbance loss of more than 20%.
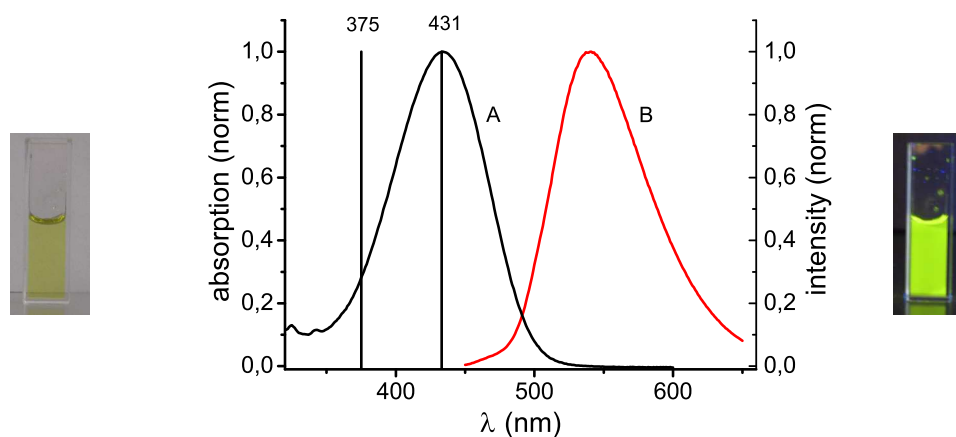
Figure 2.8: Normalized absorption spectrum (A) versus normalized emission spectrum (B) of label **2** at pH 7.0. The 375 nm laser line that is used for excitation in this experiment, and the 431 nm laser line which represents a perfect spectral match, is also shown. The picture on the left shows label **2** dissolved in water, the picture on the right shows label **2** in water excited via lab lamb.

pH dependence

Biological systems are strongly effected by pH. Enzymes for instance have a defined working optimum. In case of lactate oxidase it is 6.5 [52] and for glucose oxidase 5.1 [53]. Unfortunately, the intensity of many fluorophores like fluorescein also depends on pH which limits their applicability. The availability of a label which is not influenced by different pH values allows for higher flexibility, for optimizing experimental parameters without adverse effects on the limits of detection. The influence of the pH on the fluorescence intensity of the unreactive dye **1** and fluorescein respectively is displayed in figure 2.9. The fluorescence of fluorescein and its isothiocyanate (FITC) strongly decreases at acidic conditions. This results in reduced sensitivity under acidic conditions [54]. The fluorescence intensity of **1** (and presumably that of the dye-analyte conjugates), in contrast, is independent of pH in the range between 3 and 9. Hence, **2** is an adequate label for techniques with variable pH like electrophoresis and isoelectric focusing [55].
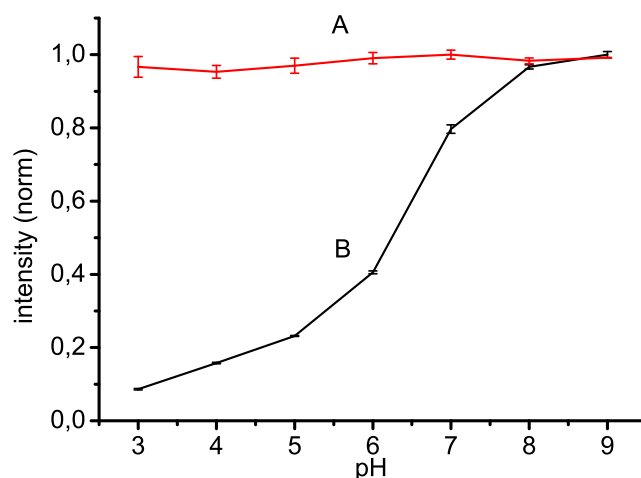
Figure 2.9: Normalized pH dependencies of dye **1** (A) and of fluorescein (B)

2.2.3 Applications of label 2

Compound **2** has been applied to a multitude of analytical problems. On the one hand it has been attached to different analytes either biological e.g. amino acids and proteins or modified silica nano particles. On the other hand it has also been used in different separation techniques like size exclusion chromatography (SEC), thin layer chromatography (TLC), capillary electrophoresis (CE) and microchip electrophoresis (MCE).

Labeling of amino acids

The amino acids L-lysine, L-serine, L-glycine, L-glutamic acid, L-aspartic acid are labeled by treating them with a solution of **2** (see figure 2.7) in bicarbonate buffer solution (pH 8.3, 50 mM) at room temperature [56]. The process is monitored via TLC (silica gel 60, EtAc/EtOH 9:1). A mixture of the precolumn labeled amino acids [57] and the free dye **1** is separated by capillary electrophoresis (see figure 2.10) which demonstrates the applicability of compound **2** for this important analytical technique [58]. The free acid **1** is used as reference instead of the label because excess NHS-ester hydrolyzes under these tagging conditions. The migration times of the labeled amino acids as well as of the free dye **1** are presented in table 2.2.
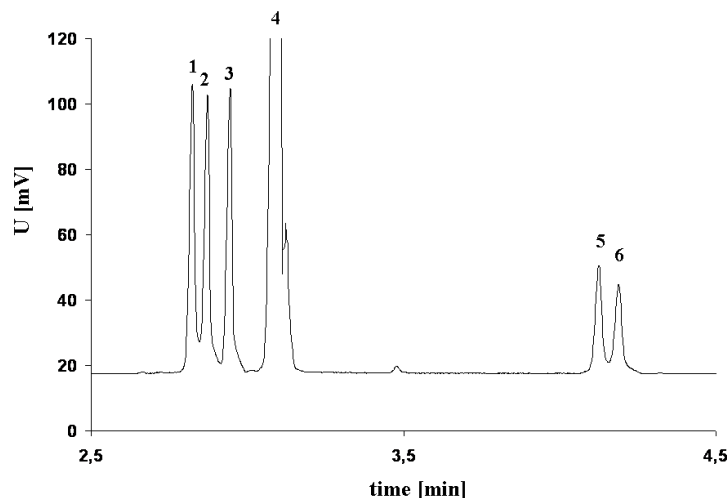
Figure 2.10: Electropherogram of the labeled amino acids and the free dye **1**

compound	migration time (min)
L-lysine (1)	2.82
L-serine (2)	2.87
L-glycine (3)	2.94
dye 1 (4)	3.10
L-glutamic acid (5)	4.12
L-aspartic acid (6)	4.19

Table 2.2: Migration times of the labeled amino acids and of the free dye **1**

These experiments were carried out at the Institute of Analytical Chemistry (Prof. D. Belder) at the University of Leipzig [58].

Labeling of proteins (BSA)

Proteins (and therefore antibodies and enzymes) are important analytes whose modification by labeling is an essential research tool in immunology and cell biology [33]. The importance of adequate markers is shown in the number of labels that are commercially on hand. The prospect of new labels is usually tested by tagging bovine serum albumin (BSA) which is a readily available and inexpensive protein. BSA is dissolved in bicarbonate buffer solution (pH 8.4, 50 mM) and label **2** is added (preparation see figure 2.7). The mixture is stirred for 12 - 15 h at room temperature and the tagged protein is purified by size exclusion chromatography (SEC) on Sephadex G-25 which is a porous polymer material. The principle of this separation technique is quite simple: small enough molecules permeate into the porous material and are retarded due to diffusion effects. Big molecules do not permeate into the pores and therefore they are not retarded. In the end, the biggest molecules of the mixture elutes first whereas the smallest ones leave the column last. In case of protein labeling, the protein-dye conjugate (highest molecular weight) eluates first, the non-labeled protein is second and finally the unbonded marker, which possesses the smallest molecular weight leaves the column (principle of SEC: see figure 2.11) [59]. This process can be easily recognized by naked eye. The yellow band of the labeled protein is immediately separated from that of the unbound dye and elutes first (see figure 2.11). The dye-protein conjugate is submitted to TOF-MS for further analyis (see data in the experimental section).

(a) [60]   (b)
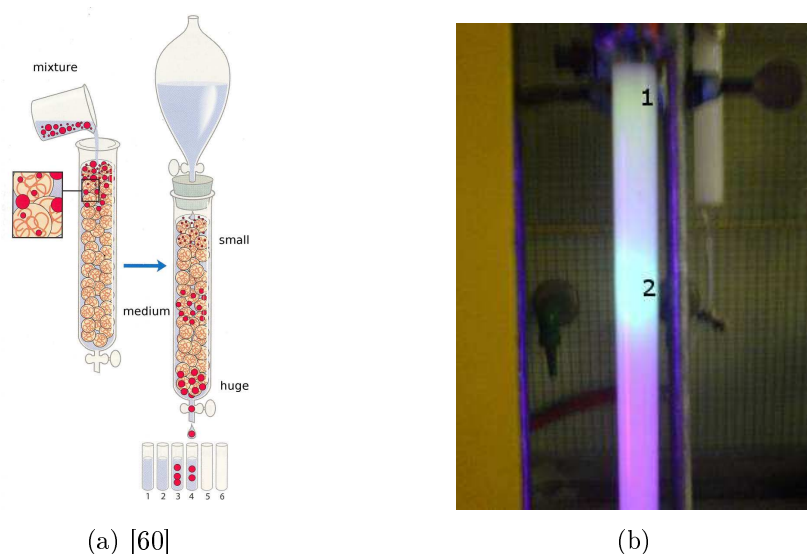
Figure 2.11: (a) Principle of SEC; (b) Purification of dye-protein conjugate: (1) unreacted label (2) labeled BSA (excitation via lab lamp)

While the absorption spectrum of the dye-protein conjugate does not differ from that of the free label, the maximum of the emission is shifted from 550 nm to 501 nm. This effect is caused by the hydrophobic environment of the label on the protein. Dye **1** also undergoes the same effect in solvents less polar than water. This indicates that **2** is located in a less polar environment when immobilized to BSA. The quantum yield of the conjugate is 0.24 which is more than twice the value of the non-conjugated label.

Labeling of silica nanoparticles

Fluorescent silica nanoparticles (FNPs) are a new and interesting class of materials. They are readily available in defined sizes and unlike non encapsulated quantum dots, they are biocompatible [61, 62]. FNPs are either prepared by doping silica nanoparticles during their synthesis with fluorophores [63] or by tagging them with a fluorescent label like compound **2** after surface modification. Amino-modification of the surface is realized by treating silica nanopowder with aminopropyltriethoxysilane (APTES) in refluxing toluene in order to introduce amino functionality. Label **2** is added to a suspension of the amino-modified silica nanoparticles in ethanol and the reaction is carried out over night (see figure 2.12). The labeled particles are collected by centrifugation and washed with ethanol to remove the unreacted label. In parallel a blank sample is prepared by combining unmodified silica nanoparticles (without amino groups) with the activated fluorophore to exclude unspecific bonding. After the centrifugation/washing steps the blank sample possesses no color whereas the amino-labeled particles are strongly colored. This labeling procedure is contrived by Mader et al. [64].
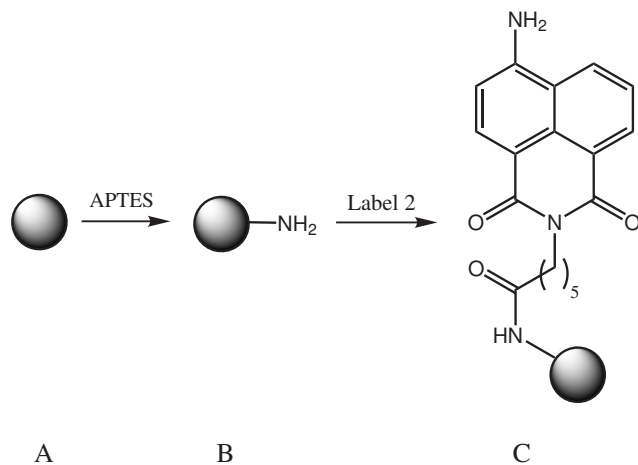
Figure 2.12: Labeling of silica nanoparticles; A: unmodified NP, B: amino-modified NP, C: labeled NP

Detection of labeled BSA via microchip electrophoresis

Microchip electrophoresis (MCE) is a miniaturized high performance separation technique which offers high separation speed, minimum sample consumption and the potential of integration in lab-on-a-chip systems [65]. The resolution depends on the application of labels suitable for electrophoretic techniques. Anionic labels for instance increase the separation time leading to peak broadening due to diffusion. Thus neutral or slightly positively charged labels usually are prefered. A drawback is the limited isomeric purity of certain commercial labels. This results in multiple signals of the dye and conjugates in the electropherogram. In combination with the low peak capacity of MCE, these avoidable signals hinder the peak identification or even an efficient separation. The applicability of label **2** (which is an isomerically pure and neutral compound) is demonstrated by separating tagged BSA from the free label via MCE. This can be done within 90 s [66]. The labeling of proteins with compound **2** is exemplified with the 65-kD protein bovine serum albumin as decribed in 2.2.3.

Separations in MCE are more challenging compared to those in CE because of less peak capacity due to the reduced separation length. Furthermore, it is difficult to separate proteins in electrophoresis because of high adsorptive interactions with the glass surface of the microfluidic device. This entails in a significant loss of separation efficiency and detection sensitivity due to peak broadening. In order to suppress those interactions an electrophoresis buffer containing 0.01% (w/w) hydroxypropyl methylcellulose (HPMC) is used as a dynamic coating. HPMC provides highest separation efficiency in the acidic pH-range [67], the HPMC works in neutral buffer too and allows the separation of the protein and the free dye (see figure 2.13). When sampling BSA solutions and separating them from free label, the electrical potentials are applied in the following order: sample inlet (A), buffer inlet (B), sample outlet (C), buffer outlet (D). The injection potentials are 493 (A), 500 (B), 0 (C) and 1330 (D) V, and the potentials for the separation are 1.6 (A), 2.0 (B), 1.5 (C) and 0 (D) kV (see figure 2.14). The limit of detection on-chip is 12.4 nM at 20 μm path length of the optical device. It is determined by a method, that uses a lysine labeled with the same fluorophore (here label **2**) as standard [58].

2.2.4   Preparation of label 5

Label **5** is obtained in a three step synthesis (see figure 2.15) by reacting 4-chloro-1,8-naphthalic anhydride and 6-aminocaproic acid with zinc acetate as catalyst to yield **3**. Compound **3** is further treated with 2 eq. of piperidine in order to introduce a piperidyl moiety and to shift the absorption maximum to the visible range of the electromagnetic spectrum. The unreactive dye **4** becomes amino-reactive by
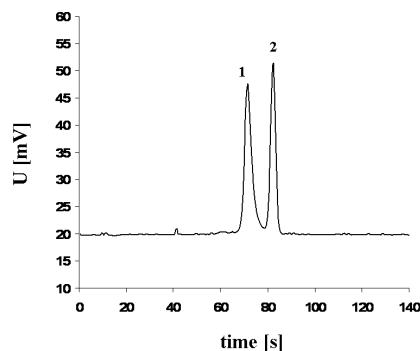
Figure 2.13: Separation of dye **1** (1) and labeled BSA (2). Experimental conditions: Separation length 3 cm, buffer pH 7 containing 0.01% of HPMC. Injected quantity of labeled BSA: nL scale
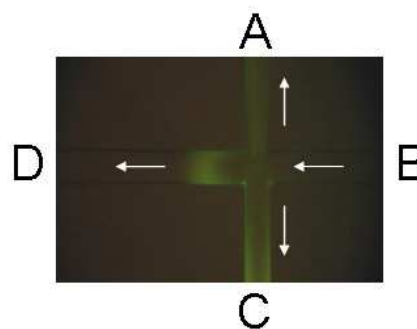
Figure 2.14: Schematic of the microchip with four ports (A, B, C, D) as used for pinched injection of the reaction mixture obtained by labeling BSA with label **2**

the same way as described in 2.2.1. Therefore, the free acid **4** is activated in-situ by converting it into its N-hydroxysuccinimidyl ester **5** using N-hydroxysuccinimide and dicyclohexylcarbodiimide in dry DMSO at room temperature. This solution is used directly for labeling and can be stored at -18°C at least for one week.
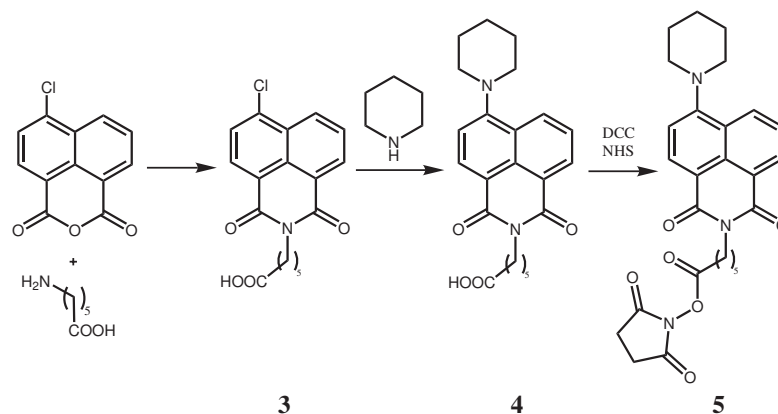
Figure 2.15: Synthetic pathway to label **5**

Dye **4** is a well known compound which is commercial available at Aurora Fine Chemicals LLC (www.aurorafinechemicals.com). Additionally, two patents dealing with this dye are published: on the one hand **4** is used as intermediate for an electroluminescent device and on the other hand it is applied as a protein

inhibitor [68, 69]. The activation of the free acid **4** as NHS-ester and its use as amino-reactive label **5** is not accomplished yet.

2.2.5 Properties of label 5

Spectroscopic properties

The absorption of label **5** in water peaks at 406 nm. Solutions of **5** exhibit a strong yellow fluorescence with an emission maximum at 538 nm in water. The molar absorption coefficient ($11.1 \cdot 10^3 \ \frac{L}{mol \cdot cm}$) and the fluorescent quantum yield (0.14) are determined in methanol due to the insufficient solubility of the label in water. The absorption and emission spectrum of **5** are shown in figure 2.16. The large Stokes' shift (132 nm) facilitates the separation of excitation and emission light which is particularly important to reduce interferences caused by background fluorescence and scattered light.
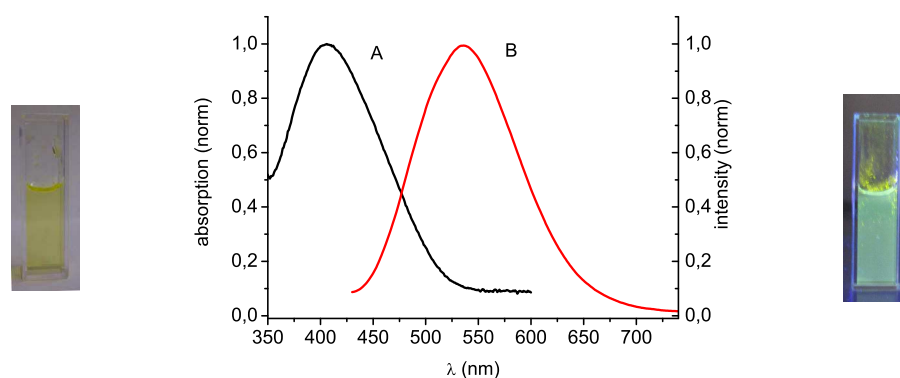
Figure 2.16: Normalized absorption spectrum (A) versus normalized emission spectrum (B) of label **5** in water. The picture on the left shows label **5** in water, the picture on the right shows label **5** in water excited via lab lamb.

2.2.6 Applications of label 5

Label **5** has been attached to amino acids as well as to bovine serum albumin as standard protein. The dye-analyte conjugates are separated and identified using different separation techniques like size exclusion chromatography (SEC), thin layer chromatography (TLC), and high-performance liquid chromatography (HPLC).

Labeling of amino acids

L-Glycine and L-aspartic acid are dissolved in bicarbonate buffer solution (pH 8.3, 50 mM) and labeled by the addition of **5** (see 2.2.4). The reaction is carried out 18 hours at room temperature. The tagged amino acids are separated and identified both by TLC (silica gel 60, butanol/acetic acid: 95/5; see table 2.3) and reversed-phase HPLC. Additionally, a mixture of the precolumn labeled amino acids and the free dye **4** is separated by HPLC (see table 2.4) proving the applicability of label **5** for this standard analytical method [70, 71].

amino acid	(R_f)
L-glycine	0.63
L-aspartic acid	0.41

compound	retention time t_R (min)
L-glycine	1.72
L-aspartic acid	1.49
free dye 4	2.20

Table 2.3: R_f of the labeled amino acids

Table 2.4: Retention time of the amino acids and of the free dye **4**

Labeling of bovine serum albumin

Compound **5** was tested as a protein label for the reasons described in 2.2.3. Hence, bovine serum albumin is dissolved in bicarbonate buffer (pH 8.3, 50 mM) and label **5** is added (preparation see 2.2.4). The mixture is stirred for 12 - 15 h at room temperature and the dye-protein conjugate is purified by size exclusion chromatography on Sephadex G-25 (see figure 2.18).
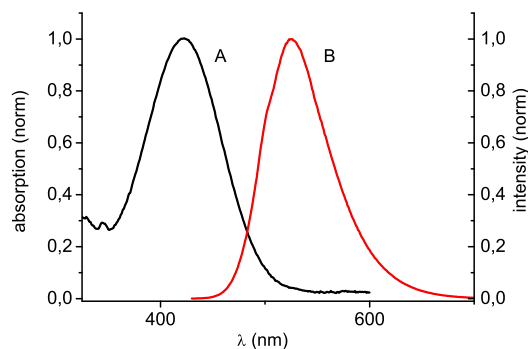
Figure 2.17:   Normalized absorption spectrum (A) versus normalized emission spectrum (B) of dye-protein conjugate in phosphate buffered saline (PBS)
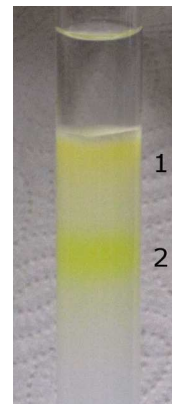
Figure 2.18: Purification of label-5-BSA conjugate via SEC; (1): unreacted label, (2): dye-protein conjugate

Figure 2.17 shows that the absorption maximum of the dye-protein conjugate is located at 424 nm, thus indicating a bathochromic shift of 18 nm compared to the free label **5**. The emission maximum is shortwave shifted and peaks at 523 nm (538 nm for the free label). This behavior is caused by the more unpolar surrounding of the protein in comparison to aqueous media.

2.2.7 Compound 4 in a sensor for oxygen

Wang et al. describes a new and simple way of oxygen sensing using a specially designed 2-color sensor film and by exploiting the specific photographic readout option of digital cameras. Compound **4** (preparation according to 2.2.4) is one of the two dyes which are applied in this technology [72].

2.2.8 Summary and evaluation of the VIS-labels

First, the two VIS labels **2** and **5** are evaluated regarding the complexity of their synthesis, the spectral properties and their qualification as amino-reactive labels. Additionally, the spectral properties of the labels as well as their protein conjugates are summarized (see table 2.5).
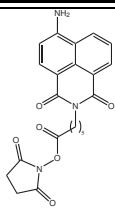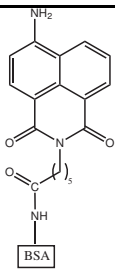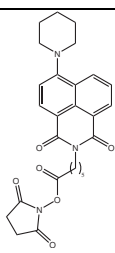
Evaluation of label 2

Label **2** is based on a known and highly photostable yellow daylight chromophore. Its synthesis is accomplished in two steps and leads to a low mol-weight, electrically neutral label that is useful for various labeling experiments (amino acids, BSA, FNPs) and separation techniques (SEC, CE, MCE). The emission maximum is comparable to that of fluorescein, but the Stokes' shift of the label and the dye-to-protein conjugate is as large as 70 nm (compared to 23 nm for fluorescein). Its photostability is distinctly better. Unlike that of fluorescein, its fluorescence is independent of pH in the electrophoretically relevant range between 3 and 9. Label **2** can be photoexcited with blue or purple diode lasers which have become very attractive light sources because of their small size, longevity, and low power consumption. On the other side, the brightness of the marker (defined as the molar absorbance at the excitation wavelength multiplied by its quantum yield) is inferior to fluorescein and most coumarins. In fact, the absorbance of fluorescein is larger by a factor of 4 at its absorption maximum (489 nm). The polar character of this label enhances its water solubility which is advantageous when tagging biological matter in aqueous media [73].

Evaluation of label 5

Label **5** is based on the same yellow daylight chromophore as label **2**. It possesses a piperidyl moiety in position 4 instead of an amino group. It exhibits similar spectroscopic properties like photostability, low molar absorbance, high quantum yield, absorption and emission maxima [74, 75]. Additionally, its Stokes' shift is as large as that of label **2** and λ_{em} peaks also at shorter wavelength after tagging proteins. The molar absorbance is higher by a factor of 1.6 compared to label **2**. The preparation requires three synthetical steps resulting in a small and neutral molecule being used to label biological analytes (amino acids, BSA). One drawback is the reduced solubility in aqueous media due to the introduction of the piperidyl moiety. Consequently, if tagging biological material the amount of label has to be restricted due to the precipitation of the dye.

Spectral properties of labels and conjugates

compound	formula	λ_{abs} (ε)	λ_{em} (ϕ)
label 2		431 nm $(6.9 \cdot 10^3 \, \frac{L}{mol \cdot cm})$	550 nm (0.1)
label 2-BSA		431 nm	501 nm (0.24)
label 5		406 nm $(11.1 \cdot 10^3 \, \frac{L}{mol \cdot cm}$ in MeOH)	538 nm (0.14 in MeOH)
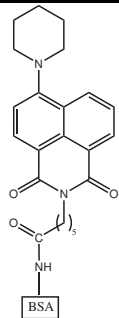
label 5-BSA		424 nm	523 nm (0.26)

Table 2.5: Properties of labels and protein conjugates; coumarin 6 is used as a standard in quantum yield determination
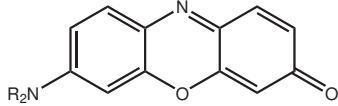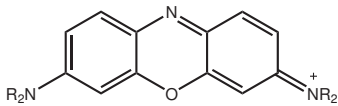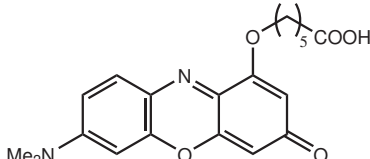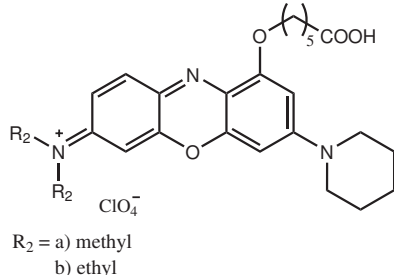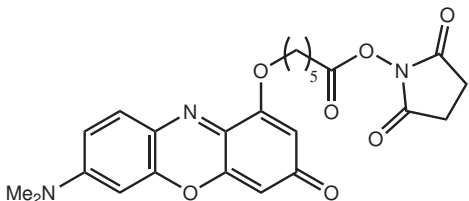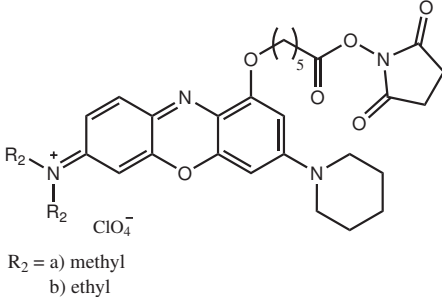
2.3   Derivatives of phenoxazines as NIR-Labels

The spectral range between 600 nm and 1000 nm is of particular intrest (compared to the UV and shortwave visible part) [76–78] because most biomatter displays less background fluorescence and straylight there [77]. Additionally, longwave radiation penetrates biomatter much more easily than shorter wavelengths which is important in biological applications. Green, yellow and (deep) red laser diodes are prefered light sources because they are affordable and compact, battery-powered and easily driven, and they are of high efficiency (in terms of conversion of electrical energy into light) [79]. Hence, there is a substantial interest in fluorescent labels for bioanalytical sciences and in combination with diode laser light sources. Numerous labels with excitation maxima of >580 nm have been reported and are available from commercial sources including Invitrogen (www.probes.com), Dyomics (www.dyomics.de), Attotec (www.atto-tec.com), ActiveMotif Chromeon (www.chromeon.de), Amersham (www.amershambiosciences.com) and others.

Among the long-wavelength emitting dyes, the oxazines and the benzoxazines (such as Nile Red and Nile Blue) are attractive due to their stability and brightness [80]. They have been used as biomarkers for nucleic acid, detection in histochemistry [81, 82], for labeling proteins [83] and for environmental analysis [84]. The state of the art, concerning oxazine-type labels, has been reviewed by Drexhage [85], Hartmann [86], Tung [87] and Simmonds/Briggs [88], for instance. Deeply colored oxazines possess a mesomeric donor-acceptor chromophoric system. Oxazinones, of type **B** (see table 2.6), are strongly solvatochromic (e.g. orange and fluorescent in non-protic solvents, red in methanol, purple and weak fluorescent in water). Diamino-substituted oxazines of type **C** (see table 2.6) are blue and hardly solvatochromic. They display good water solubility due to their cationic nature, often undergo an increase in fluorescence quantum yield upon

conjugation, and are enabled to structural modification, thus various functional groups can be introduced.

In this section novel phenoxazine labels are presented. These compounds are advantageous because far-visible or near infrared dyes can be obtained by a simple condensation reaction. Hence, all the advantages (mentioned above) for a label operating in this highly desirable spectral region are achieved within a few synthetic steps. Two types of phenoxazines (**B** and **C**) represents the basic chromophores of the labels presented in table 2.6. These two chromophores are functionalized with different groups resulting in a broad field of application. On the one hand there are the classic amino-reactive markers derivatized by a C-6 linker carrying a carboxy group (compounds **8** and **13a/b**) which can be activated via its N-hydroxysuccinimidyl ester (compounds **9** and **14a/b**). On the other hand there are the clickable labels (compound **16** and **18**) which can be used in click chemistry, a concept described in 2.1.2. These labels provide the opportunity to simplify existing and to generate new strategies of labeling. The different sythetic strategies, spectral properties and applications are presented in the following sections.

B	C
8	13a/b
9	14

| 16 | 18 |

Table 2.6: Chromophores of the purple oxazines **B** and the blue oxazines **C**, the free acids **8** and **13a/b**, the corresponding amino-reactive labels **9** and **14a/b** as well as the click-labels **16** and **18**

2.3.1 Preparation of label 9
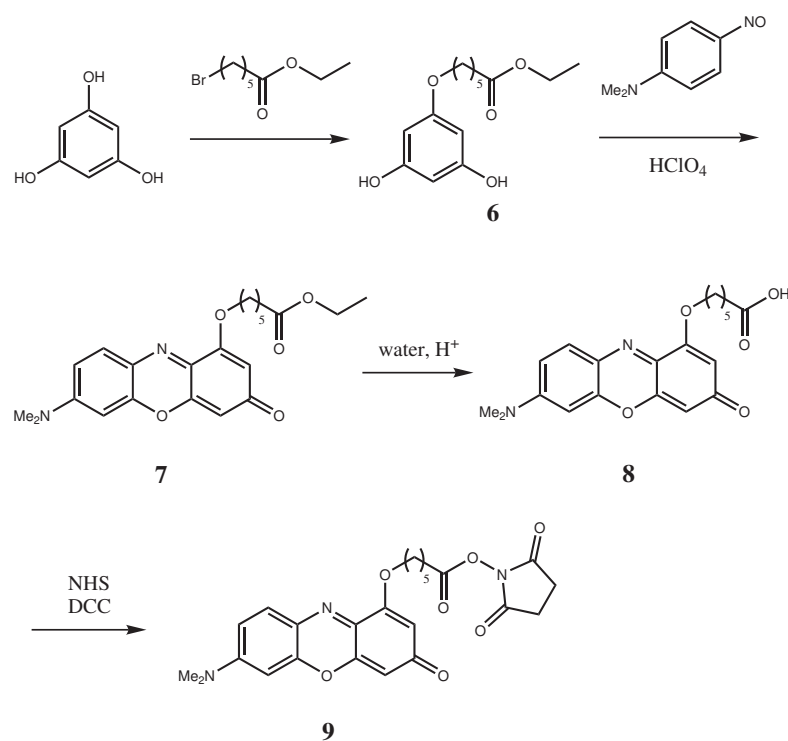
Figure 2.19: Synthetic pathway to the purple phenoxazine label **9**

Label **9** is synthesized in four steps as shown in figure 2.19. Phlorogluci-nol (a cheap and easily available starting material) is functionalized with ethyl-bromo-hexanoate to obtain the monosubstituted intermediate **6** [89]. Ethyl-bromo-hexanoate is prepared by esterification of 6-amino-hexanoic acid according to [90].

Next, the phenoxazine dye **7** is prepared by condensation of **6** with p-nitroso-N,N-dimetylaniline [91,92]. Finally, the carboxylic ester is hydrolyzed under acidic conditions to obtain the free acid **8**. This dye can be easily converted in-situ into its NHS-ester **9** using DCC and NHS [93]. The solution of the activated dye is directly used for labeling and can be stored at -18°C at least for one week.

2.3.2   Properties of label 9

The free acid **8** is used to determine the spectroscopic properties instead of label **9** as the NHS-ester functionality does not change the spectroscopic behavior of the chromophore.

Spectroscopic properties
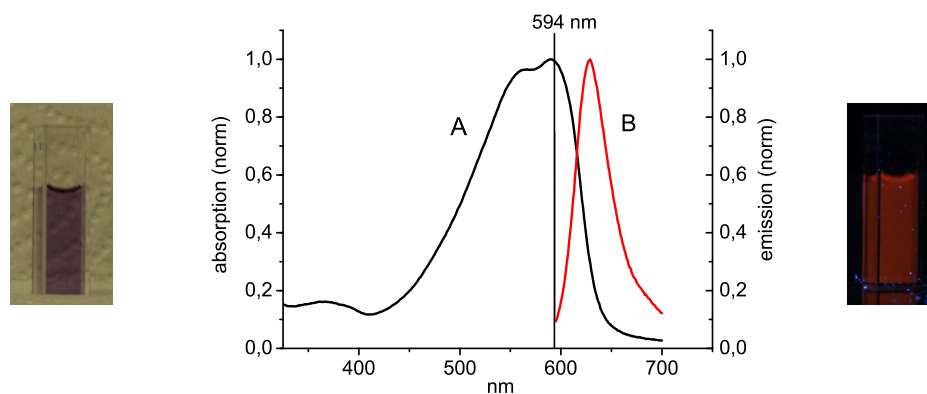
Figure 2.20: Normalized absorption spectrum (A) versus normalized emission spectrum (B) of dye **8** in water; Helium-Neon laser line at 594 nm which represents a perfect spectral match is also shown. The photos show compound 8 dissolved in water: unexcited (left) and excited via lab lamb (right).

The absorption and emission spectra of the purple phenoxazine (free acid) **8** exhibit a broad absorption band with a maximum at 589 nm and a shoulder at 565 nm (see figure 2.20). The emission peaks at 630 nm and the Stokes' shift is 32 nm. Compound **8** displays strong solvatochromism like other dyes of the Nile Red type. The absorption/emission maxima in water (589/630 nm) are shortwave shifted to 557/619 nm in methanol and to 510/580 nm in toluene. Hence, the respective label is a feasible probe for intra-protein (local) polarity [94,95]. The molar absorbance of **8** is $3.8 \cdot 10^4 \; \frac{L}{mol \cdot cm}$ and quantum yield in aqueous solution is 0.05 determined with Nile Red (QY of 0.018 [96]) as standard.

pH dependence

Compound **8** is excited at its absorption maximum (598 nm), and the change of the fluorescence intensity with pH is measured at its emission maximum (630 nm). The fluorescence of **8** drops at low pH which can be explained by its chemical structure. Dye **8** is an uncharged and slightly basic molecule whose nitrogen atoms (dimethylamine group and heterocycle) can be protonated. The resulting positive charge is most likely mesomerically distributed over the whole electron system and thus affects emission intensity. Figure 2.21 shows the absorption spectrum of dye **8** which is shortwave shifted by the transition from an alkaline or neutral ($\lambda_{abs} = 598$ nm) to an acidic aqueous medium ($\lambda_{abs} = 551$ nm). Therefore, the excitation intensity at 598 nm as well as the emission intensity at 630 nm decreases under acidic conditions.
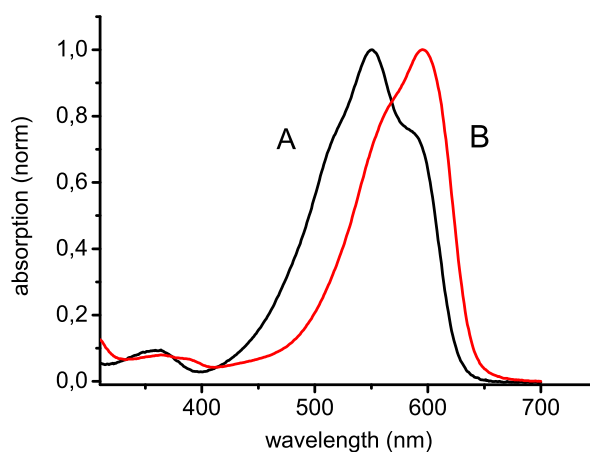
Figure 2.21: Normalized absorption spectra of the purple phenoxazine **8** in (A) 0.1 M HCl and in (B) 0.1 M NaOH or 50 mM phosphate buffer (PB) of pH 7

2.3.3   Applications of label 9

In order to demonstrate the scope of label **9**, it is used to tag a various number of analytes containing an amino group: from important biological analytes like peptides and proteins to silica nanoparticles which are a new and biocompatible material with a growing number of applications.

Labeling of peptides

Bradykinin consists of nine amino acids. This peptide enlarges blood vessels and therefore it decreases blood pressure making bradykinin an important analyte in medicine and biochemistry [97]. The peptide is labeled by treating it with a solution of **9** overnight at room temperature. The labeled bradykinin is separated from the unreacted dye by microchip electrophoresis (electropherogram see figure 2.22, migration time see table 2.7) in the same manner as described in section 2.2.3. This experiment shows the application of label **9** in MCE. The label exhibits a neutral and low weight chromophore which is an advantage in electrophoresis (like label **2**). Additionally, label **9** operates in the highly desired near infrared region of the electromagnetic spectrum and can be excited with small laser diodes. Hence, in the small separation system (MCE) and detection device (laser diode, fluorescence detection) two criteria for a future lab-on-a-chip system are fulfilled. The MCE experiment is carried out at the Institute of Analytical Chemistry (Prof. D. Belder) at the University of Leipzig.
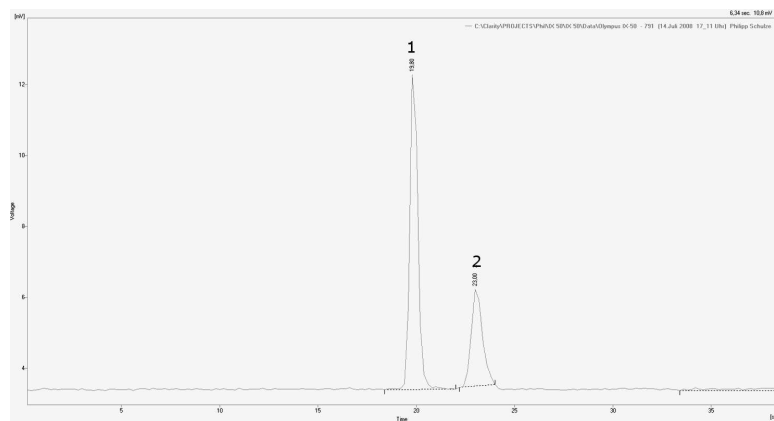
Figure 2.22: Separation of the labeled bradykinin (1) and dye **8** (2). Experimental conditions: Separation length 3 cm, buffer PBS pH 7. Injected quantity of labeled bradykinin: nL scale

compound	migration time in sec
bradykinin (1)	19.8
dye 8 (2)	23.00

Table 2.7: Migration time of the labeled bradykinin as well as of the free dye **8**

Labeling of bovine serum albumin

Like in the case of bradykinin, the labeling is carried out over night at room temperature. The protein is purified by size exclusion chromatography and submitted to TOF-MS analysis (see data in the experimental section). The effect of BSA on fluorescence intensity of the dye is checked via BSA titration. Here, 5 μL (c = 0.054 M) of non-reactive dye **8** is added to a buffered solution (PBS, 50 mM, pH 7) of BSA in concentrations between 0 and 1000 mg/L. No significant change in fluorescence intensity can be observed, indicating that there is no disturbance of the fluorescent measurement by non-covalent dye-protein interaction. The photophysical properties of the non-reactive dye with those of the dye-protein conjugate are presented for comparison in table 2.8. Quantum yields are determined in phosphate buffer (pH 7, 50 mM). Nile Red is used as standard.

compound	λ_{abs}	λ_{em} (ϕ)
dye 8	565 nm (shoulder) 589 nm	630 nm (0.05)
labeled BSA	558 nm	627 nm (0.04)

Table 2.8: Photophysical properties of dye **8** and labeled BSA

While the emission spectra and the quantum yields of the dye-protein conjugate of the purple phenoxazine does not significantly deviate from that of the unreactive dye, the absorption spectrum of the protein conjugate varies, resulting in a different shape of the bands (see figure 2.23). This effect is only visible after the covalent attachment of the fluorophore to the protein. The absorption spectrum is unchanged if only the non-reactive dye is added to a BSA solution. Hence, the change of only the absorption band is a useful tool which indicates a successful covalent labeling.

Labeling of silica nanoparticles

The labeling of silica nanoparticles (SiNPs) with **9** is a forward-looking application. Both, the easy affordable and biocompatible SiNPs and a far-visible compound adequate for laser excitation are combined. The tagging is realized by two different methods **A** and **B**:

Method A: Silica nanopowder from Nanostructure&Amorphous Materials Inc. (www.nanoamor.com) is treated with APTS in order to obtain amino-modified material. Label **9** is added to a suspension of the amino-modified silica nanopowder in ethanol and the reaction is carried out over night. The amino-labeled particles are collected by centrifugation (6000 rpm, 10 min) and washed with ethanol
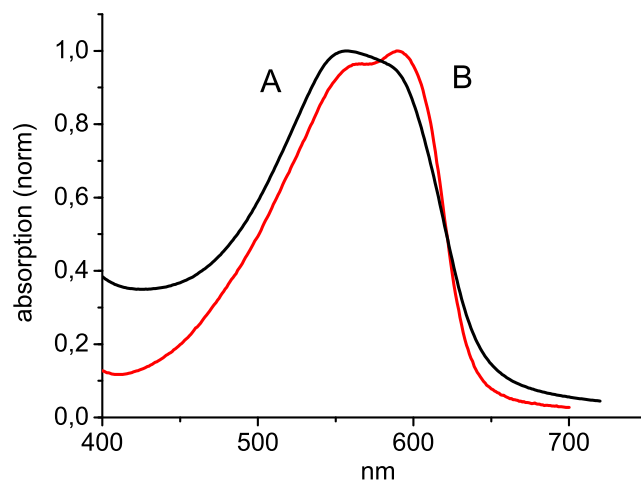
Figure 2.23: Normalized absorption spectrum of dye-BSA conjugate (A) versus normalized absorption spectrum of dye **8** in water (B)

(3 times) removing the unreacted label. In parallel a blank sample is prepared by combining unmodified SiNPs (without amino groups) with the activated fluorophore. After the centrifugation/washing steps the blank sample shows almost no color whereas the amino-labeled particles are strongly colored.

Method B: Unfunctionalized SiNPs are prepared by the Stöber method [98]. A mixture of APTS in ethanol and label **9** are stirred over night in order to receive labeled silane. This dye-silane conjugate is directly used to label the SiNPs. These labeled SiNPs are purified by SEC on Sephadex LH-20 (see figure 2.24). The particles modified with fluorophores are obtained by collecting the colored fraction that leaves the column first. The second colored band that moves much slower contains the unreacted reagents and is discarded. In parallel a blank sample is prepared to exclude unspecific binding of the fluorophore to the particle surface. Therefore, alcosol containing particles are diluted with ethanol. The unreactive dye **8** (free acid) is also dissolved in ethanol and added to the particle solution. The mixture is stirred over night and purified by SEC as described above. The resulting SiNPs possess no significant fluorescence.

The emission maximum of the labeled SiNPs (method **A** and **B**) is bathochromically shifted (λ_{em} = 626 nm) in comparison to the unreacted label (λ_{em} = 619 nm; see figure 2.25). The emission spectra of the labeled SiNPs and the unreacted reagent are recorded in ethanol and therefore blue shifted as compared to the spectra in aqueous media.
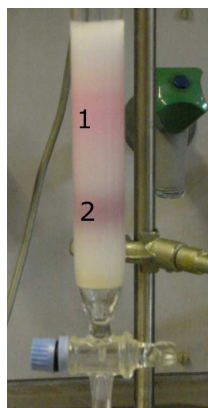
Figure 2.24: Separation of unreacted dye (1) and labeled particles (2) on Sephadex LH-20
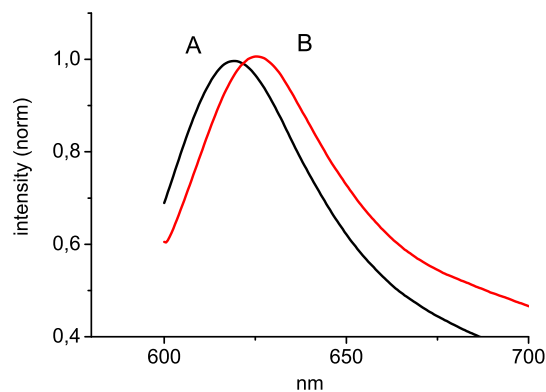
Figure 2.25: Normalized emission spectra of dye **8** (A) and the labeled particles (B) in ethanol

2.3.4   Preparation of labels 14a/b

The blue phenoxazine labels **14a/b** (see figure 2.26) are prepared in five synthetic steps. The two labels differ only in the replacement of a dimethylamino group (label **14a**) by a diethylamino group (label **14b**). Both syntheses start from phloroglucinol. Treatment with piperidine yields compound **10** [99]. The intermediate **11** is obtained by reaction with ethyl-bromohexanoate which is prepared by the esterification of 6-amino-hexanoic acid [90]. The condensation with p-nitroso-N,N-dimethylaniline or p-nitroso-N,N-diethylaniline leads to the phenoxazine **12a** or **12b**, the acidic-catalyzed hydrolysis to the free acids **13a** and **13b** by analogy to the purple phenoxazine. In the last step, the free acids are activated by treating them with DCC and NHS in dry DMSO which results the corresponding NHS-esters **14a** and **14b**. The solutions of the labels can also be stored at -18°C at least for one week.
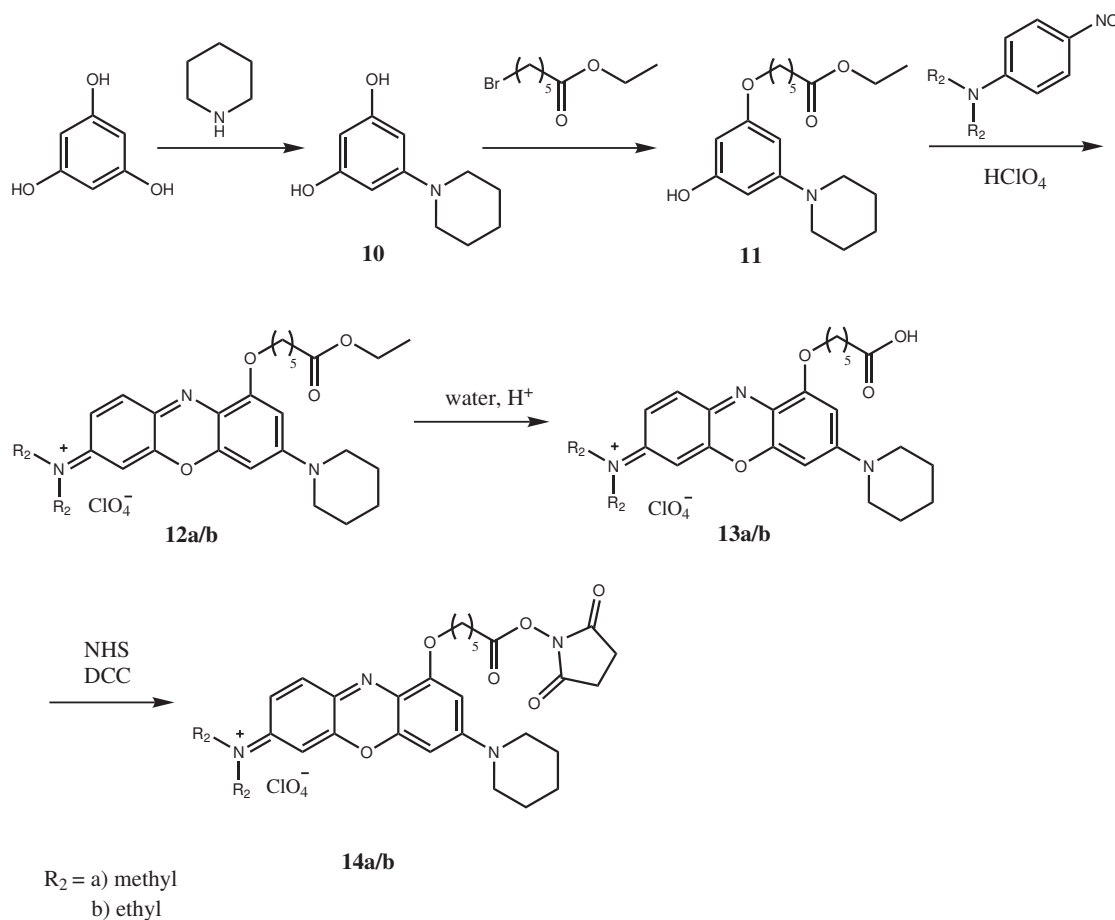
Figure 2.26: Synthetic pathway to the blue phenoxazine labels **14a/b**

2.3.5 Properties of labels 14a/b

The free acids **13a/b** are used to determine the spectroscopic properties instead of labels **14a/b** as the NHS-esters functionalities do not change the spectroscopic behavior of the chromophores.

Spectroscopic properties

Due to different electron acceptors (a carbonyl group of the purple phenoxazine **8** and an iminium group of **13a/b**) the absorption as well as the emission of the blue phenoxazines are bathochromatically shifted as shown in figure 2.27 and 2.28. The absorption maximum peaks at 648 nm ($\lambda_{shoulder} = 598$ nm) for **13a** and 652 nm ($\lambda_{shoulder} = 602$ nm) for **13b**. Therefore, the two labels can be excited with the 635 nm diode laser which is widely used in fluorescence instrumentation such as cell sorters and imagers. Molar absorbance of **13a** is $7.1 \cdot 10^4 \ \frac{L}{mol \cdot cm}$ and $7.0 \cdot$

$10^4 \frac{L}{mol \cdot cm}$ for **13b**. The fluorescent emission peaks at 670 nm for **13a** and at 671 nm for **13b**. Both exhibit a quantum yield in water of 0.004 whereas Nile Blue (QY is 0.004 [100] in water) is used as standard. The two phenoxazines show a blue color in water with a red fluorescence after photoexcitation.
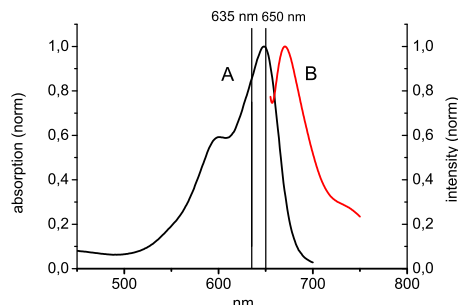
Figure 2.27: Normalized absorption spectrum (A) versus normalized emission spectrum (B) of dye **13a**. The lines at 635 nm and 650 nm of the laser are also depicted.
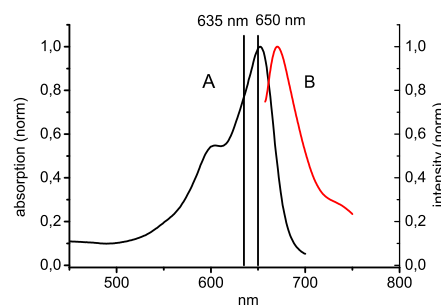
Figure 2.28: Normalized absorption spectrum (A) versus normalized emission spectrum (B) of dye **13b**. The lines of the 635 nm and 650 nm laser are also shown.

These compounds are much less solvatochromic and therefore the absorption/emission maxima are much less shifted in methanol solution (639/663 nm for **13a** and 643/666 nm for **13b**) compared to the purple phenoxazine.

pH dependence

The effect of pH on the fluorescence of the the blue phenoxazine dyes is studied for the pH range 3 to 9. Both dyes are excited at their maximum in aqueous media and the change of their fluorescence intensity is measured. It turns out that the emission intensity of **13a/b** and therefore the intensity of the corresponding NHS-esters do not depend significantly on pH in comparison to the purple phenoxazine **8** which intensity decreases under acidic conditions (see figure 2.29 and section 2.3.2). The reason for the different pH sensibility of the purple and the blue phenoxazines is due to their different structure. Compound **8** and label **9** are neutral molecules which can be protonated at their nitrogen atoms. This has an influence on the mesomeric system of the dyes and hence to their emission intensity. The blue phenoxazines already carry a positive charge which renders an additional protonation on the mesomeric system improbable. So, there is no remarkable effect of pH on the emission intensity of the blue dyes.
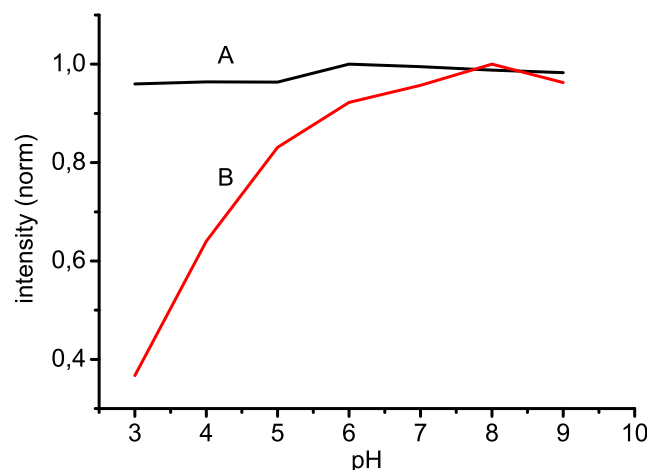
Figure 2.29: Normalized pH dependencies of dye **13a** (A) and the purple phenoxazine **8** (B) between pH 3 and pH 9

2.3.6 Applications of labels 14a

In order to demonstrate the application of the blue phenoxazines as amino-reactive labels, compound **14** has been attached to amino acids as well as to bovine serum albumin as standard protein. The dye-analyte conjugates are separated and identified using size exclusion chromatography (SEC) and thin layer chromatography (TLC). Tagging experiments are carried out with compound **14a** due to the fact that the two blue labels only differ insignificantly in their spectroscopic and structural properties.

Labeling of amino acids

The amino acids L-leucine, L-serine, L-glycine, L-glutamic acid, L-aspartic acid are dissolved in bicarbonate buffer (pH 8.3, 50 mM) and labeled by treating them with solutions of **14a** overnight at room temperature. The process is monitored via TLC (silica gel 60, butanol/acetic acid/water: 60/20/20) and the retention times are depicted in table 2.9.

compound	R_f
L-serine	0.31
L-aspartic acid	0.35
L-glycine	0.36
L-glutamic acid	0.4

L-leucine	0.42

Table 2.9: R_f of the labeled amino acids

Labeling of bovine serum albumin

Bovine serum albumin (BSA) serves as a model protein in this labeling experiments. Similar to the amino acids, a solution of **14a** in DMSO is added to BSA in bicarbonate buffer (pH 8.3, 50 mM). The tagging is carried out over night and at room temperature. The labeled protein is purified by size exclusion chromatography (see figure 2.30) and analyzed by TOF-MS (see data in the experimental section). The effect of BSA on fluorescence intensity of the dye is checked via BSA titration in the same manner as shown in 2.2.7: 5 μL (c = 0.054 M) of non-reactive dye is added to BSA in phosphate buffer solution (pH 7, 50 mM). Concentrations of BSA solutions range between 0 and 1000 mg/L. No significant change in fluorescence intensity can be observed, indicating that the fluorescent measurement are not disturbed by non-covalent dye-protein interaction.
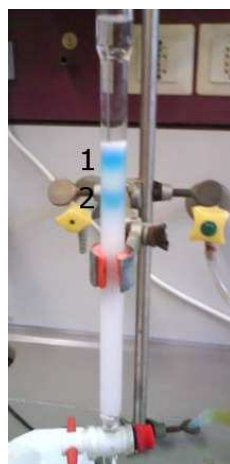
Figure 2.30: Purification of label-14a-BSA conjugate via SEC; unreated label (1), dye-protein conjugate (2)
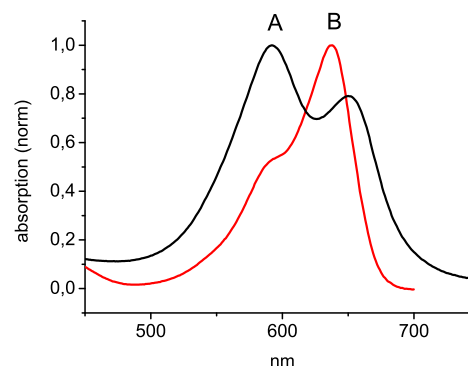
Figure 2.31: Normalized absorption spectrum of dye-BSA conjugate (A) versus normalized absorption spectrum of dye **13a** (B) in water

Figure 2.31 shows that the absorption spectrum of the dye-protein conjugate (A) differ from that of the free dye **13a** (B) resulting in a different shape of the bands. This effect can also be observed in case of the purple label **9** and is only visible after covalent labeling. The absorption spectrum is not altered if the non-reactive dye only is added to a BSA solution. Hence, the change of the

absorption spectrum is a useful indicator for successful labeling. Tabel 2.10 lists the photophysical properties of the non-reactive dye in comparison with those of the dye-protein conjugate. Quantum yields are determined in phosphate buffer solution (pH 7, 50 mM) with Nile Blue as standard.

compound	λ_{abs}	λ_{em} (ϕ)
dye 13a	598 nm (shoulder)	670 nm
	648 nm	(0.004)
labeled BSA	592 nm	677 nm
	641 nm	(0.003)

Table 2.10: Photophysical properties of dye **13a** and labeled BSA

2.3.7   Preparation of label 16
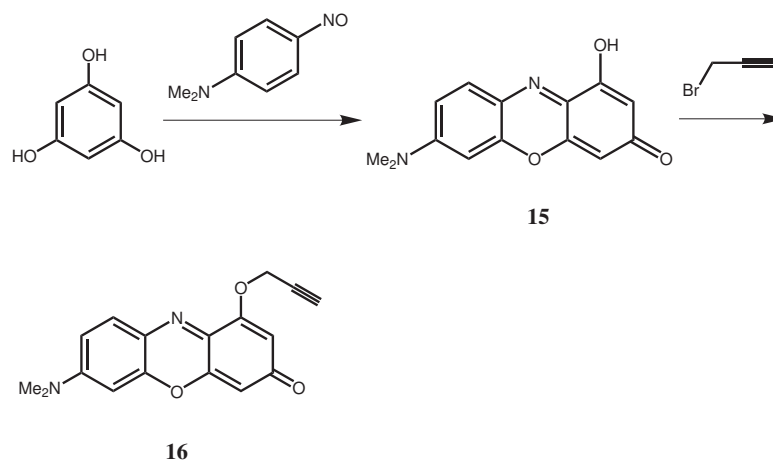
Figure 2.32: Synthetic pathway to the purple click-label **16**

The motivation behind the synthesis of label **16** lies in the combination of the innovative concept of click-chemistry with the advantageous spectral properties of the purple chromophore **B** (see table 2.6). The preparation of this compound is accomplished in two steps leading to a low mol-weight and far-visible click-label (see figure 2.32). The phenoxazinone **15** is synthesized by the condensation of phloroglucinol and p-nitroso-N,N-dimethylaniline according to Kotoucek et al. [91]. The alkyne linker is introduced by the reaction of **15** with propargyl bromide giving click-label **16**. Further activation steps, essential for all amino-reactive labels, are not necessary. This work was done in cooperation with Dr. Xiaohua Li where Dr. Li was responsible for the second part of the synthesis.

2.3.8   Properties of label 16

Spectroscopic properties

Label **16** is a representative of purple phenoxazines (see table 2.6, chromophore **B**). Figure 2.33 shows a broad absorption band with a maximum at 596 nm (shoulder at 561 nm) and a molar absorbance of $3.5 \cdot 10^4 \ \frac{L}{mol \cdot cm}$. The emission peaks at 630 nm and the Stokes' shift is 34 nm. The dye exhibits a strong solvatochromism whereby the absorption/emission maxima in water (596/630 nm) are shortwave shifted to 550/620 nm in methanol. Quantum yield of **16** is 0.12 (Nile Red as standard, QY in methanol 0.08 [101]) which is determined in methanol due to its poor solubility in water.
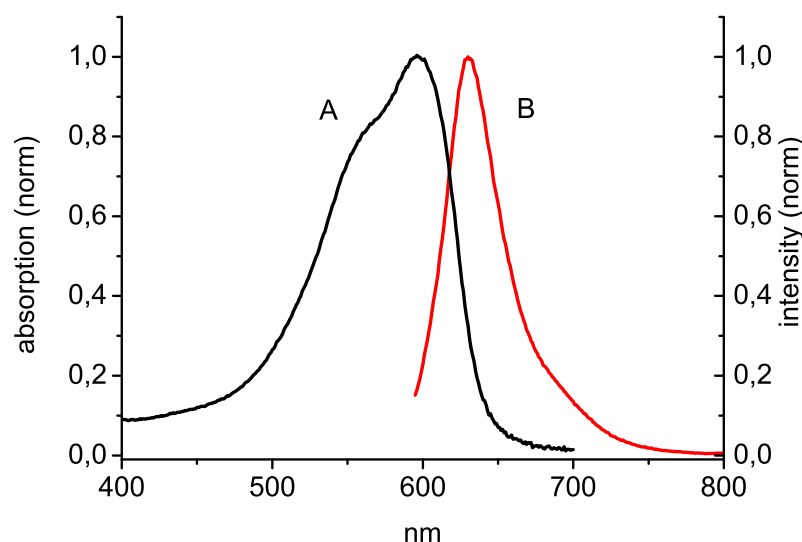
Figure 2.33: Normalized absorption spectrum (A) versus normalized emission spectrum (B) of **16**

2.3.9   Applications of label 16

Clickable fluorophore for biological application

Kele et al. modifies an azido sugar as a model framework with compound **16** because sugars are important biological molecules (see figure 2.34) [41]. The click reaction demonstrates the application of the label for bioorthogonal tagging because of the extreme rareness of azido and alkyne moieties in biological systems [102,103].

It also turns out that the spectral properties of the dye do not change upon conjugation. Additionally, label **16** operates in the far-visible part of the electromagnetic spectrum and therefore interferences caused by biological background fluorescence are reduced.
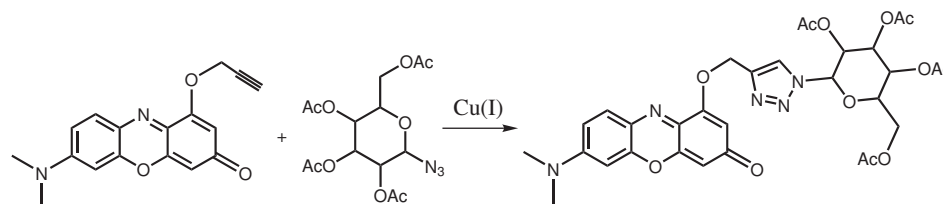
Figure 2.34: Click-reaction to label azido-sugars as model scaffold

Labeling of upconverting particles

Fluorescent labeling of upconverting particles (μm or nm size) with label **16** is carried out by Mader et al. to obtain particles with dual emission. The emission depends on whether the upconverting part is photoexcited at 980 nm or the organic dye at 596 nm. It is combined by clicking compound **16** to a silica-coated and azido-modified upconverting particle. The particle consists of inorganic, upconverting material (La_2O_2S for μ-particles; $NaYF_4$ for nano-particles) which is doped with Yb^{3+} and Er^{3+} [104]. The spectroscopic properties of label **16** slightly deviate after the covalent attachment to the surface of the particles. The absorption peaks at 590 nm and the emission at 620 nm [105].

2.3.10 Preparation of label 18

Label **18** is created as a click-label which is operating in the NIR-part (600-1000 nm) of the electromagnetic spectrum. Little effort has been made to develop such labels in this spectral region which is of certain advantage especially when working with biological material. There are no interferences caused by the biological background luminescence and low energy radiation is in position to deeply penetrate skin and tissue. Additionally, label **18** is cationic and therefore its water solubility is enhanced. This is benificial when working with biological analytes in aqueous media. Label **18** is obtained in three synthetic steps with phloroglucinol as starting molecule. Treatment with piperidine yiels **10**. The intermediate **17** is prepared by reaction with propargyl bromide and condensation with p-nitroso-N,N-dimethylaniline leading to the molecule of interest **18** in the last step (see figure 2.35).
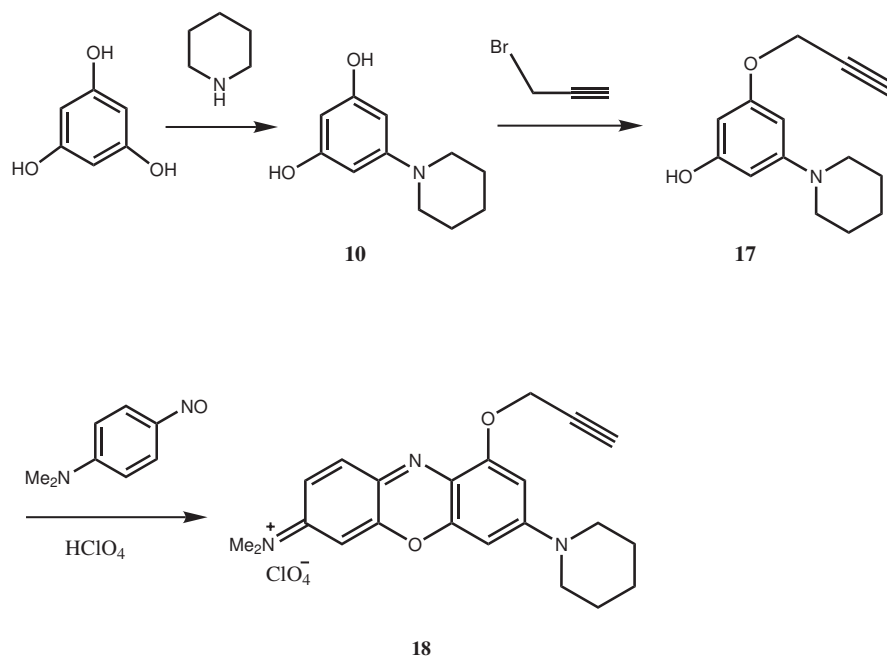
Figure 2.35: Synthetic pathway to the blue click-label **18**

2.3.11 Properties of label 18

Spectroscopic properties

In contrast to the purple click label **16** the absorption and the emission spectrum of the blue phenoxazine **18** are bathochromically shifted (see figure 2.36). This is caused by the replacement of the carbonyl group by an iminium moiety and is also observed for the blue amino-reactive phenoxazines (see 2.3.5). The absorption spectrum of the blue click label shows a broad band with a maximum at 651 nm and a shoulder at 599 nm. Therefore, it can be excited with the 635 nm diode laser. The molar absorbance of **18** is $7.3 \cdot 10^4 \frac{L}{mol \cdot cm}$ and the emission peaks at 674 nm with a quantum yield of 0.009 in aqueous solution (Nile Blue is used as standard, QY is 0.004 [100]).

2.3.12 Application of label 18

Clickable fluorophore for biological application

Kele et al. also uses compound **18** to tag an azido sugar for the same reasons as described in 2.3.9 (see figure 2.37). The advantages of **18** compared to the purple click label **16** are the more favorable spectroscopic properties (NIR instead of far-visible, excitation with the widespread 635 nm laser diode) and the enhanced water
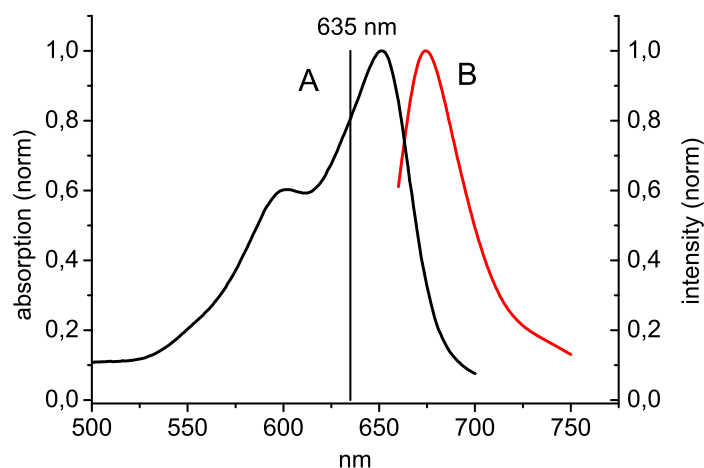
Figure 2.36: Normalized absorption spectrum (A) versus normalized emission spectrum (B) of **18**. The line of the 635 nm laser diode is also shown.

solubility caused by the positively charged chromophore of the blue phenoxazine.
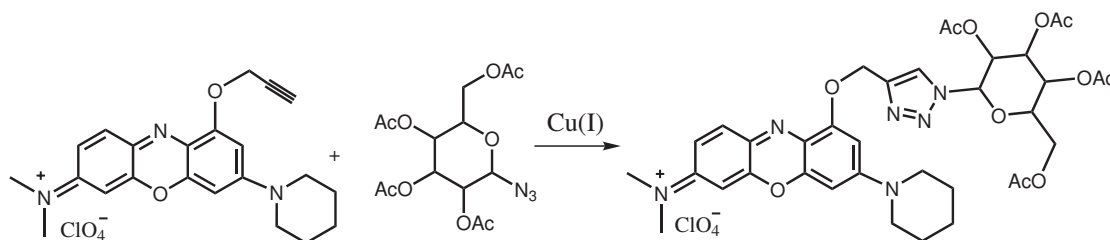
Figure 2.37: Click-reaction to label azido sugars as model scaffold

2.3.13   Summary and evaluation of the NIR-labels

In this section, the NIR-dyes are evaluated regarding the complexity of their synthesis, the spectral properties and their qualification as appropriate labels. Additionally, the spectral properties of these dyes and their corresponding conjugates are summarized (see table 2.11).

Evaluation of dye 8

The structures and the spectroscopic properties of dye **8** and its corresponding label **9** are related to Nile Red. The absorption coefficient ($3.8 \cdot 10^4 \; \frac{L}{mol \cdot cm}$) for

instance is identical with that of Nile Red, a well-established laser dye and stain for biological material [106, 107].

Preparation is carried out in four synthetic steps leading to a low mol-weight, electrically neutral and far-visible label that is proven to be useful for various tagging experiments (peptide, BSA, silica nanoparticles) and separation techniques (SEC, MCE). The feasible usage as a probe for intra-protein (local) polarity due to its strong solvatochromism demonstrates the broad application of the purple phenoxazine. A similar label is established by the group of Briggs et al. but this compound is distinctly bigger in size [108]. The solubility in aqueous media is unfortunately limited as expected for neutral organic compounds. Hence, in biological application the amount of label has to be restricted in regard of the possible precipitation of the dye.

Evaluation of dye 13a/b

Dye **13a** and **13b** as well as their NHS-esters (**14a/b**) are operating beyond 600 nm (NIR-dyes). These blue phenoxazines are capable of being excited via the 635 nm or 650 nm laser diode which is a small, widespread and stable light source. Their absorption coefficients ($\sim 7.0 \cdot 10^4 \ \frac{L}{mol \cdot cm}$) are twice as high as those of the purple phenoxazines (**8/9**) and comparable to Nile Blue ($7.6 \cdot 10^4 \ \frac{L}{mol \cdot cm}$ [109]). Additionally, the blue phenoxazines are positively charged which makes them more soluble in aqueous media than the neutral/purple compounds. This is advantageous while working with biological material. **13a/b** and their NHS-esters are synthesized in four to five steps thus creating two easily affordable compounds for different labeling experiments.

Drexhage and Marx (Boehring Mannheimer GmbH) [110] synthesize dyes and labels related in structure and spectroscopic properties. Compared to the blue phenoxazines described in a patent of Boehring Mannheimer GmbH, dye **13a/b** and their corresponding labels are not functionalized at the push and pull system of the chromophore which is disadvantageous for the spectral properties of the label in terms of molar absorbance and brightness (defined as the product of ε and quantum yield).

Evaluation of dye 16

Label **16** is derived from compound **8** (alternatively from label **9**) due to a transfer of the advantageous characteristics (e.g. easy synthesis and spectral range) to a clickable compound. The only difference between these two phenoxazines lies in the replacement of the linker (**8** is carrying a carboxylic acid) with an alkyne linker. Hence, the spectroscopic properties (see tabel 2.11), the strong solvatochromism and the solubility in water are very similar to compound **8**. Compound **16** is

prepared in only two synthetic steps leading to a compound which proved its broad applicability in clicking biological material and upconverting particles. Especially the relatively simple synthesis from cheap and easily affordable starting materials makes this label an interesting clickable fluorophore.

Evaluation of dye 18

Label **18** is a clickable derivative of the blue phenoxazine **13a** (alternatively of the amino-reactive label **14a**) in which the amino-reactive linker is replaced by an alkyne moiety. Their spectroscopic properties (longwave part of the spectrum) are very similar to compound **13a** (see table 2.11). This is highly desirable due to reduced background fluorescence caused by the analytes. Compared to label **16** the structure (positive charge) of the blue click-label enhances its water solubility which is important in biological applications. The synthesis consists of three steps with cheap and easily affordable starting materials similar to label **16**.

Spectral properties of dyes and conjugates

compound	formula	λ_{abs} (ε)	λ_{em} (ϕ)
dye 8		565 nm (shoulder) 598 nm ($3.8 \cdot 10^4$ $\frac{L}{mol \cdot cm}$)	630 nm (0.05)
dye 8-BSA conjugate		558 nm	627 nm (0.04)
dye 13a		598 nm (shoulder) 648 nm ($7.1 \cdot 10^4$ $\frac{L}{mol \cdot cm}$)	670 nm (0.004)
dye 13a-BSA conjugate		592 nm 641 nm	677 nm (0.003)
dye 13b		602 nm (shoulder) 652 nm ($7.0 \cdot 10^4$ $\frac{L}{mol \cdot cm}$)	671 nm (0.004)
dye 16		561 nm (shoulder) 596 nm ($3.5 \cdot 10^4$ $\frac{L}{mol \cdot cm}$)	630 nm (0.12 in MeOH)
dye 18		599 nm (shoulder) 651 nm ($7.3 \cdot 10^4$ $\frac{L}{mol \cdot cm}$)	674 nm (0.009)

Table 2.11: Properties of NIR-dyes and their protein conjugates in water; Nile Red and Nile Blue are used as standards in quantum yield determination

2.4 Azido- and thiol-labels based on purple and blue phenoxazines

Table 2.12 itemizes two azido-labels suitable for click chemistry as well as two thiol-reactive labels and their spectral properties. Both classes are base on developments described in 2.3. The synthesis and the application of these dyes are carried out by Jana Kleim in her diploma thesis which I co-supervised. The aim of her thesis is the preparation of azido click-labels attachable to alkyne moieties. Furthermore, this azido dyes are modified by click chemistry leading to highly selective thiol labels (theory described in 2.1). Synthesis, properties and application of the new labels are depicted in [111] and [112].
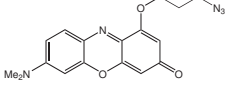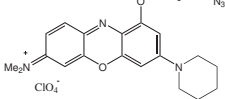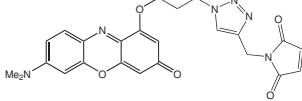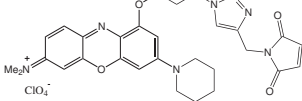
formula	λ_{abs} (ε)	λ_{em} (ϕ)
	595 nm ($1.73 \cdot 10^4$ $\frac{L}{mol \cdot cm}$)	629 nm (0.012)
	649 nm ($5.3 \cdot 10^4$ $\frac{L}{mol \cdot cm}$)	669 nm (0.014)
	597 nm ($2.2 \cdot 10^4$ $\frac{L}{mol \cdot cm}$)	628 nm (0.023)
	650 nm ($4.5 \cdot 10^4$ $\frac{L}{mol \cdot cm}$)	668 nm (0.015)

Table 2.12: Structure and spectroscopic properties of azido- and thiol-labels based on purple and blue phenoxazines

Chapter 3

New fluorescent PET-probes for H$_2$O$_2$ sensing

3.1 Background

PET is the abbreviation for **P**hotoinduced **E**lectron **T**ransfer and describes an electron tranfer from a PET-donor to an excited fluorophore (acceptor) which influences the luminescence intensity of the acceptor [113]. In the research of this phenomenon great efforts have been undertaken to generate specific luminescence probes for various applications. The build-up as well as the functioning of a PET-probe is illustrated in figure 3.1. The probe contains three components [114]:

- a fluorophore (acceptor);

- a spacer group; and

- a receptor (donor).

Hence, the design is highly versatile with regard to individual purposes. The choice of the fluorophore is determined by the required excitation and emission wavelengths. Working with tissue for instance demands long wavelength irradiation and therefore NIR-dyes. The molecule of interest determines the constitution of the receptor e.g. crown ethers for sensing metal ions [115] or a piperazine moiety for the measurement of pH [116]. The spacer facilitates the PET-effect which is a long range process [117].

The **off-mode** of the probe represents the quenching of the photo-excited fluorophore caused by the electron transfer of the analyte-free receptor (donor). In the **on-mode** the excitation of the fluorophore entails luminescence due to the fact that the electron transfer from the donor to the acceptor is blocked by the formation of a receptor analyte-bond (see figure 3.1) [118].
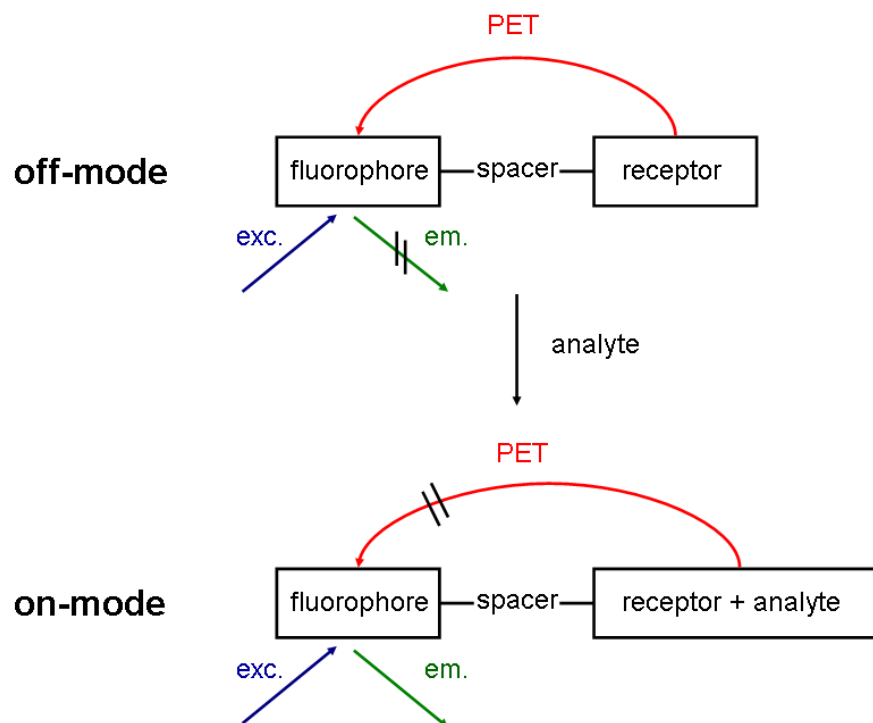
Figure 3.1: Fluorophore-spacer-receptor scheme of a PET-probe

Soh et al. [119] explains this behavior in terms of a molecular orbital energy diagram of the PET-probe. Figure 3.2 illustrates the two cases whether or not an electron transfer from the donor to the acceptor is possible. If the energy level of the highest occupied molecular orbital (HOMO) of the donor (receptor) is high enough an electron transfer to the HOMO of the excited acceptor (fluorophore) occurs and the quantum yield of the fluorophore is low (**part (a)**). The interaction of an analyte with the receptor stabilizes the HOMO of the donor which is then energetically located below the fluorophore's HOMO. Hence, the PET-effect is suspended and the quantum yield of the fluorophore increases (**part (b)**). The design of an efficient PET-probe depends on the energy level of the HOMO of an excited acceptor which has to be located between the HOMO energy levels of the analyte-free donor and the analyte-bound donor. De Silva et al. [120] denotes a more easier criterium for the formation of PET-probes: In the **off-mode** (PET occurs) the oxidation potential of the receptor is smaller than that of the acceptor. In the **on-mode** (PET is suspended) the binding of an analyte molecule significantely disturbs the oxidation potential of the receptor which is therefore higher than that of the fluorophore. Furthermore, it is important that the redox potential of the fluorophore is much less influenced by the analyte compared to

the receptor [117].
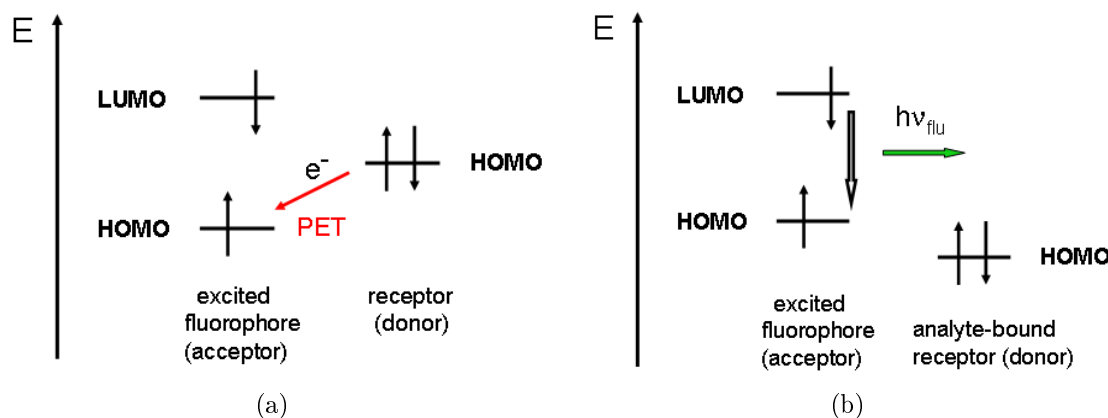
Figure 3.2: (a) analyte-free situation in which an electron transfer occurs (off-mode) (b) analyte-bound situation in which the PET effect is blocked (on-mode)

3.1.1 Development and application of PET-probes

In 1976 Wang and Morawetz presented the first probe harnessing the principle of PET [121]. Figure 3.3 depicts the structure of dibenzylamine containing the three required components. The compound possesses a fluorophore (two benzyl moieties, blue) with excitation and emission in the UV region of the electromagnetic spectrum. Two methylene groups (black) space the fluorophores from the aliphatic amine receptor (red) which is capable for sensing H^+. The fluorescence intensity increases after protonation.
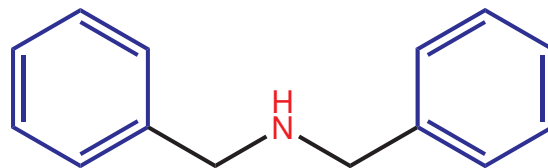
Figure 3.3: Structure of dibenzylamine with the three essential components PET probes highlighted: fluorophore, spacer, receptor

Dibenzylamine is not an ideal PET-probe. On the one hand it operates in the unfavorable UV region of the spectrum and on the other hand it is not specific regarding H^+. The probe also reacts with Zn^{2+} and acetic anhydride. In the following years PET-probes have been improved concerning their specifity and their spectral properties. Also the number of analytical problems tackled by probes

dealing with the concept of PET increased and today some of them are commercially available e.g. for blood analytes (Na^+, K^+, Ca^{2+}) [122]. Figure 3.4 shows a coumaryl-crown ether that selectively detects the toxin "saxitoxin" in the presence of Na^+, K^+ [123]. Beside the high selectivity the excitation and emission properties are bathochromatically shifted in comparison to dibenzylamine. Additionally, figure 3.4 outlines the three structural components (fluorophore, spacer, receptor) which all PET probes have in common.
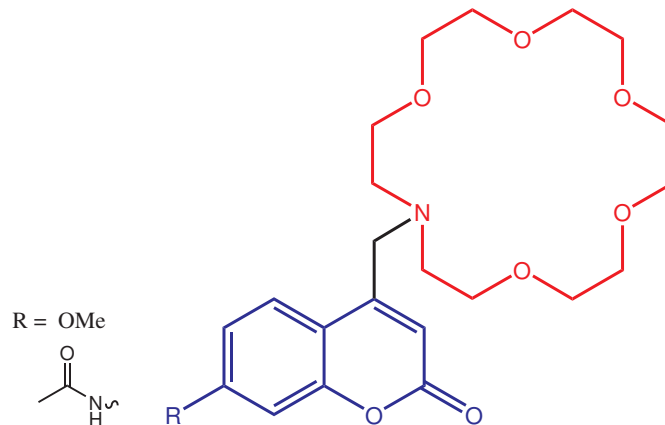
Figure 3.4: Structure of coumaryl-aza-crown derivatives for sensing saxitoxin: fluorophore, spacer, receptor

3.1.2   PET-probes for hydrogen peroxide sensing

State of the art

Hydrogen peroxide (H_2O_2) is one representative of the so-called "reactive oxygen species" (ROS) besides singlet oxygen, hydroxyl radicals, and superoxide anion. These species are associated with various pathological conditions: if their physiological concentration is exceeded ROS indicate oxidative stress in vivo [124,125]. Additionally, H_2O_2 is vasoactive and it appears in inflammations and hypoxia-reoxygenation [126, 127]. Knowledge of the behavior of this important analyte, especially in biological systems is insufficient due to the lack of appropriate detection methods [119]. Fluorescent analysis is especially useful for measurements in living cells and tissue because a continuous observation is possible [128]. Unfortunately, only a few fluorescent probes for detecting H_2O_2 e.g. naphthofluorescein disulfonate (NFDS-1) [129] are known. The number of probes based on the PET-effect is even smaller. Soh et al. presents a H_2O_2 PET-probe (DPPEA-HC) using a diphenylphosphine moiety as receptor group which is spaced from the coumarin fluorophore by two methylene groups [130]. Fluorescence intensity

of the probe depends on the PET-effect from the diphenylphosphine donor to the hydroxycoumarin acceptor. If the receptor (red) reacts with H_2O_2 it is oxidised to a diphenylphosphine oxide moiety (green) as shown in figure 3.5. The electron transfer is blocked and the fluorescence intensity increases.
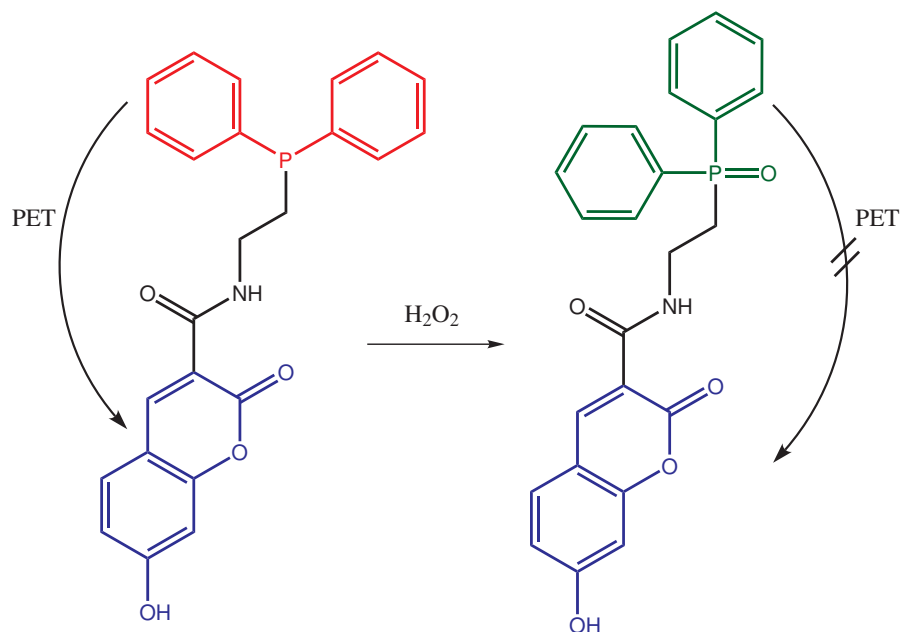
Figure 3.5: (left) Structure of DPPEA-HC in its off-mode showing weak/no fluorescence and (right) in its on-mode (DPPEA-HC-oxide) with suppressed PET and bright fluorescence; fluorophore, spacer, receptor, analyte-bound receptor

Novel developments

Inspired by this principle and the advantages of a fluorescent PET-probe for H_2O_2 sensing we present both the synthesis and the application of two novel probes based on 4-amino-1,8-naphthalimide derivatives. This important yellow daylight fluorophore is widely used as acceptor in PET-probes for sensing anions [131] or metal ions [132] due to its favorable characteristics. It operates in the visible part of the electromagnetic spectrum and exhibits advantageous photophysical properties e.g. a large Stokes' shift and insensitivity to pH [133]. P-Anisidine and p-aminophenol, respectively, are the receptors of choice which are spaced by two methylene groups. Both compounds **21** and **26** are additionally functionalized by the introduction of a C-6 linker carrying a carboxy group (or the ethyl ester). Therefore, the probes can be activated by DCC and NHS giving the corresponding amino-reactive NHS-esters which can be attached to polymeric supports in order

to obtain a sensor device. Table 3.1 shows the basic structure of the naphthalimide **A** (same as in chapter 2) and the hydrogen peroxide probes **21** and **26**.
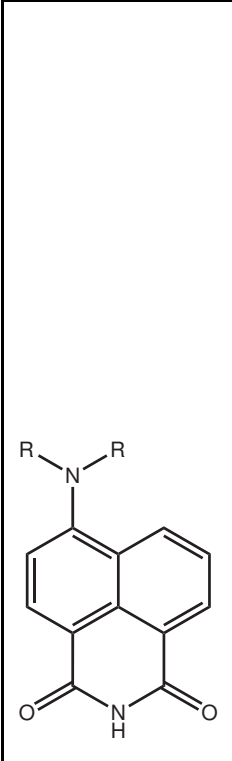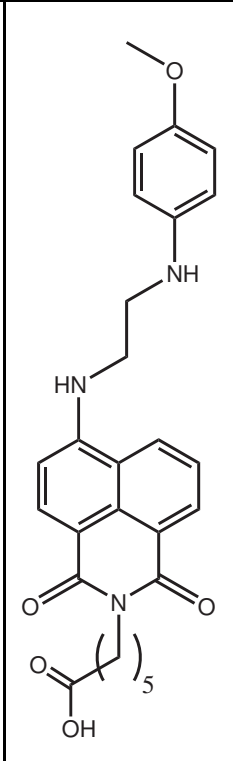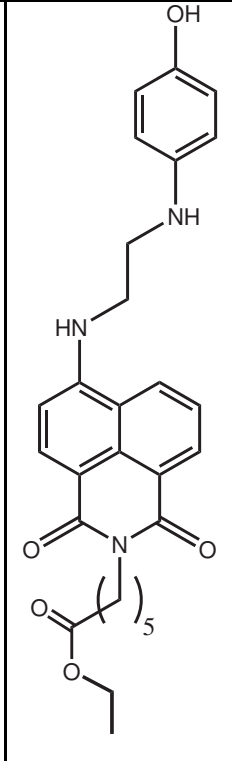
A	21	26

Table 3.1: Basic structure of 1,8-naphthalimide **A** (R = variable moieties) and of probes **21** and **26**

These PET-probes work in the same manner as described above. Figure 3.6 illustrates this principle and the three essential components for PET-probes (colored) for compound **26**. Hence, the electron transfer of the receptor (p-amino-phenol) diminishes the fluorescence intensity of the excited naphthalimide in absence of H$_2$O$_2$. If H$_2$O$_2$ oxidizes the p-aminophenol moiety the electron transfer is suspended and the fluorescence intensity increases. The oxidation behavior of the p-aminophenol moiety receptor group is related to the hydroquinone/quinone system which is shown in part (b) of figure 3.6. The mechanism of the oxidation of probe **21**, especially of the p-anisidine moiety is unknown. A possible theory is a one-electron oxidation by the generation of a radical cation as described by Simon et al. [134].
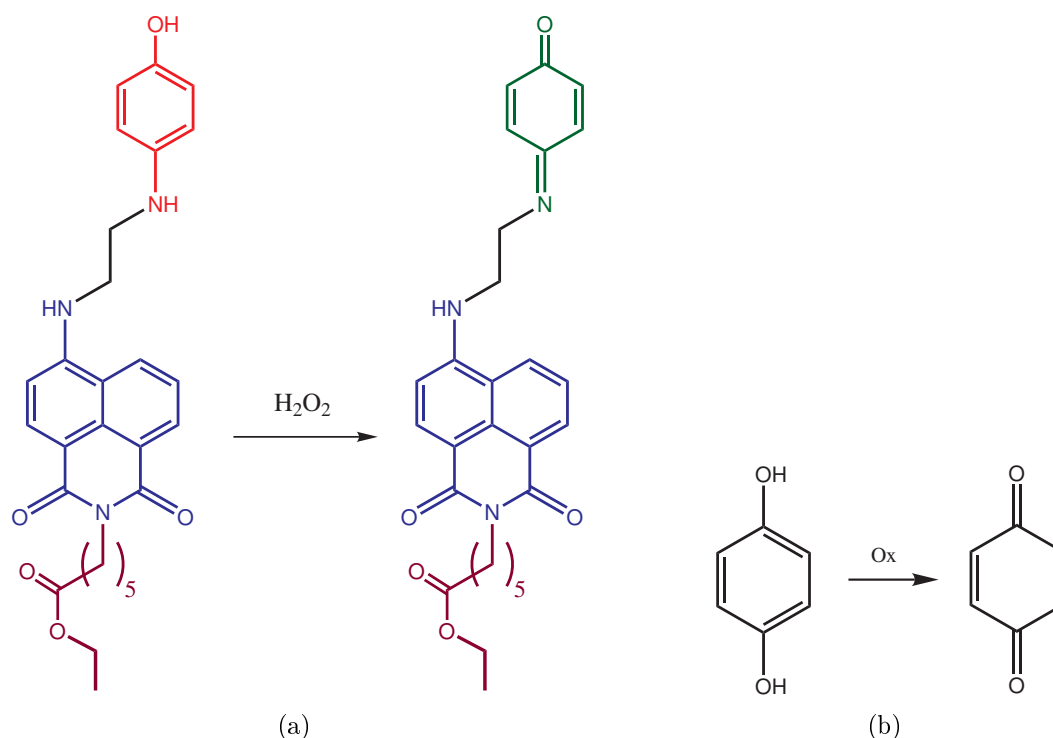
Figure 3.6: (a) Structure of probe **26** (left) for sensing hydrogen peroxide as well as of probe **26-oxidized** (right); fluorophore, spacer, receptor, analyte-bound receptor; (b) principle of the related hydroquinone/quinone system

3.1.3 Preparation of probe 21

Probe **21** is obtained in a four step synthesis (see figure 3.7). P-Anisidine and N-(2-bromoethyl)-phthalimide as cheap and easily affordable starting materials are reacted to give compound **19**. The phthalimide moiety of **19** is cleaved by the treatment with hydrazine monohydrate in boiling ethanol to yield the primary amine **20**. The substitution of the chloro group of compound **3** (synthesis described in 2.2.4) by the amino group of **20** finally yields product **21**. The acid moiety of the probe is made amino-reactive in order to attache the probe to a polymeric support containing amino groups. Therefore, compound **21** is converted into its N-hydroxysuccinimidyl ester **21-NHS** using NHS and DCC in dry DMSO at room temperature. The in-situ prepared solution is used directly and the activated compound can be stored at -18°C at least for one week.
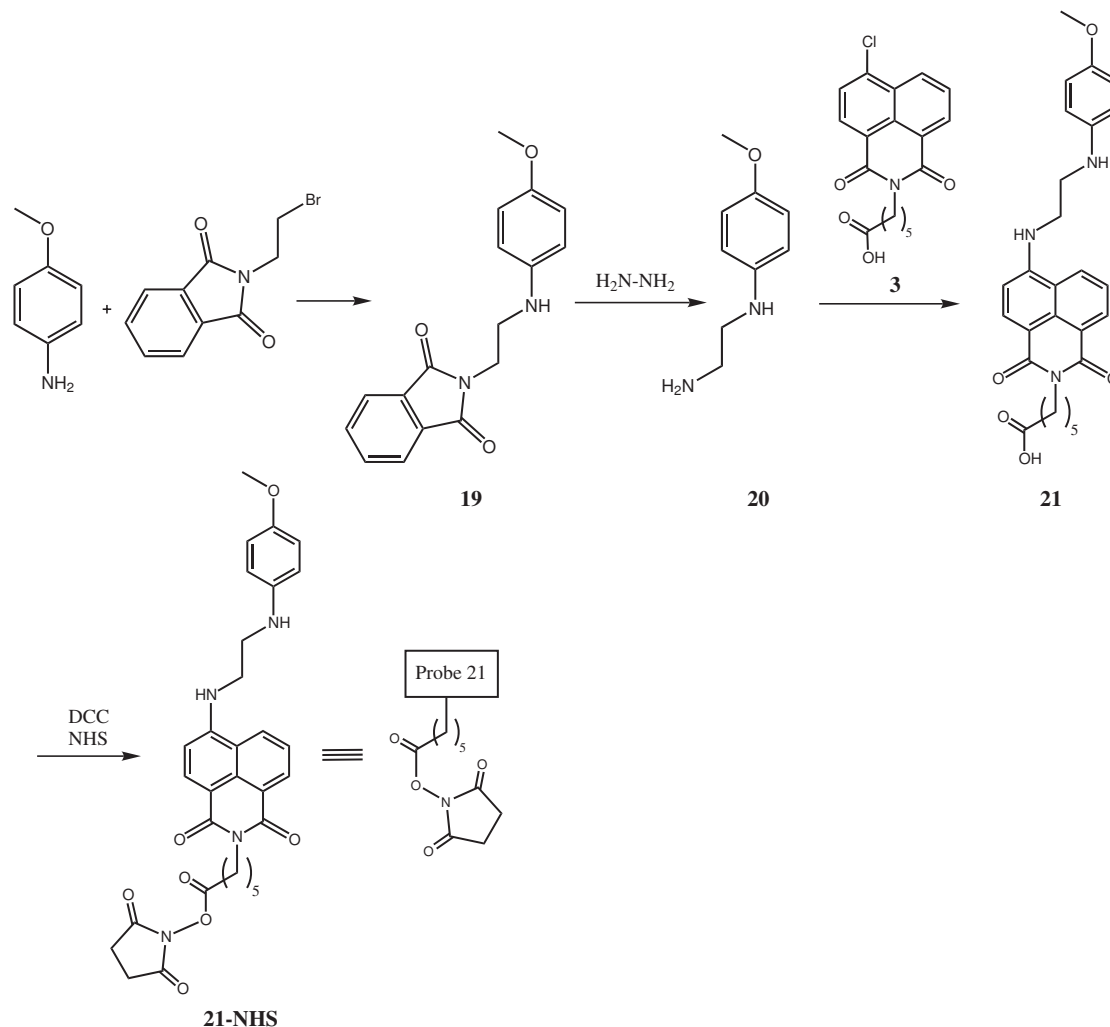
Figure 3.7: Synthetic pathway to probe **21** and its activation (probe **21-NHS**)

3.1.4 Properties of probe 21

Spectroscopic properties

The spectroscopic properties of probe **21** are related to those of VIS-labels **2** and **5** (presented in section 2.2) due to the 1,8-naphthalimide moiety (a common fluorophore). The absorption of **21** peaks at 455 nm in phosphate buffer solution (pH 8, 50 mM). The molar absorption coefficient ε amounts to $6.0 \cdot 10^3 \; \frac{L}{mol \cdot cm}$ which is as low as the ε of label **2** ($6.9 \cdot 10^3 \; \frac{L}{mol \cdot cm}$). Compound **21** exhibits a yellow fluorescence in aqueous solutions with an emission maximum at 536 nm. The large Stokes' shift of 81 nm makes it easier to distinguish between the exciting and emitting light which is particularly important to reduce interferences caused

by background fluorescence and scattered light. The normalized absorption and emission spectra of probe **21** are shown in figure 3.8.
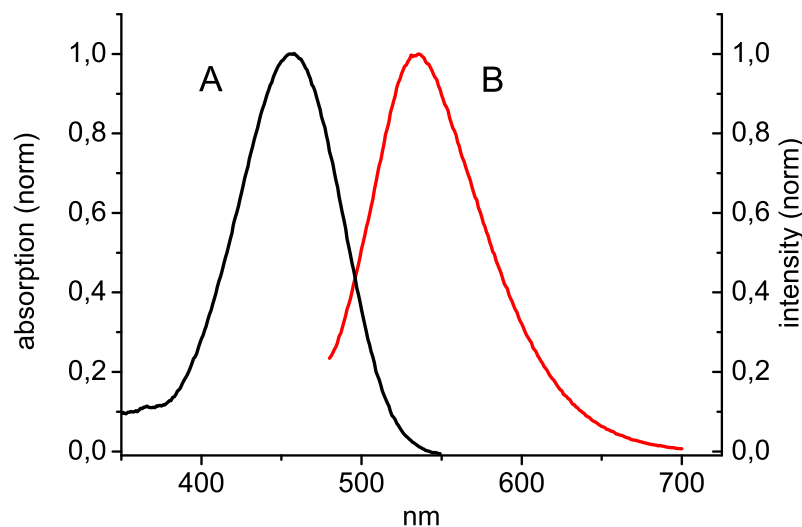
Figure 3.8: Normalized absorption spectrum (A) versus normalized emission spectrum (B) of probe **21** in phosphate buffer solution (pH 8, 50 mM)

3.1.5 Applications of probe 21

In this section the potential of compound **21** as a capable fluorescent PET-probe for hydrogen peroxide is proven. Therefore, the fluorescence response of the probe in terms of various analyte concentrations, ranging from 10 μM to 1 mM, is tested. Furthermore, probe **21** is covalently attached to a polymeric support (O-(2-aminoethyl)-cellulose) to generate a sensor device in the future.

PET-probe for sensing hydrogen peroxide

The ability of probe **21** for hydrogen peroxide detection is tested in this section. Figure 3.9 illustrates the first experiment in which a defined concentration of the analyte ($c_{H_2O_2}$ = 1 mM) is added to a solution of **21** ($c_{probe-21}$ = 10 μM) in phoshate buffer solution (pH 8, 10 mM) at 25°C. Part **(a)** of figure 3.9 shows the emission spectra of probe **21** and the increase of the fluorescence intensity within 30 minutes after the addition of H_2O_2. Hence, the interaction between the receptor group (p-anisidine moiety) and the analyte as well as the ability of compound **21** to sens H_2O_2 is proven. Part **(b)** of figure 3.9 shows a time course experiment clarifying

the time-dependent change of the fluorescence intensity. After the addition of H_2O_2 a linear increase of the fluorescence intensity (curve **A**) denotes the early stages of the reaction. This linear increase ends at about 500 s (8 min) and the reaction stops after 1500 s (25 min) where the intensity does not rise anymore. Curve **B** shows the growth of the signal of a blank sample containing only probe **21** in buffer solution. Hence, a continuously increase of the fluorescence intensity is observed. This behavior of a blank sample is also monitored by Soh et al. for the DPPEA-HC H_2O_2-probe [130]. Additionally, the time course experiment illustrates that photobleaching can be easily observed after 1500 s (25 min) and it occurs both for blank **B** and the sample **A**.

(a)   (b)
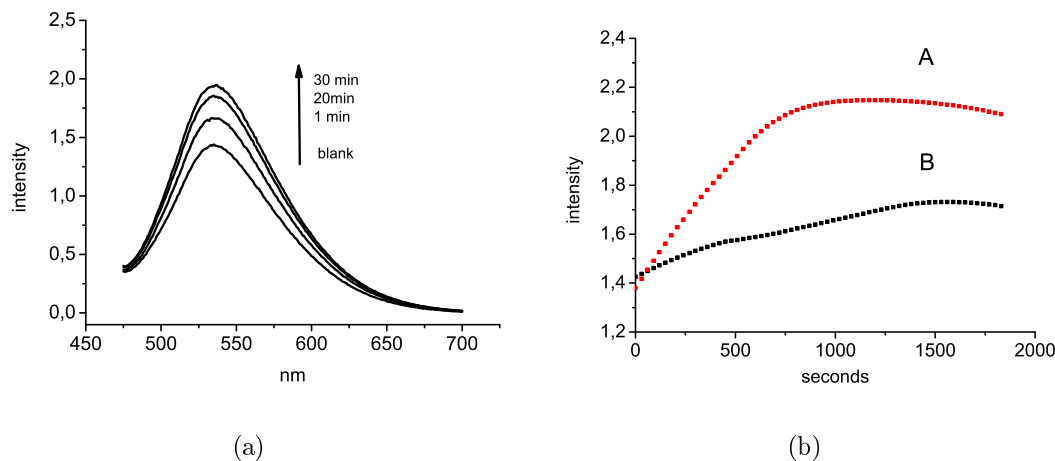
Figure 3.9: (a) Emission spectra of probe **21** (c = 10 μM) with increase of fluorescence intensity after addition of H_2O_2 (c = 1 mM); (b) time course of fluorescence intensity at 25°C in phoshate buffer solution (pH 8, 10 mM): **A** after addition of H_2O_2 (c = 1 mM) and **B** blank sample (excitation at 450 nm, emission at 530 nm)

The second experiment deals with the development of an appropriate calibration curve for H_2O_2. Therefore, the fluorescence intensity of probe **21** is measured in the presence of various concentrations of H_2O_2 ranging from 10 μM to 1 mM. The measurements are carried out in phosphate buffer solution of pH 8 (10 mM) guaranteeing the deprotonation of the amino group in a slightly alkaline medium. Hence, the protonation of the receptor can be excluded which would otherwise enhance the background signal of the analyte-free probe. The temperature is constantly kept at 25°C and the measurements of the different concentrations are conducted after 30 minutes of reaction time each. A time delay assures a fluorescent measurement at its maximum (depicted in figure 3.9 part (**b**)) and therefore a maximum of sensitivity. This is especially important at low analyte concentra-

tions. A feasible fluorescent measurement can also be performed after 600 s (10 min). This time delay is more expedient for an analytical assay. Figure 3.10 shows two calibration curves of probe **21** for hydrogen peroxide. They are established by five point calibrations of the relative fluorescence intensity ($\frac{I}{I_0}$). The concentrations of H_2O_2 amount to 10 μM, 20 μM, 50 μM, 250 μM or 500 μM and 1000 μM whereas the concentration of probe **21** is either 10 μM (curve **A**) or 5 μM (curve **B**). The calibration curves rise exponentially and they are fitted by Origin with a coefficient of determination (R^2) of 0.9 each. As can be seen in figure 3.10 probe **21** is appropriate for H_2O_2 sensing in the μM range. Additionally, the two calibration curves **A** and **B** yield that a probe concentration of 10 μM should be recommended for analytical applications. In comparison to $c_{(probe-21)} = 5$ μM the increase of $\frac{I}{I_0}$ is much higher and a change of the fluorescence intensity at $c_{(H_2O_2)} = 10$ μM is not observed any longer at $c_{(probe-21)} = 5$ μM.
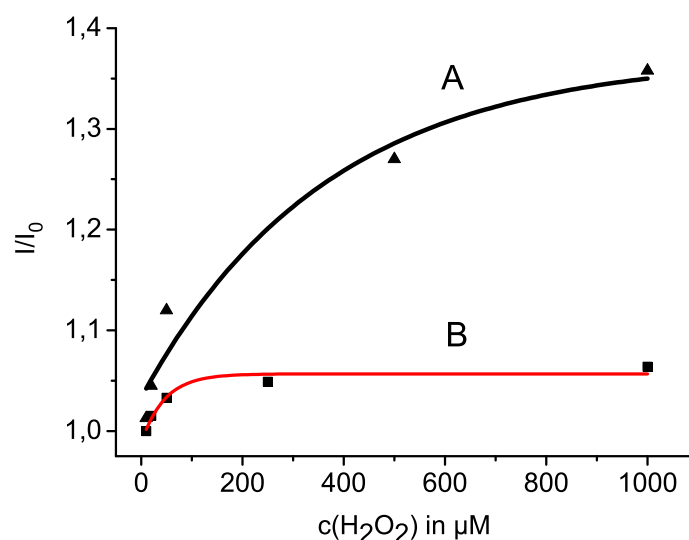
Figure 3.10: Relative fluorescence intensity ($\frac{I}{I_0}$) of probe **21** (**A:** $c_{(probe-21)} = 10$ μM; **B:** $c_{(probe-21)} = 5$ μM) in the presence of H_2O_2 of various concentrations after 30 min

Covalent attachment to cellulose

Probe **21** is covalently attached to amino-modified cellulose in order to develop a H_2O_2-sensor. This tagged polymer can be spread on a foil support e.g. polyester in order to generate a sensor stripe [135]. In continuous application like flow-through

cells the probe is protected from washing-off due to its covalent attachment. In this thesis only the attachment to a polymeric support is performed. Therefore, probe **21-NHS** (preparation described in 3.1.3) is added to an ethanolic suspension of O-(2-aminoethyl)-cellulose. The reaction is carried out over night and the labeled polymer is collected by centrifugation. Several washing steps with ethanol are necessary to remove the unbound probe. A blank sample is prepared simultaneously by combining non-activated probe with the amino-modified cellulose. After the centrifugation/washing steps the blank sample shows almost no color whereas the probe-bound cellulose is strongly colored. The procedure is derived from labeling amino-modified silica particles (see 2.2.3).
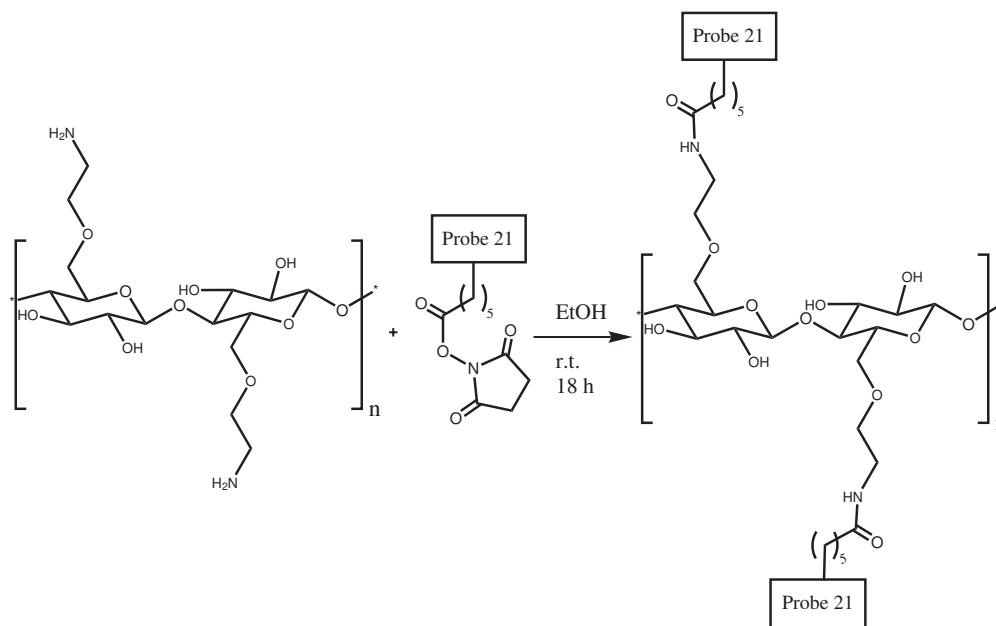
Figure 3.11: Covalent attachment of probe **21-NHS** to O-(2-aminoethyl)-cellulose as polymeric support

3.1.6 Preparation of probe 26

The preparation of probe **26** is carried out in five synthetic steps (see figure 3.12) starting by the esterification of compound **3** (synthesis described in 2.2.4) with ethanol to yield **22**. Compound **23** is obtained by the substitution of the chloro moiety of the ester treating it with monoethanolamine. The hydroxy group of **22** is replaced by a chloro moiety in order to generate an appropriate leaving group (compound **24**). Therefore, **23** reacts with triphenylphosphine and CCl_4 in acetonitrile. In the last step p-aminophenol which is protected as TMS-ether **25** is

introduced yielding probe **26**. The cleavage of the protecting group occurs during the reaction/purification of the last step.
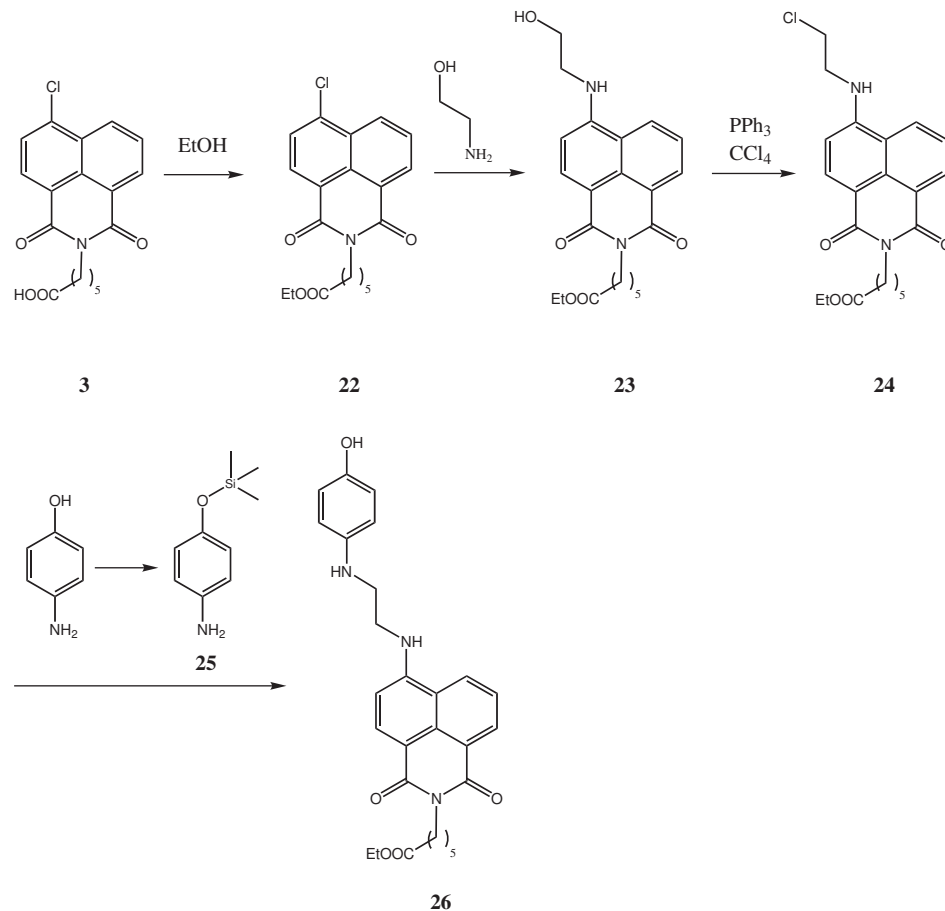
Figure 3.12: Synthetic pathway to probe **26**

3.1.7   Properties of probe 26

Spectroscopic properties

The spectroscopic properties of probe **26** are, like those of **21** related to the VIS-labels **2** and **5** (presented in section 2.2). The absorption maximum of **26** peaks at 439 nm and its emission maximum is settled at 543 nm (yellow fluorescence) in phosphate buffer solution (pH 8, 50 mM). The molar absorption coefficient amounts to $5.8 \cdot 10^3 \ \frac{L}{mol \cdot cm}$) which is almost identical to probe **21** ($6.0 \cdot 10^3 \ \frac{L}{mol \cdot cm}$). The large Stokes' shift of **26** (104 nm) facilitates the separation of exciting and

emitting light reducing the interferences caused by background fluorescence and scattered light.

3.1.8   Applications of probe 26

In this section, the capability of compound **26** as valuable fluorescent PET-probe for hydrogen peroxide is proven. Therefore, the fluorescence response of the probe depending on various analyte concentrations, ranging from 10 μM to 1 mM, is tested.

PET-probe for sensing hydrogen peroxide

The ability of probe **26** for sensing H_2O_2 is tested in a likewise manner as of probe **21**. In the first experiment compound **26** ($c_{probe-26}$ = 1 μM) solved in phosphate buffer solution (pH 8, 10 mM) is treated with hydrogen peroxide ($c_{H_2O_2}$ = 1 mM) at a constant temperature of 25°C. Figure 3.13 shows the rise of the fluorescence intensity whithin 30 min (part **(a)**) and the increase of the fluorescence signal at λ_{em} = 530 nm (λ_{exc} = 450 nm) depending on time (part **(b)**). This measurement yields that after 20 minutes there is hardly any change of the signal thus indicating the end of the reaction.

(a)   (b)
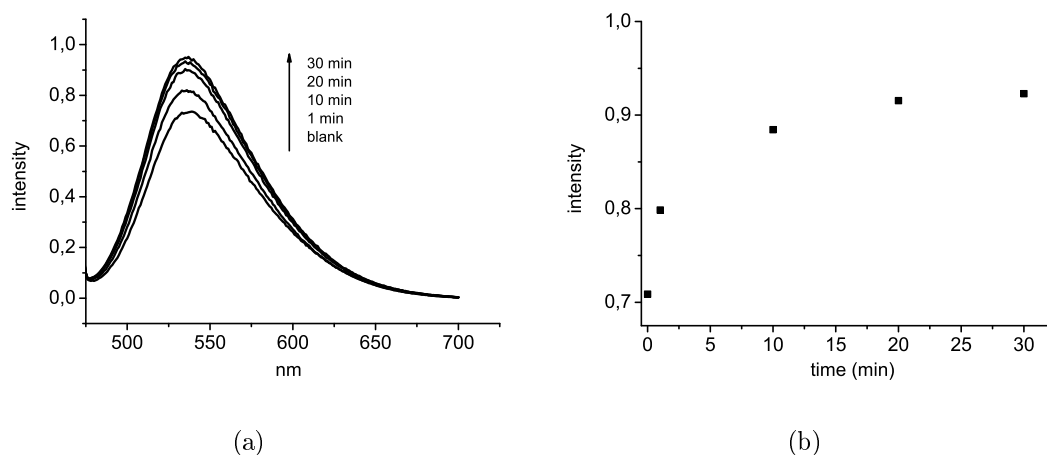
Figure 3.13: (a) Emission spectra of probe **26** (c = 1 μM) and the increase of fluorescence intensity after addition of H_2O_2 (c = 1 mM); (b) time-dependent fluorescence intensity in phosphate buffer (pH 8, 10 mM) after the addition of H_2O_2 (c = 1 mM) (excitation at 450 nm, emission at 530 nm)

The challenge of the second experiment is the development of a calibration curve for H_2O_2. Fluorescence intensity of probe **26** is measured in the presence of

various concentrations of H_2O_2 ranging from 10 μM to 1 mM in the same way as described in section 3.1.5 in phosphate buffer solution (pH 7, 10 mM) and 25°C. After 30 minutes of reaction time the probe is excited at 450 nm and emission at 530 nm is measured. The time delay ensures a fluorescent measurement at its maximum (depicted in figure 3.13 part (**b**)) as well as a maximum of sensitivity. A feasible fluorescent measurement can also be performed after 600 s (10 min) likewise to probe **21** in terms of analytical applications. Figure 3.14 illustrates a four point calibration of the relative fluorescence intensity ($\frac{I}{I_0}$) for probe **26**. The concentrations of H_2O_2 are 10 μM, 20 μM, 100 μM and 1000 μM whereas the concentration of probe **26** amouts 5 μM. The calibration curve rises exponentially and is fitted by Origin with a coefficient of determination (R^2) of 0.97. This measurement was performed by Dominik Grögel within his PhD work.
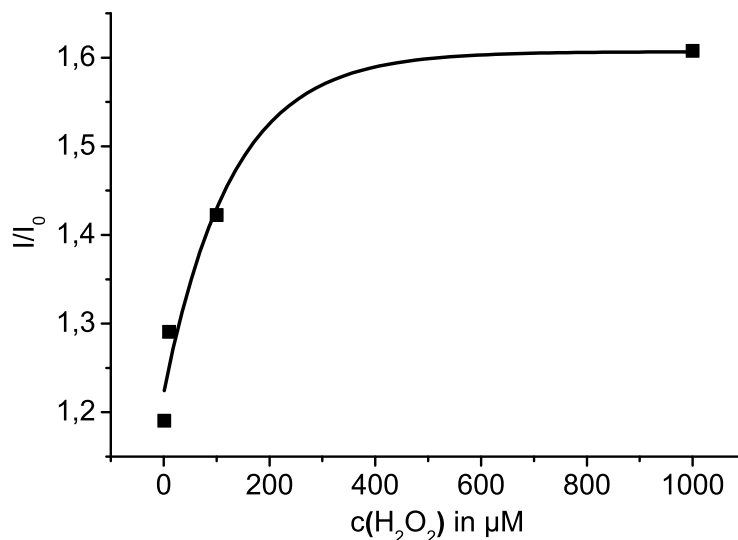
Figure 3.14: Relative fluorescence intensity ($\frac{I}{I_0}$) of probe **26** after 30 min (c = 5 μM) in presence of H_2O_2 at various concentrations.

3.1.9 Summary and evaluation of the H_2O_2 probes

The probes **21** and **26** are evaluated regarding the complexity of their synthesis, their spectral properties and their qualification as probes for sensing hydrogen peroxide. Additionally, the spectral properties of the probes are summerized in table 3.2.

Evaluation of probe 21

Probe **21** is based on the 1,8-napththalimide as highly photo- and chemoresistive yellow daylight fluorophore. The preparation is carried out in few synthetic steps with good to excellent yields. The purification of all steps is accomplished by recrystallisation which saves time and money compared to column chromatography. The emission maximum is comparable to that of fluorescein, but the Stokes' shift is considerably longer than that of fluorescein (70 nm vs. 23 nm). Probe **21** can be photoexcited with blue or purple diode lasers which have become very attractive light sources owing to their small size, longevity, and low power consumption. One drawback is the low molar absorption of only $6.0 \cdot 10^3 \frac{L}{mol \cdot cm}$. This problem can be solved by attaching probe **21** to a polymeric support (shown in 3.1.5) in order to enhance the concentration of probe molecules and to develop a sensor device. The p-anisidine moiety emerges as a good receptor for H_2O_2 in a PET-probe which diminish the fluorescence intensity of the fluorophore depending on the analyte concentration. In summary, probe **21** is appropriate for H_2O_2 sensing in the μM range, operating in the visible part of the electromagnetic spectrum and can be covalently attached to polymeric supports.

Evaluation of probe 26

Probe **26** is derived from the same yellow daylight chromophore as probe **21**. Hence, the spectroscopic properties like photo- and chemostability, the location of the absorption and emission maxima as well as the molar absorption are comparable. The only deviation is a receptor moiety in the form of a hydroxy group instead of a methoxy group resulting in nearly the same sensitivity for H_2O_2. The preparation of probe **26**, however, requires five to six (free acid) synthetic steps as opposed to four steps of compound **21**. Especially the introduction of the receptor group (p-aminophenol) is of low yield (only 6%) and requires a time-consuming purification by column chromatography. Furthermore, a stock solution of probe **26** in DMSO can only be stored for a short periode of time (about 10 h) before it will no longer respond to H_2O_2.

Spectral properties of probes 21 and 26
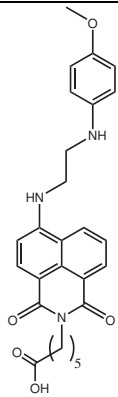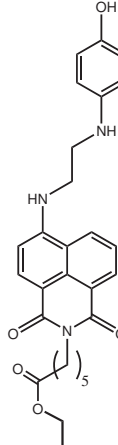
compound	formula	λ_{abs} (ε)	λ_{em}
probe 21		455 nm $(6.0 \cdot 10^3 \; \frac{L}{mol \cdot cm})$	536 nm
probe 26		439 nm $(5.8 \cdot 10^3 \; \frac{L}{mol \cdot cm})$	543 nm

Table 3.2: Spectroscopic properties of probes **21** and **26**

Chapter 4

Experimental Part

4.1 General Remarks

4.1.1 Reagents and Buffers

Reagents

All reagents and solvents are supplied by Sigma-Aldrich (www.sigmaaldrich.com) and Merck (www.merck.de). They are used without further purification if not stated. Deuterated solvents like dimethyl sulfoxide-d_6 are obtained from Deutero GmbH (www.deutero.de). Tetramethylsilane (TMS) is used as an external standard for NMR measurements.

Buffers

Buffers which are prepared during this work.

1. Bicarbonate Buffer (BCB) of pH 8.3 or 8.4, 50 mM:
   2.1 g of sodium hydrogencarbonate is dissolved in 500 mL of doubly distilled water. A very small amount of sodium azide is added to avoid a fungus infest.

2. Phosphate Buffer (PB) of pH 7.2, 100 mM:
   17.8 g of $Na_2HPO_4 \cdot 2\,H_2O$ is dissolved in 1000 mL of doubly distilled water. A very small amount of sodium azide is added to avoid a fungus infest.

3. Phosphate Buffer (PB) of pH 7.0 or 8.0, 10 mM:
   1.78 g of $Na_2HPO_4 \cdot 2\,H_2O$ is dissolved in 1000 mL of doubly distilled water. A very small amount of sodium azide is added to avoid a fungus infest.

The final pH value is adjusted with 0.1 N HCl and 0.1 N NaOH solution [136].

4.1.2   Chromatography

Thin-layer (TLC) and liquid chromatography (LC)

TLC is used to monitor the progress of the syntheses as well as for overcoming various separation problems, thus silica gel 60 F_{254} aluminium sheets are purchased from Merck. Column chromatography is performed for purifying organic compounds using silica gel 60 provided by Merck, too. The dimension of the column are:

length: from 36 cm to 66 cm

diameter: 3.5 cm

Size-exclusion chromatography (SEC)

The conjugates (tagged proteins and particles) are purified by SEC using Sephadex G-25 or Sephadex LH-20 purchased from Pharmacia AB Biotechnology. The length of the column is 23 cm with a diameter of 2.6 cm. Phosphate buffer solution (Sephadex G-25) or ethanol (Sephadex LH-20) serves as eluents.

Capillary electrophoresis CE

A self-made system equipped with a HCN 35-35000 power supply (www.fug-elektronik.de) is used for capillary electrophoresis along a fluorescence detector (Argos 250B, from Flux Instruments, Pfaffenhofen a.d. Glonn, Germany). 50 μm fused silica capillaries are obtained from Polymicro (www.polymicro.com).

Microchip capillary electrophoresis MCE

Microchip electrophoresis is performed on a microscope-based instrument as described in [137] with the exception that all data are acquired and processed using an INT-9 analog-to-digital converter along with Clarity Chromatography Station software (www.dataapex.com). The Borofloat^{TM} microchips are obtained from Micronit (www.micronit.com).

High-Performance Liquid Chromatography HPLC

All HPLC studies are performed at room temperature, using a Kontron 422 solvent pump and a Kontron 432 UV detector set at 406 nm. Chromatographic retention data are recorded with Kontron Data software (420-MT2, version 3.90, 1992, www.kontron.de). Sample introduction is undertaken manually with a 20 μL loop. All experiments are performed with flow rates of 1 mL/min and a mobile phase

composed of acetonitrile and water 90:10 (v/v). Additionally, TFA is added to the mobile phase (0.1 %, v/v). A LiChrospher 100 CH-18/2 analytical column is used as stationary phase.

4.1.3 Spectroscopy

^{1}H-NMR and ^{13}C-NMR spectra are acquired on an Advance 300 spectrometer (www.bruker-biospin.com). Absorption spectra are recorded on either a Cary 50 Biospectrophotometer (www.varianic.com) or a Jasco V-650 (www.jasco.co.uk). Emission spectra are measured using a Jasco FP-6200 spectrofluorometer or an Aminco Bowman luminescence spectrometer (www.polytec.de). A PDL 800-B picosecond pulsed diode laser ($\lambda_{em} = 375$ nm) from PicoQuant (www.picoquant.com) is used for laser excitation. Mass spectra are collected on either a ThermoQuest Finnigan TSQ 7000 for electrospray ionisation (www.thermo.com) or a LCMS-2010 (www.shimadzu.com) with a self-made nanospray ionisation probe using graphite coated nanospray needles (www.proxeon.com). High resolution Mass Spectra as well as the MALDI-TOF are measured using the Central Analytical Department at the University of Regensburg, Germany. Attenuated total reflection (ATR) IR spectroscopy is carried out on a Excalibur FTS 3000 spectrometer (from Biorad; www.bio-rad.com), equipped with a Golden Gate Diamond Single Reflection ATR-System (from Specac: www.specac.com).

4.1.4 Determination of the molar absorption coefficients and quantum yields

The quality of a fluorophore (color strength and brightness) depends on both molar absorption and on quantum yield [5]. Hence, the determination of these spectral parameters is essential for the characterisation of new dyes and labels.

Molar absorption coefficient

The molar absorption coefficient $\varepsilon(\lambda)$ is derived from **Lambert-Beer law** (see equation 4.1).

$$A = \varepsilon(\lambda) \cdot c \cdot d \tag{4.1}$$

This law is only valid if the concentration c $(\frac{mol}{L})$ of the analyte is very low. The determination of $\varepsilon(\lambda)$ requires very pure and dry compounds of exact quantities dissolved in appropriate solvents (mainly double destilled water) for a stock solution. Three different concentrations are prepared to minimize the error of measurement. This method is called "dry weight determination" according to Hong et al. [138, 139].

Quantum yield

The quantum yield (QY) is the emission effenciency of a given fluorophore and defined by equation 4.2 [140]:

$$QY = \frac{photons\ emitted}{photons\ absorbed} \tag{4.2}$$

It is measured relatively to a reference which is a fluorophore of known quantum yield. The reference for labels and probes based on the 1,8-naphthalimide is coumarin 6, that for the red or the blue phenoxazine is Nile Red or Nile Blue respectively. The QY is determined using equation 4.3 [141, 142]:

$$\phi_F = \phi_{Ref} \cdot \frac{A_{Ref} \cdot I_F \cdot n_F^2}{A_F \cdot I_{Ref} \cdot n_{Ref}^2} \tag{4.3}$$

Abbreviations

ϕ_F = unknown quantum yield of the fluorophore

ϕ_{Ref} = quantum yield of the reference

A_F = absorbance of the fluorophore at the excitation wavelength

A_{Ref} = absorbance of the reference at the excitation wavelength

I_F = area under the corrected emission spectra of the fluorophore

I_{Ref} = area under the corrected emission spectra of the reference

$n_{F/Ref}$ = refractive indices of the solvents of the fluorophore/reference

4.2 Synthesis and Application

4.2.1 Synthesis of label 2

Preparation of 6-(6-amino-1,3-dioxo-1H,3H-benzo[de]isoquinolin-2-yl)-hexanoic acid (1)

4-Amino-1,8-naphthalic anhydride (50 mg, 0.23 mmol) and 6-amino caproic acid (31 mg, 0.23 mmol) are dissolved in 10 mL of dry dimethylformamide. N,N-diisopropyl-ethylamine (0.08 mL, 0.46 mmol) is added as base, and $Zn(OAc)_2$ is used in catalytic quantity (5 mg). Water is excluded by adding a 4-Å molecular sieve. The reaction mixture is kept at 90°C for 48 h. The solvent is evaporated,
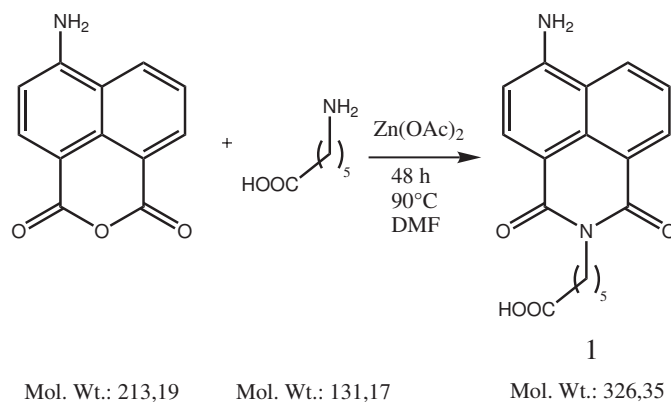
Figure 4.1: Preparation of compound **1**

and the crude yellow compound **1** is purified by column chromatography (silica gel 60/ethyl acetate) to yield a yellow solid (62 mg, 62%; see figure 4.1). PI-EI-MS: [M$^{+\cdot}$] (calculated): 325.1267 Da; [M$^{+\cdot}$] (found): 325.1260; ^{1}H-NMR (DMSO-d$_6$): δ= 8.60 (d, 1 H), 8.42 (d, 1 H), 8.18 (d, 1 H), 7.65 (m, 1 H), 7.44 (s, 2 H), 6.84 (d, 1 H), 3.98 (t, 2 H), 2.2 (t, 2H), 1.7-1.5 (m, 4 H), 1.4-1.23 (m, 2H). IR (ATR-System): ν = 3412 cm^{-1}, 3362 cm^{-1}, 3255 cm^{-1}, 2927 cm^{-1}, 2825 cm^{-1}, 1660 cm^{-1}, 1629 cm^{-1}, 1569 cm^{-1}, 1530 cm^{-1}, 1377 cm^{-1}. m.p: 209 - 210°C.

In-situ preparation of 6-(6-amino-1,3-dioxo-1H,3H-benzo[de]isoquinolin 2-yl)-hexanoic acid 2,5-dioxo-pyrrolidin-1-yl ester (2)
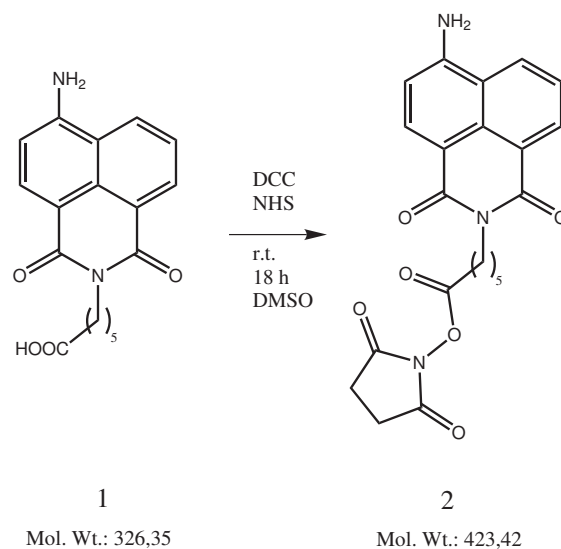

Figure 4.2: Preparation of compound **2**

1 mg (3 μmol) of compound **1**, 0.53 mg (4.5 μmol) of NHS and 0.95 mg (4.5 μmol) of DCC are dissolved in 200 μL of dry DMSO. The mixture is stirred for 18 h at room temperature and is used for labeling without further purification. Thin layer chromatography (silica gel 60; ethyl acetate and ethanol, 9/1) is applied to monitor the formation of the NHS-ester over time (see figure 4.2).

4.2.2   Labeling experiments with label 2

Labeling of amino acids

1 mg of L-lysine, L-serine, L-glycine, L-glutamic acid, L-aspartic acid are dissolved in 1 mL of bicarbonate buffer (pH 8.4, 50 mM) and cooled down to 4°C. 4 μL of activated dye is added to each 45 μL of analyte solution and stirred for 1 h at room temperature. The reaction progress is checked by thin layer chromatography (silica gel 60, ethyl acetate and ethanol: 9/1). All solutions are shortly centrifuged to remove particles (see 4.2.3) before being diluted to lower concentrations suitable to electrophoresis.

Labeling of BSA

5 mg of bovine serum albumin is dissolved in 1 mL of a 50 mM bicarbonate buffer solution of pH 8.4. Then, 5 μL of the label **2** is added. The mixture is stirred for 12 - 15 h. Purification and separation, respectively is carried out both on MCE and SEC (see 4.2.3). The MALDI-TOF mass spectrum (using sinapic acid as the matrix) shows a broad peak between 66,260 Da and 67,600 Da, with a maximum at 66,790 Da. Obviously peak broadening is the result of multiple labeling of BSA by label **2**.

Labeling of amino-modified silica nanoparticles

Silica nanopowder (amorphous-SiO_2) is purchased by Nanostructure & Amorphous Materials Inc. (www.nanoamor.com) and used as received. 1 g of the silica powder is dispersed in 100 mL of toluene by sonification and stirring. The solution is heated to reflux thus 1 mL aminopropyltriethoxysilane (APTES) is added drop-wise. Refluxation is continued for 5 h. Afterwards, the particles are collected by centrifugation (6000 rpm, 10 min.), washed with ethanol (3 times) and dried at 50°C. Dye **1** (2.6 mg, 8.1 μmol, 1 eq.), DCC (3.3 mg, 16.2 μmol, 2 eq.) and NHS (1.9 mg, 16.2 μmol, 2 eq.) are stirred in 100 μL DMSO over night. 5 mg of the amino-modified silica nanoparticles are suspended in 1 mL of ethanol and 5 μL of the label is added. The reaction is carried out over night and the labeled particles are collected by centrifugation (6000 rpm, 10 min.) and washed with ethanol (3 times). In parallel a blank sample is prepared by combining 5 mg of unmodified

silica nanoparticles with 5 μL of mixture with the activated fluorophore (following the same protocol). After the centrifugation/washing steps the blank sample shows almost no color whereas the amino-labeled particles are intensively colored.

4.2.3 Label 2-analyte conjugate in separation experiments

Separation of labeled amino acids by CE

The labeled amino acids are introduced in a 64 cm ($\varnothing = 50$ μm) long fused silica capillary by electrokinetic injection (7 s, 5 kV, 10 μA). Separation (25 kV, 68 μA) is performed in phosphate buffer (pH 7, 50 mM) as it provides the best separation efficiency for the test mixture. Peak assignments are performed using the standard addition procedure. The detector contains a standard filter set which is originally developed for fluorescein tagged probes ($\lambda_{exc} = 450$ - 480 nm, $\lambda_{em} > 495$ nm).

Separation of labeled BSA by MCE

The Borofloat^{TM} microchips with a standard cross layout are of the following dimensions: injection channel 8 mm, separation channel 85 mm, height 30 μm, width 50 μm. Conditioning of the chip is performed by rinsing for 3 min with 1 M NaOH and 1 min with water before the introduction of separation buffer which contains 0.01% (w/w) hydroxypropyl methylcellulose (HPMC) as dynamic coating. Pinched injection is applied for 35 s. When sampling BSA solutions and separating it from free label, the electrical potentials are applied in the following order: sample inlet (A), buffer inlet (B), sample outlet (C), buffer outlet (D). The injection potentials are 493 (A), 500 (B), 0 (C) and 1330 (D) V, and the potentials for the separation are 1.6 (A), 2.0 (B), 1.5 (C) and 0 (D) kV (see figure 4.3).
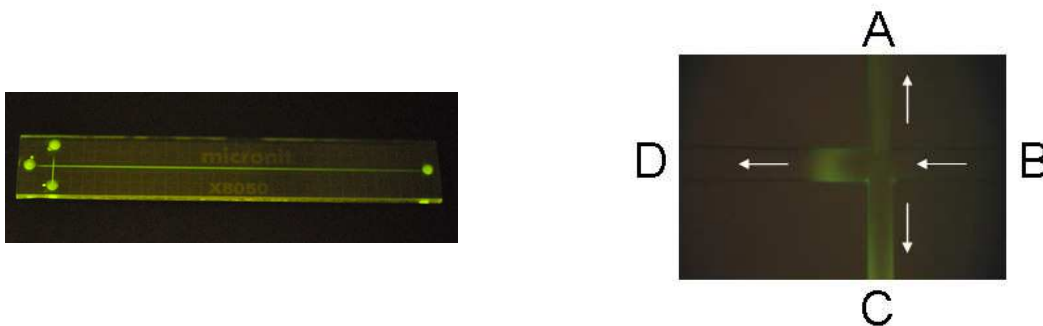
Figure 4.3: (left) Standard cross layout of borofloat microchips containing dye **1**; (right) Schematic view of the microchip with four ports (A, B, C, D)

Separation of labeled BSA by SEC

The conjugate is separated from the untagged protein as well as from the non-reacted label using Sepadex G-25 as stationary phase and phosphate buffer solution (pH 7.2, 50 mM) as the eluent. The extract of the dye-protein conjugate has a yellow color.

4.2.4 Synthesis of label 5

Preparation of 6-(6-Chloro-1,3-dioxo-1H,3H-benzo[de]isoquinolin-2-yl)-hexanoic acid (3)
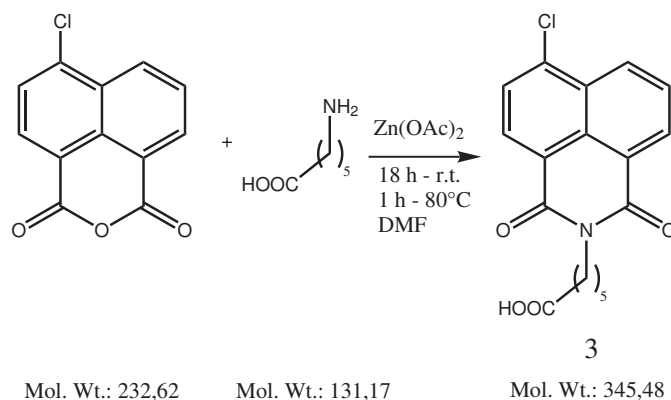
Figure 4.4: Preparation of compound **3**

A yellow suspension of 2.5 g (0.01 mol) 4-chloro-1,8-naphthalic anhydride and 1.7 g (0.01 mol) of 6-aminocaproic acid in 70 mL DMF is stirred at r.t. for 18 hours and then heated to 80°C for 1 hour. Zinc acetate is added as a catalyst. The reaction mixture is then poured into 350 mL of water and the resulting pale yellow precipitate is filtered off and washed with cold water. The crude product is dissolved in 100 mL of boiling ethanol and filtered hot. The filtrate is left to cool down to room temperature over night [143,144]. The yellow crystals are filtered off and washed with cold ethanol. The wet product **3** is dried in vacuum (see figure 4.4). Yield: 2.5 g (72 %, yellow crystalls); m.p.: 140°C; ^{1}H-NMR (DMSO-d$_6$): δ = 8.6 - 7.5 (m, 5 H), 4.0 (t, 2H), 2.2 (t, 2 H), 1.7 - 1.25 (m, 6 H); ^{13}C-NMR (DMSO-d$_6$): δ = 174.3, 162.7, 162.4, 137.2, 131.3, 130.6, 129.7, 128.3, 128.1, 128.0, 127.4, 122.4, 121.1, 39.5, 33.4, 27.0, 25.9, 24.1; elementary analysis (calaculated): C 62.52 %, H 4.66 %, N 4.05 % (found): C 62.28 %, H 4.61 %, N 3.89 %.

Preparation of 1,3-Dioxo-6-piperidin-1-yl-1H,3H-benzo[de]isoquinolin-2-yl)-hexaonic acid (4)

2 g of **3** (0.0058 mol) and 0.85 mL (0.0086 mol) of piperidine are dissolved in 40 mL of DMF and heated to 90°C for 18 hours. 0.9 g of K_2CO_3 is added as base. The mixture is filtered and poured into 150 mL of water. The solution is acidified to pH 6 and the crude product precipitated. It is filtered off and washed three times (50 mL) with cold water. The wet product is dried over silica gel and purified by recrystallisation in ethanol (see figure 4.5) [145]. Yield: 1.6 g (69 %, yellow crystals) m.p.: 169°C - 170°C; ^{1}H-NMR (CDCl$_3$): δ = 8.56 (dd, 1 H), 8.49 (d, 1 H), 8.38 (dd, 1 H), 7.67 (m, 1 H), 7.17 (d, 1 H), 4.13 (t, 2H), 3.22 (dd, 4 H), 2.36 (t, 2 H), 1.93 - 1.83 (m, 4 H), 1.81 - 1.64 (m, 6 H), 1.55 - 1.41 (m, 2 H); ^{13}C-NMR (CDCl$_3$): δ = 178.9, 164.6, 164.1, 157.3, 132.7, 131.1, 130.6, 129.9, 126.3, 125.4, 123.1, 115.9, 114.7, 54.6, 39.9, 33.8, 27.8, 26.6, 26.2, 24.4, 24.3; elementary analysis (calaculated): C 70.03 %, H 6.64 %, N 7.10 % (found): C 70.04 %, H 7.00 %, N 7.08 %.
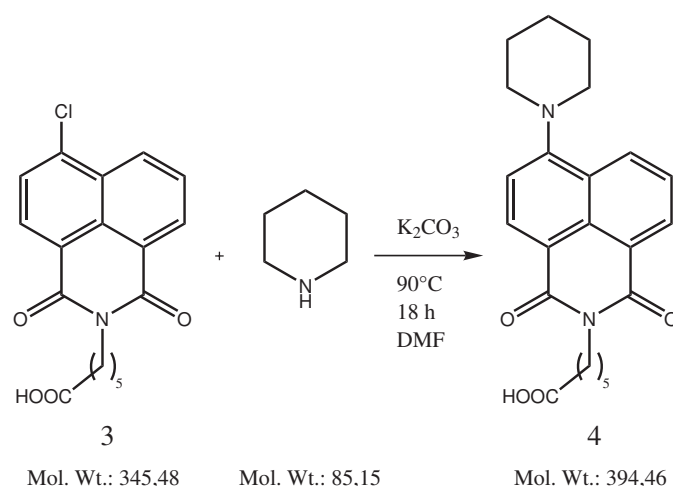
Figure 4.5: Preparation of compound **4**

In-situ preparation of 6-(1,3-Dioxo-6-piperidin-1-yl-1H,3H-benzo[de]isoquinolin-2-yl)-hexanoic acid 2,5-dioxo-pyrrolidin-1-yl ester (5)

2 mg (4 μmol) of compound **4**, 0.7 mg (6 μmol) of NHS and 1.2 mg (6 μmol) of DCC are dissolved in 400 μL of dry DMSO. The mixture is stirred for 18 h at room temperature and used for labeling without further purification. Thin layer chromatography (silica gel 60; ethyl acetate) is applied for monitoring NHS-ester formation (see figure 4.6).
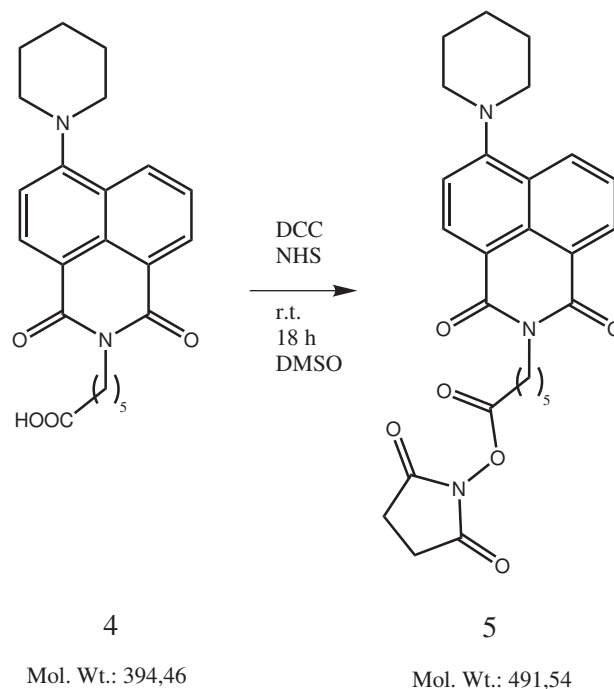
Figure 4.6: Preparation of compound **5**

4.2.5 Labeling experiments with label 5

Labeling of amino acids

1 mg of L-glycine and L-aspartic acid are dissolved in 1 mL of bicarbonate buffer (pH 8.4, 50 mM) and cooled down to 4°C. 5 μL of the activated dye is added to each 200 μL of analyte solution and stirred for 18 h at room temperature. The reaction progress is observed by thin layer chromatography (silica gel 60, butanol/acetic acid: 95/5). The solutions are centrifuged shortly to remove particles before HPLC separation (see 4.2.6).

Labeling of BSA

5 mg of bovine serum albumin is dissolved in 1 mL of a 50 mM bicarbonate buffer solution of pH 8.4. Then, 5 μL of label **5** is added. The mixture is stirred for 12 - 15 h. SEC is used for the purification and separation of the dye-protein conjugate (see 4.2.6).

4.2.6 Label 5-analyte conjugate in separation experiments

Separation of labeled amino acids by HPLC

50 μL of the labeled glycine and the labeled aspartic acid, respectively, are diluted with 200 μL of acetonitrile/water (90/10, v/v) and filtered before being introduced to the HPLC system. A blank sample of dye **4** is measured in order to collect the retention time of the non-reacted and hydrolyzed label. It is prepared in the same manner as label **5** but without any activation steps. All separations are carried out by an isocratic mode using acetonitrile/water (90/10, v/v) with 0.1 % TFA (v/v) as mobile phase. The UV detector is set at 406 nm which is the absorption maximum of dye **4** in water.

Separation of labeled BSA by SEC

The dye-protein conjugate is separated from the untagged protein as well as from the unreacted label using Sepadex G-25 as stationary phase and phosphate buffer solution (pH 7.2, 50 mM) as the eluent. The extract of the dye-protein conjugate possesses a yellow color.

4.2.7 Synthesis of label 9

6-(3,5-Dihydroxyphenoxy)-hexanoic acid ethyl ester (6)
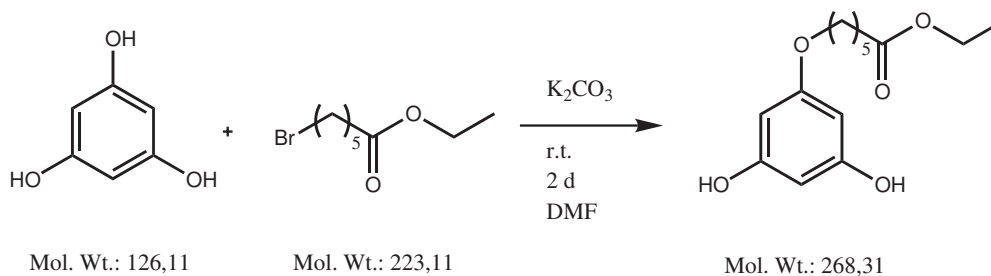
Figure 4.7: Preparation of compound **6**

A mixture of 0.5 g (3.96 mmol) phloroglucinol, 0.7 mL (3.06 mmol) of ethyl-bromohexanoate and 1.1 g (7.9 mmol) of potassium carbonate are stirred in dimethylformamide (20 mL) at room temperature for two days [146]. The mixture is diluted with 150 mL of water and acidified with H_2SO_4 to pH 3 [147]. The reaction mixture is extracted three times with ethyl acetate. The combined organic layers are dried with sodium sulfate. The solvent is evaporated and **6** is

purified by column chromatography (silica gel 60; diethyl ether/petroleum ether: 1/1) to yield a colorless oil (0.32 g, 30 %, see figure 4.7); R_f (silica gel 60; diethyl ether/petroleum ether: 90/10): 0.5; ^{1}H-NMR (CDCl$_3$): δ = 7.0 (s, 2 H), 6.0 (m, 1 H), 5.95 (m, 2 H), 4.12 (q, 2 H, ^{3}J(H,H) = 7.13 Hz), 3.72 (t, 2 H, ^{3}J(H,H) = 6.31 Hz), 2.3 (t, 2 H, ^{3}J(H,H) = 7.41 Hz), 1.75-1.5 (m, 4 H), 1.41-1.29 (m, 2 H), 1.25 (t, 3 H, ^{3}J(H,H) = 7.13 Hz); ^{13}C-NMR (CDCl$_3$): δ = 174.19, 159.89 (1C), 156.49, 94.89, 93.85, 66.70, 59.92, 33.25, 27.61, 24.39, 23.53, 13.07; IR (ATR): ν = 3349 cm^{-1}, 2987 cm^{-1}, 2941 cm^{-1}, 2874 cm^{-1}, 1697 cm^{-1}, 1599 cm^{-1}, 1506 cm^{-1}, 1473 cm^{-1}, 1416 cm^{-1}, 1376 cm^{-1}; HR-MS (EI$^.$-MS): [M$^{+.}$] (calculated): 268.1311, [M$^{+.}$] (found): 268.13086.

6-(7-Dimethylamino-3-oxo-3H-phenoxazin-1-yloxy)-hexanoic acid ethyl ester (7)
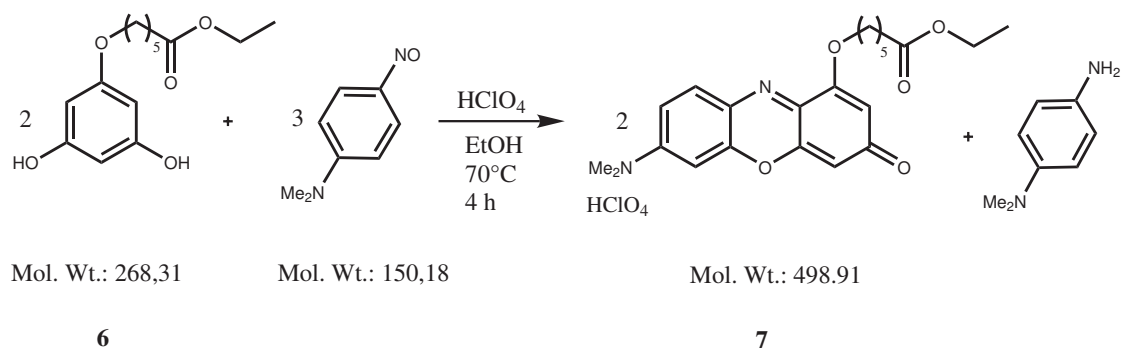
Figure 4.8: Preparation of compound **7**

Compound **6** (0.32 g; 1.19 mmol) and 4-nitroso-N,N-dimetylaniline (0.27 g; 1.79 mmol) are dissolved in ethanol. 0.15 mL (1.79 mmol) of perchloric acid is added and the mixture is heated to 70°C for 4 hours. After 4 hours the hot mixture is filter and remains at room temperature over night for crystallization. The product is yielded as violet crystals (0.20 g, 33 %, see figure 4.8); R_f (silica gel 60; ethyl acetate): 0.46; mp.: 138°C; ^{1}H-NMR (DMSO-d$_6$): δ = 7.84 (d, 1 H, ^{3}J(H,H) = 9.60 Hz), 7.5 (dd, 1 H, ^{3}J(H,H) = 2.74 Hz, 9.60), 7.05 (d, 1 H, ^{3}J(H,H) = 2.74 Hz), 6.53 (d, 1 H, ^{3}J(H,H)=2.19 Hz), 6.49 (d, 1 H, ^{3}J(H,H)=2.19 Hz), 4.16 (t, 2 H, ^{3}J(H,H)=6.31 Hz), 4.04 (q, 2 H, ^{3}J(H,H) = 7.13 Hz), 3.4 (s, 6 H), 2.3 (t, 2 H, ^{3}J(H,H) = 7.41 Hz), 1.92-1.72 (m, 2 H), 1.70-1.54 (m, 2 H), 1.52-1.38 (m, 2 H), 1.17 (t, 3 H, ^{3}J(H,H) = 7.13 Hz); ^{13}C-NMR (CDCl$_3$): 185.84, 173.55, 158.07, 153.76, 149.53, 146.85, 137.1, 132.18, 125.19, 110.09, 107.02, 103.36, 96.37, 69.11, 60.29, 40.4, 34.2, 28.07, 25.51, 24.68, 14.26; IR (ATR): ν = 3160 cm^{-1}, 3091 cm^{-1}, 2944 cm^{-1}, 1710 cm^{-1}, 1643 cm^{-1}, 1602 cm^{-1}, 1566 cm^{-1}, 1536 cm^{-1}, 1507 cm^{-1}, 1480

cm^{-1}; EI$^-$-MS: [M$^{+\cdot}$] (calculated): 398.1842 Da; EI$^-$-MS: [M$^{+\cdot}$] (found): 398.1843 Da.

6-(7-Dimethylamino-3-oxo-3H-phenoxazin-1-yloxy)- hexanoic acid (8)
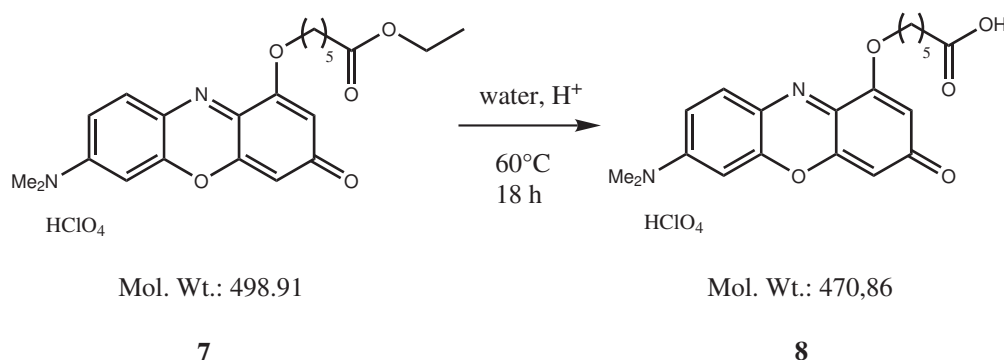
Figure 4.9: Preparation of compound **8**

Compound **7** (0.14 g; 0.28 mmol) is dissolved in 10 mL of acetone and diluted with 20 mL of water. Perchloric acid is added in catalytic quantities and the reaction mixture is heated to 60°C for 18 hours. Product **8** crystallizes after cooling to room temperature yielding a violet product (0.1 g, 75 %). R$_f$ (silica gel 60; ethanol): 0.26; ^{1}H-NMR (MeOD): δ = 7.89 (d, 1 H,^{3}J(H,H)= 9.88 Hz), 7.5 (dd, 1 H, ^{3}J(H,H) = 2.74 Hz), 7.0 (d, 1 H, ^{3}J(H,H) = 2.74 Hz, 9.88 Hz), 6.52 (m, 2 H), 4.22 (t, 2 H, ^{3}J(H,H) = 6.58 Hz), 3.47 (s, 6 H), 2.36 (t, 2 H, ^{3}J(H,H) = 7.13 Hz), 2.03-1.9 (m, 2 H), 1.8-1,67 (m, 2 H), 1.66-1.5 (m, 2H); IR (ATR): ν = 3100 cm^{-1}, 2957 cm^{-1}, 2872 cm^{-1}, 1731 cm^{-1}, 1650 cm^{-1}, 1609 cm^{-1}, 1578 cm^{-1}, 1547 cm^{-1}; EI$^-$-MS: [M$^{+\cdot}$] (calculated): 371.1529 Da; EI$^-$-MS: [M$^{+\cdot}$] (found): 371.1518 Da.

In-situ preparation of 6-(7-Dimethylamino-3-oxo-3H-phenoxazin-1-yloxy)-hexanoic acid 2,5 dioxo-pyrrolidin-1-yl ester (9)

1 mg (2.1 μmol) of free acid **8**, 0.6 mg (5.3 μmol) of NHS and 1.1 mg (5.3 μmol) of DCC are dissolved in 100 μL of dry DMSO. Triethylamine is added as a base in slight excess and the mixture is stirred for 18 h at room temperature. Thin layer chromatography (TLC) is used to monitor the formation of the NHS-ester (see figure 4.10). The solution is then used without further purification for labeling purposes.
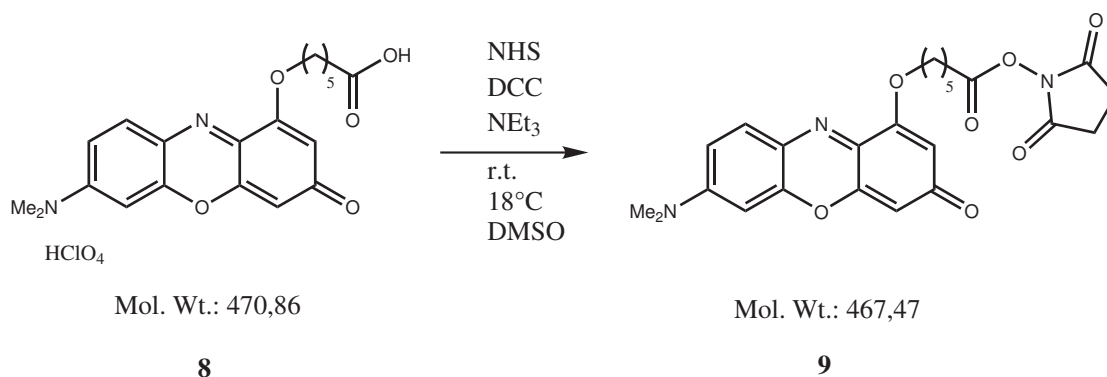
Figure 4.10: Preparation of compound **9**

4.2.8 Labeling experiments with label 9

Labeling of bradykinin

1 mg bradykinin is dissolved in 1 mL of bicarbonate buffer (50 mM, pH 8,4) and cooled to 4°C. 5 μL of the activated dye is added to 45 μL of analyte solution and stirred over night at room temperature. The reaction progress is observed by thin layer chromatography (silica gel 60, EtAc/EtOH 9:1).

Labeling of BSA

5 mg of BSA is dissolved in 1 mL of a 50 mM bicarbonate buffer solution of pH 8.4. Then, 5 μL of label **9** (c = 0.021 M) is added. The mixture is stirred for 12 - 15 h at room temperature. The labeled protein is purified by size exclusion chromatography on Sephadex G-25 (50 mM phosphate buffer, pH 7.3). The MALDI-TOF mass spectrum of the purple phenoxazine (using sinapic acid as the matrix) with BSA shows a broad peak between 66,100 Da and 69,000 Da, with a maximum at 67,100 Da.

Methods for labeling the silica nanoparticles (SiNPs)

Method A: Silica nanopowder (amorphous-SiO_2) can be purchased by Nanostructure & Amorphous Materials Inc. (www.nanoamor.com) and used without further treatment. 1 g of the silica powder is dispersed in 100 mL of toluene by sonification and stirring. The solution is heated to reflux before 1 mL aminopropyltriethoxysilane (APTES) is added dropwise and refluxed for another 5 h. Afterwards, the particles are collected by centrifugation (6000 rpm, 10 min.), washed with ethanol (3 times) and dried at 50°C. The purple dye **8** (3 mg, 8.1 μmol, 1 eq.), DCC (3.3 mg, 16.2 μmol, 2 eq.) and NHS (1.9 mg, 16.2 μmol, 2 eq.) are stirred in 100

μL of DMSO over night. 5 mg of the amino-modified silica nanoparticles are suspended in 1 mL of ethanol. 5 μL of the label are added and the solution is stirred over night. The amino-labeled particles are once more collected by centrifugation (6000 rpm, 10 min) and washed with ethanol (3 times). In parallel a blank sample is prepared by combining 5 mg of unmodified silica nanoparticles with 5 μL of the mixture with the activated fluorophore using the same protocol. After the centrifugation/washing steps the blank sample possesses almost no color whereas the amino-labeled particles are strongly colored.

Method B: Silica nanoparticles are prepared by the Stöber method: A mixture of 50 mL of ethanol, 1 mL of distilled water, and 1 mL of ammonia solution (25 % in water) is heated to 40°C. Tetraethylorthosilicate (TEOS, 1.5 mL, 6.73 mmol) is added and the solution is slowly stirred for 3 h at 40°C. Further TEOS (1.0 mL, 4.48 mmol) is added and the stirring is continued for another 3 h. In parallel, a dye-silane coniugate is prepared. Therefore, the purple dye **8** (3 mg, 8.1 μmol, 1 eq.), DCC (3.3 mg, 16.2 μmol, 2 eq.) and NHS (1.9 mg, 16.2 μmol, 2 eq.) are stirred in 100 μL DMSO over night in order to obtain the purple label **9**. A solution of aminopropyltriethoxysilane (APTES; 1.9 μL, 8.1 μmol, 1 eq.) in 50 μL of ethanol is added and the mixture is stirred over night. The SiNPs and the dye-silane conjugate are used without further purification. 1 mL of the alcosol containing particles are diluted with 1 mL of ethanol and 10 μL of the dye-silane conjugate mixture is added. The fluorescent SiNPs are purified by size exclusion chromatography on a column ($\varnothing$ 3 cm, height 14 cm) containing Sephadex LH-20 (from GE Healthcare; www.gehealthcare.com) using ethanol as the eluent. The fluorophore-modified particles are obtained by collecting the colored fraction that first leaves the column. The second colored band that moves much slower contains the unreacted reagents and is discarded.

4.2.9 Label 9-analyte conjugate in separation experiments

Separation of labeled bradykinin by MCE

The Borofloat^{TM} microchips with a standard cross layout have the following dimensions: injection channel 8 mm, separation channel 85 mm, height 30 μm, width 50 μm. The chip is conditioned by flushing it 3 min with 1 M NaOH and 1 min with water before filling it with separation buffer (50 mM phosphate buffer, pH 7.2). Pinched injection is applied for 35 s. When sampling bradykinin solution and separating it from free label, the electrical potentials are applied in the following order: sample inlet (A), buffer inlet (B), sample outlet (C), buffer outlet (D). The injection potential are 750 (A), 680 (B), 0 (C) and 2330 (D) V, and the potentials for the separation are 2243 (A), 2645 (B), 2198 (C) and 0 (D) V (same as for label 2-BSA conjugate, see figure 4.3).

Separation of labeled BSA by SEC

The purification of the labeled protein is carried out by size exclusion chromatography using Sepadex G-25 as stationary phase and phosphate buffer (pH 7.2, 50 mM) solution as the eluent. The extract of the dye-protein conjugate has a purple color and leaves the column first.

4.2.10   Synthesis of labels 14a/b

5-Piperidin-1-yl-benzene-1,3-diol (10)

10

Mol. Wt.: 126,11   Mol. Wt.: 85,15   Mol. Wt.: 193,24
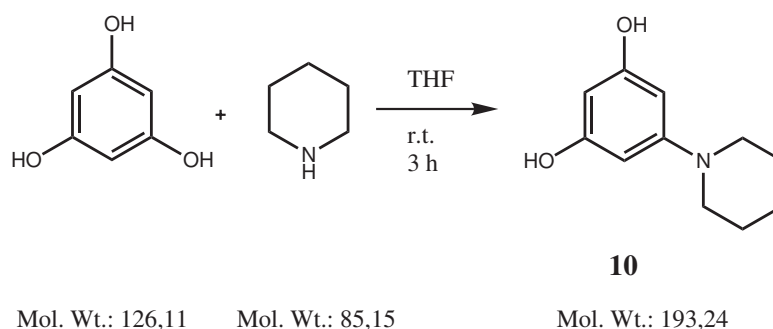
Figure 4.11: Preparation of compound **10**

Compound **10** (see figure 4.11) is prepared according to the method described in a patent [99]. Phloroglucinol (1 g; 8 mmol) is dissolved in 20 mL of THF and 0.785 mL (8 mmol) of piperidine is added. The reaction mixture is stirred for 3 h at room temperature. The solvent is evaporated and the product is purified by recrystallization in ethanol/water (ratio: 1/1). The product is obtained as pink crystals (0.6 g, 39%); mp: 194°C (same as in literature); ^{1}H-NMR (DMSO-d$_6$): δ = 8.85 (s, 2 H), 5.75 (d, 2 H, ^{3}J(H,H) = 1.92 Hz), 5.65 (t, 1 H, ^{3}J(H,H) = 1.92 Hz), 3.0 (m, 4 H), 1.6-1.4 (m, 6 H); ^{13}C-NMR (DMSO-d$_6$): δ = 158.59, 153.33, 94.32, 93.62, 49.37, 25.08, 23.94; IR (ATR): ν = 3235 cm^{-1}, 2963 cm^{-1}, 2958 cm^{-1}, 2858 cm^{-1}, 1604 cm^{-1}, 1509 cm^{-1}, 1437 cm^{-1}, 1380 cm^{-1}, +p-ESI-MS: [MH$^+$] (calculated): 194.1, +p-ESI-MS: [MH$^+$] (found): 194.3.

6-(3-Hydroxy-5-piperidin-1-yl-phenoxy)-hexanoic acid ethyl ester (11)

A mixture of 0.5 g (2.59 mmol) of compound **10**, 0.46 mL (2.59 mmol) of ethyl-bromohexanoate and 1.1 g (7.9 mmol) of potassium carbonate are stirred in dimethylformamide at room temperature for two days (see figure 4.12). The mixture is filtered and the solvent is evaporated. The crude product is purified by column chromatography (silica gel 60; diethyl ether/petroleum ether: 60/40) to
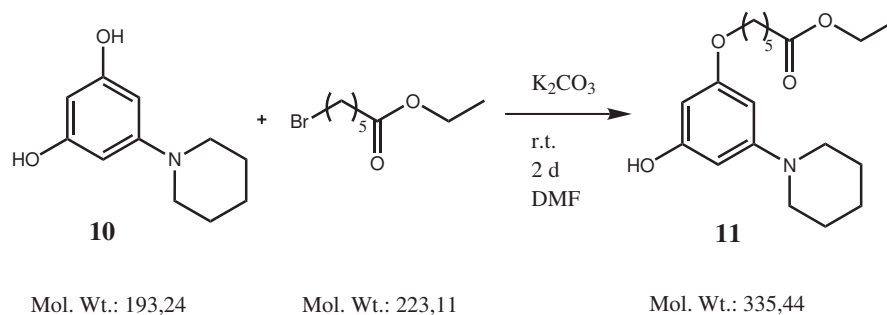
Figure 4.12: Preparation of compound **11**

yield a colorless oil (0.27 g, 31%); R_f (silica gel 60; diethyl ether/petroleum ether: 70/30): 0.65; ^{1}H-NMR (CDCl$_3$): δ = 6.05 (m, 1 H), 6.0 (m, 1 H), 5.87 (m, 1 H), 4.13 (q, 2 H, ^{3}J(H,H) = 7.13 Hz), 3.81 (t, 2 H, ^{3}J(H,H) = 6.58 Hz), 3.05 (t, 4 H, ^{3}J(H,H) = 5.21 Hz), 2.31 (t, 2 H, ^{3}J(H,H) = 7.41 Hz), 1.8-1.37 (m, 12 H), 1.24 (t, 3 H, ^{3}J(H,H) = 7.13 Hz); ^{13}C-NMR (CDCl$_3$): 173.08, 159.84, 156.65, 152.81, 95.84, 95.04, 92.37, 66.44, 59.40, 49.67, 33.26, 27.90, 24.60, 24.45, 23.67, 23.26; IR (ATR): ν = 3406 cm^{-1}, 2935 cm^{-1}, 2858 cm^{-1}, 2808 cm^{-1}, 1733 cm^{-1}, 1591 cm^{-1}, 1503 cm^{-1}, 1452 cm^{-1}.

[9-(5-Ethoxycarbonylpentyloxy)-7-piperidin-1-yl-phenoxazin-3-ylidne] -dimethyl-ammonium perchlorate (12a)
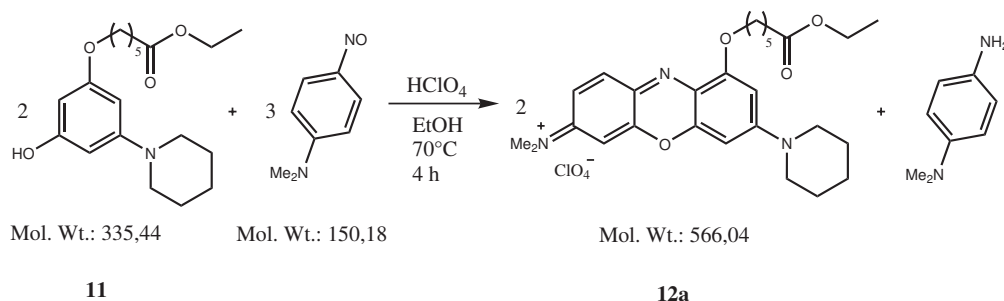
Figure 4.13: Preparation of compound **12a**

Compound **11** (0.2 g; 0.6 mmol) and 0.15 g (0.9 mmol) of 4-nitroso-N,N-dimetylaniline are dissolved in ethanol. 0.08 mL (0.9 mmol) of perchloric acid is added and the mixture is heated to 70°C for four hours. The mixture is filter hot and the product crystallizes at room temperature over night. **12a** (see figure 4.13) is yielded as dark-blue crystals (0.174 g, 49 %); R_f (silica gel 60; butanol/acetic acid/water: 60/20/20): 0.48; mp : 179°C-180°C; ^{1}H-NMR (acetone-d$_6$): δ = 7.78 (d, 1 H, ^{3}J(H,H) = 9.60 Hz), 7.31 (dd, 1 H, ^{3}J(H,H) = 2.44 Hz, 9.60 Hz), 6.88 (d,

1 H, ^{3}J(H,H)=2.44 Hz), 6.85 (d, 1 H, ^{3}J(H,H) = 2.74 Hz), 6.81 (d, 1 H, ^{3}J(H,H) = 2.44 Hz), 4.34 (t, 2 H, ^{3}J(H,H) = 6.31 Hz), 4.01 (q, 2 H, ^{3}J(H,H) = 7.13 Hz), 4.0 (m, 4 H), 3.43 (s, 6 H), 2.35 (t, 3 H, ^{3}J(H,H) = 7.41 Hz), 2.0-1.9 (m, 2 H), 1.83 (m, 6 H), 1.77-1.6 (m, 2 H), 1.64-1.52 (m, 2 H), 1.25 (t, 3 H, ^{3}J(H,H) = 7.13 Hz), ^{13}C-NMR (CDCl$_3$): δ = 173.60, 160.59, 158.74, 158.43, 158.07, 150.43, 149.33, 134.76, 131.82, 116.43, 97.11, 96.88, 92.98, 60.52, 50.98, 44.66, 41.48, 34.55, 29.18, 27.48, 26.29, 25.36, 24.74, 14.62; IR (ATR): ν = 2947 cm^{-1}, 2863 cm^{-1}, 1726 cm^{-1}, 1651 cm^{-1}, 1592 cm^{-1}, 1485 cm^{-1}, 1405 cm^{-1}, 1343 cm^{-1}; PI$^-$-LSI$^-$-MS: [M$^+$] (calculated): 466.2706 Da; [M$^+$] (found): 466.2694 Da.

[9-(5-Ethoxycarbonylpentyloxy)-7-piperidin-1-yl-phenoxazin-3-ylidene]-diethyl-ammonium perchlorate (12b)
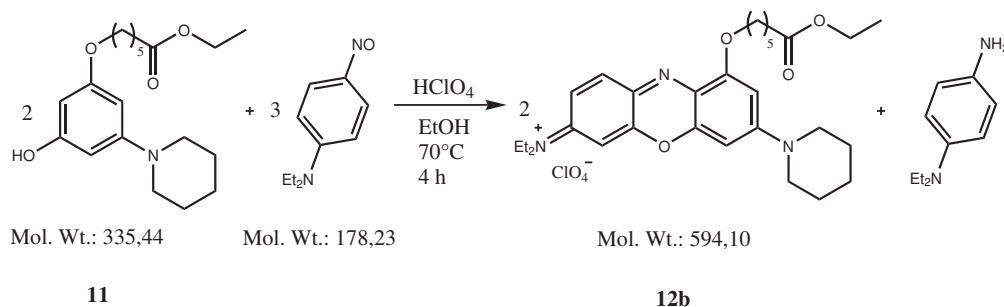
Figure 4.14: Preparation of compound **12b**

0.2 g (0.6 mmol) of compound **11** and 0.16 g (0.9 mmol) of 4-nitroso-N,N-dietylaniline are dissolved in ethanol. 0.08 mL (0.9 mmol) of perchloric acid is added and the mixture is heated to 70°C for four hours. Afterwards the mixture is filter hot and the product crystallizes at room temperature over night. **12b** (see figure 4.13) is yielded as dark-blue crystals (0.140 g, 41 %); R$_f$ (silica gel 60; butanol/acetic acid/water: 60/20/20): 0.65; ^{1}H-NMR (CDCl$_3$): δ = 7.75 (d, 1 H), 7.0 (dd, 1 H), 6.67 (d, 1 H), 6.64 (d, 1 H), 6.55 (d, 1 H), 4.26 (t, 2 H), 4.1 (q, 2 H), 3.84 (m, 4 H), 3.64 (q, 4 H), 2.35 (t, 3 H), 2.05-1.5 (m, 12 H), 1.34 (t, 6 H), 1.24 (t, 3 H); ^{13}C-NMR (CDCl$_3$): δ = 172.68, 158.44, 156.49, 154.25, 148.29, 147.76 , 133.5, 129.97 (1C), 128.96, 113.97, 95.16, 94.95, 91.43, 69.24, 59.27, 49.41, 45.46, 33.16, 27.28, 25.58, 24.44, 23.64, 22.93, 13.26 , 11.78; PI$^-$-LSI$^-$: [M$^+$] (calculated): 494.3019 Da; [M$^+$] (found): 494.3011 Da; IR (ATR): ν = 3024 cm^{-1}, 2941 cm^{-1}, 1724 cm^{-1}, 1622 cm^{-1}, 1513 cm^{-1}, 1453 cm^{-1}, 1406 cm^{-1}, 1260 cm^{-1}.
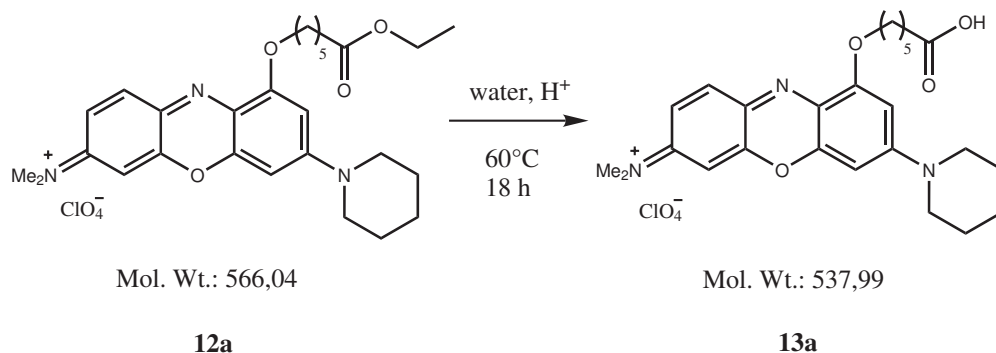
Figure 4.15: Preparation of compound **13a**

[9-(5-Carboxypentyloxy)-7-piperidin-1-yl-phenoxazin-3-ylidene] -dimethyl-ammonium perchlorate (13a)

Compound **12a** (0.14 g; 0.25 mmol) is dissolved in 10 mL of acetone and diluted with 20 mL of water. Perchloric acid is added in catalytic quantities and the reaction mixture is heated to 60°C for 18 h in order to hydrolyze the ester (see figure 4.15). After cooling to room temperature, the free acid **13a** is extracted three times with DCM. The combined organic layers are dried over Na_2SO_4. After the solvent is evaporated, the product is obtained as a dark blue solid. The purity is checked by TLC. Yield: 0.12 g (90 %); R_f (silica gel 60; butanol/acetic acid/water: 60/20/20): 0.85; ^{1}H-NMR (methanol-d_4): $\delta = 7.79$ (d, 1 H, ^{3}J(H,H) = 9.60 Hz), 7.23 (dd, 1 H, ^{3}J(H,H) = 2.61 Hz, 9.60 Hz), 6.83 (d, 1 H, ^{3}J(H,H) = 2.47 Hz), 6.81 (d, 1 H, ^{3}J(H,H) = 2.61 Hz), 6.69 (d, 1 H, ^{3}J(H,H) = 2.33 Hz), 4.27 (t, 2 H, ^{3}J(H,H) = 6.45 Hz), 3.9 (m, 4 H), 3.34 (s, 6 H), 2.36 (t, 2 H, ^{3}J(H,H) = 3.57 Hz), 2.05-1.94 (m, 2 H), 1.87-1.78 (m, 6 H), 1.78-1.67 (m, 2 H), 1.66-1.55 (m, 2 H); LSI$^-$-MS: [M$^+$] (calculated): 438.2393 Da; LSI$^-$-MS: [M$^+$] (found): 438.2383 Da; IR (ATR): ν = 2918 cm^{-1}, 2845 cm^{-1}, 1710 cm^{-1}, 1654 cm^{-1}, 1595 cm^{-1}.

[9-(5-Carboxypentyloxy)-7-piperidin-1-yl-phenoxazin-3-ylidene] -diethyl-ammonium perchlorate (13b)

0.14 g (0.23 mmol) of **12b** is dissolved in 10 mL of acetone and diluted with 20 mL of water. Perchloric acid is added in catalytic quantities and the reaction mixture is heated to 60°C for 18 hours (see figure 4.16). After cooling to room temperature the deprotected dye **13b** is extracted three times with DCM. The combined organic layers are dried over Na_2SO_4. After the solvent is evaporated the purity of the product is checked by TLC. Yield: 0.11 g (82 %); R_f (silica gel 60; butanol/acetic acid/water: 60/20/20): 0.61; ^{1}H-NMR (methanol-d_4): $\delta = 7.75$ (d, 1 H), 7.21 (dd, 1 H), 6.81-6.6 (m, 3 H), 4.23 (t, 2 H), 3.91-3.83 (m, 4 H), 3.7
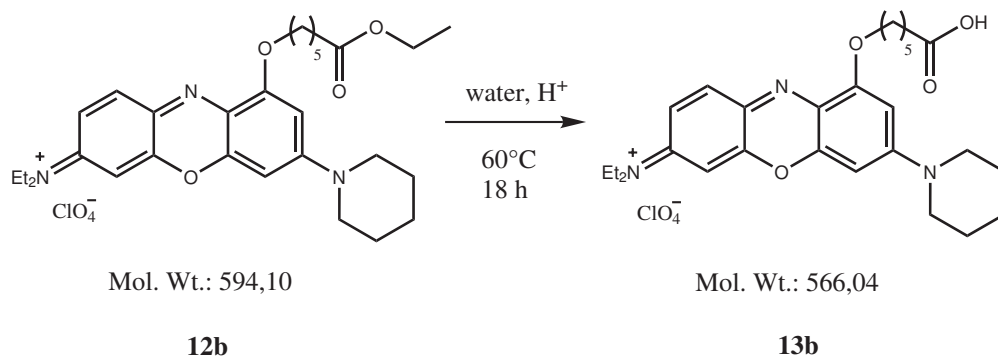
Figure 4.16: Preparation of compound **13b**

(q, 4 H), 2.25 (t, 2 H), 2.1-1.9 (m, 2 H), 1.89-1.76 (m, 6 H), 1.76-1.48 (m, 4 H), 1.32 (t, 6 H); LSI$^-$-MS: [M$^+$] (calculated): 466.2706, [M$^+$] (found): 466.2701; IR (ATR): $\nu = 2921$ cm^{-1}, 2854 cm^{-1}, 1651 cm^{-1}, 1595 cm^{-1}, 1564 cm^{-1}.

Common method for preparation of NHS-esters 14a and 14b

13a R = Me, Mol. Wt.: 537,99

13b R = Et, Mol. Wt.: 566,04

14a R = Me, Mol. Wt.: 635,06

14b R = Et, Mol. Wt.: 663,12
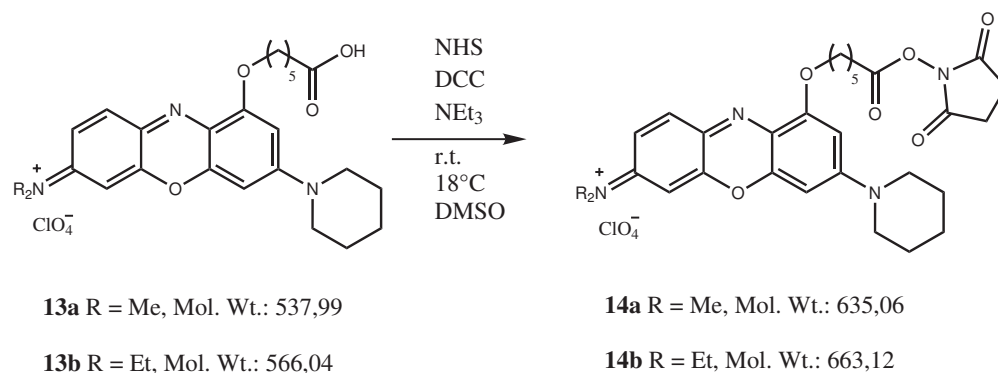
Figure 4.17: Preparation of the NHS-esters **14a** and **14b**

The carboxy groups of the blue oxazines **14a** and **14b** respectively are made amino-reactive (to become "labels") by converting them into esters of N-hydroxysuccinimide that readily react with amines, preferably at pH values above 8 (see figure 4.17). The respective free acid (1 mg of either **13a** or **13b**), NHS (molar ratio: free acid/NHS is 1/2), and DCC (molar ratio: free acid/DCC is 1/2) are dissolved in 100 μL of dry DMSO. Triethylamine is added as a base in slight excess, and the mixture is stirred for 18 h at room temperature. Thin layer chromatography (TLC) is applied to monitor the formation of the NHS-ester and the obtained solution is used without further purification for labeling experiments.

4.2.11   Labeling experiments with label 14a

Labeling of amino acids

1 mg of L-glycine, L-serine, L-leucine, L-aspartic acid and L-glutamic acid are dissolved in 1 mL of bicarbonate buffer (50 mM, pH 8.3) each and cooled to 4°C. 5 μL of label **14a** (c = 0.054 M) is added to each 45 μL of analyte solution and stirred over night at room temperature. The reaction progress is monitored by thin layer chromatography (silica gel 60, butanol/acetic acid/water: 60/20/20).

Labeling of BSA

5 mg of bovine serum albumin is dissolved in 1 mL of a 50 mM bicarbonate buffer of pH 8.4. Then, 5 μL of the label (c(14a) = 0.054 M) is added. The mixture is stirred for 12 - 15 h at r.t. [148]. The labeled protein is purified by size exclusion chromatography. The MALDI-TOF mass spectrum (using sinapic acid as the matrix) of the labeled BSA shows a broad peak between 66,400 Da and 71,400 Da, with a maximum at 68,000 Da.

4.2.12   Label 14a-analyte conjugate in separation experiments

Separation of labeled amino acids by TLC

The separation of the tagged amino acids from the unreacted label **14a** as well as from the hydrolyzed NHS-ester (free acid **13a**) is carried out using silica gel 60 as stationary phase and a butanol/acetic acid/water (60/20/20, v/v) mixture as eluent.

Separation of labeled BSA by SEC

The purification of the labeled protein is performed by size exclusion chromatography using Sepadex G-25 as stationary phase and phosphate buffer solution (pH 7.2, 50 mM) as eluent. The extract of the dye-protein conjugate is at deep blue color and leaves the column first (see figure 2.31).

4.2.13   Synthesis of labels 16

7-Dimethylamino-1-hydroxy-phenoxazin-3-one (15)

The synthesis of phenoxazinone **15** which is shown in figure 4.18 is carried out according to Kotoucek et al. [91].

Mol. Wt.: 126,11   Mol. Wt.: 150,18   Mol. Wt.: 292,72
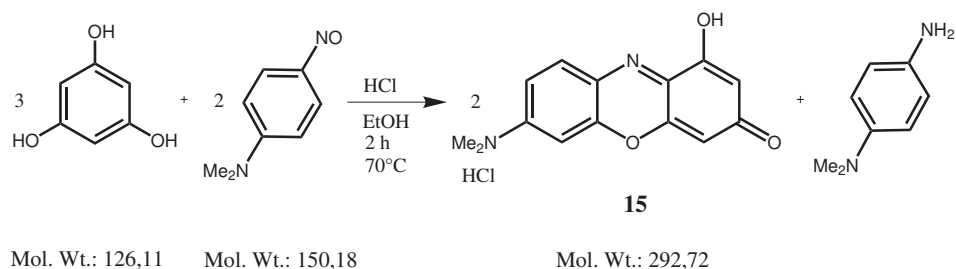
Figure 4.18: Preparation of compound **15**

7-Dimethylamino-1-prop-2-ynyloxy-phenoxazin-3-one (16)

Mol. Wt.: 292,72   Mol. Wt.: 118,96   Mol. Wt.: 294,30

15   **16**
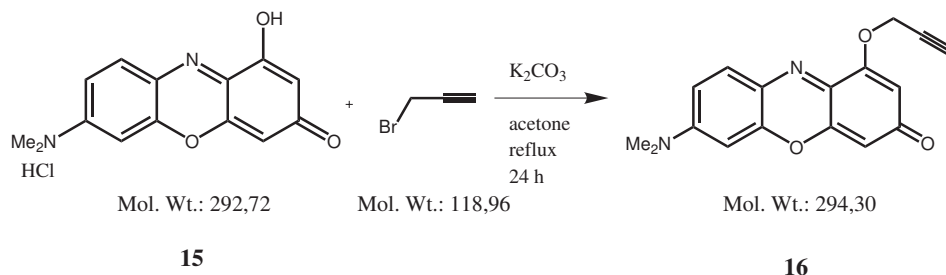
Figure 4.19: Preparation of compound **16**

147 mg (0.5 mmol) of 7-dimethylamino-1-hydroxy-phenoxazone is refluxed with (82 mg, 0.55 mmol) of propargyl bromide and 207 mg of K_2CO_3 in acetone for 24 h. After cooling, the reaction is filtered, concentrated on a rotavapor, and then purified by flash chromatography (see figure 4.19). Yield: 76.5 mg (52%); m.p.>300°C. ^{1}H NMR (CDCl$_3$): δ = 7.70 (d, ^{3}J(H,H) = 7.5, 1H), 6.71 (m, 1H), 6.44 (s, 1H), 6.44 (s, 1H), 6.26 (s, 1H), 6.15 (s, 1H). PI-EI [M^{+}] (calculated): 294.1004; (found): 294.1002.

4.2.14   Labeling experiments with label 16

Labeling of azido sugar

The tagging experiment shown in figure 4.20 is performed by Kele et al. [41]. Therefore, 1 eq. of label **16** and 1.1 eq. of the azido sugar are stirred in acetonitrile/water (1/1, v/v). CuI (10 %) is added as catalyst and triethylamine (20 %) is used as base. The reaction is carried out for 16 hours at room temperature. Yield 45 %; ^{1}H NMR (DMSO-d$_6$) δ = 8.62 (1H, s), 7.57 (1H, d, ^{3}J(H,H) = 8.8 Hz), 6.78 (1H, d, ^{3}J(H,H) = 8.8 Hz), 6.58 (1H, s), 6.41 (1H, d, ^{3}J(H,H) = 9.3 Hz), 6.19 (1H, s), 5.92 (1H, s), 5.71 (1H, t, ^{3}J(H,H) = 9.3 Hz), 5.56 (1H, t, ^{3}J(H,H) = 9.3 Hz),

5.19 (1H, t, ^{3}J(H,H) = 9.9 Hz); 5.23 (2H, s), , 4.38 (1H, m), 4.38 (1H, m), 3.09 (6H,s), 2.02 (3H, s), 2.00 (3H, s), 1.96 (3H, s), 1.79 (3H, s); ^{13}C NMR (HMQC) δ = 131.0, 123.9, 110.2, 106.7, 101.7, 95.6, 83.3, 71.7, 69.5, 67.0, 61.2, 61.1, 39.5, 20.0, 19.9, 19.7, 19.4; HR-MS (ESI):[MH$^+$] (calculated): 668.2204, [MH$^+$] (found): 668.2197.
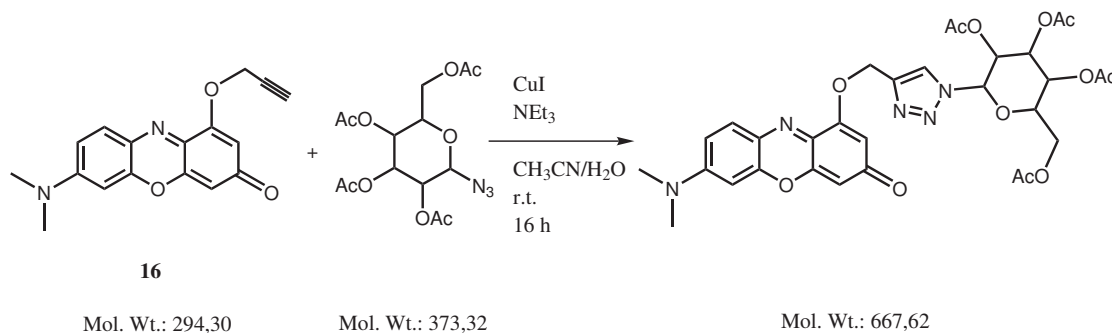
Figure 4.20: Click reaction of compound **16** with an azido sugar as a building block

4.2.15 Synthesis of labels 18

3-Piperidin-1-yl-5-prop-2-ynyloxy-phenol (17)
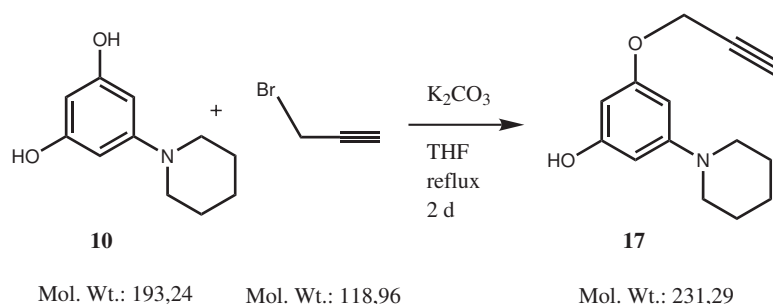
Figure 4.21: Preparation of compound **17**

0.5 g (2.6 mmol) of 5-(piperidin-1-yl)benzene-1,3-diol **10** (synthesis described in 4.2.10) and propargyl bromide (0.23 mL, 2.6 mmol) is refluxed in THF for 2 days. 360 mg of K$_2$CO$_3$ is used as base. After cooling, the reaction mixture is filtered hot, concentrated, and purified by column chromotography (silica gel 60, diethyl ether/petroleum ether: 60/40, v/v) to get a colorless oil (see figure 4.21). Yield: 0.21 g (35 %). R$_f$ = 0.51, ^{1}H-NMR (DMSO-d$_6$): δ = 6.01 (1H, t, ^{3}J(H,H) = 1.9 Hz), 5.96 (1H, t, ^{3}J(H,H) = 1.9 Hz), 5.83 (1H, t, ^{3}J(H,H) = 1.9 Hz), 5.23

(1H, t, ^{3}J(H,H) = 1.1 Hz), 4.53 (2H, d, ^{3}J(H,H) = 2.5 Hz), 3.12-3.04 (4H, m), 2.50 (1H, t, ^{3}J(H,H) = 2.5 Hz), 1.80-1.62 (6H, m).

Dimethyl(7-piperidin-1-yl-9-prop-2-ynyloxy-phenoxazin-3-ylidene)-ammonium perchlorat (18)
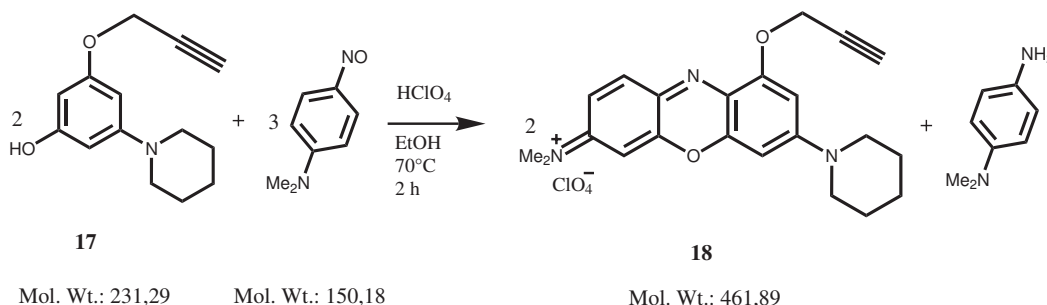
Figure 4.22: Preparation of compound **18**

Compound **17** (0.2 g, 0.86 mmol) is reacted with p-nitroso-N,N-dimethylaniline (0.19 g, 1.3 mmol) and 0.14 mL (1.3 mmol) of perchloric acid. The reaction is performed in ethanol at 70°C for 2 hours. The crude product is recrystallized in ethanol to yield dark blue crystals. Yield: 0.12 g (30 %); ^{1}H-NMR (acetone-d$_6$): δ = 7.79 (1H, d, ^{3}J(H,H) = 9.6 Hz), 7.35 (1H, dd, ^{3}J(H,H) = 2.7Hz, 9.6Hz), 6.89 (1H, d, ^{3}J(H,H) = 2.5Hz), 6.84 (1H, d, ^{3}J(H,H) = 2.7 Hz), 5.19 (2H, d, ^{3}J(H,H) = 2.5 Hz), 3.46 (6H, s); 3.97.4.05 (4H, m), 3.35 (1H, t, ^{3}J(H,H) = 2.5Hz), 1.78.1-87 (6H, m); 3.35 (1H, t, ^{3}J(H,H) = 2.5Hz); IR (ATR): ν = 3266 cm^{-1}, 2921 cm^{-1}, 2859 cm^{-1}, 1651 cm^{-1}, 1540 cm^{-1}, 1487 cm^{-1}, 1487 cm^{-1}. HR-MS (PI-EI): [M$^+$] (calculated): 362.1863, [M$^+$] (found): 362.1877.

4.2.16 Labeling experiments with label 18

Labeling of azido sugar

The tagging experiment shown in figure 4.23 is also performed by Kele et al. [41]. 1 eq. of label **18** and 1.1 eq. of the azido sugar are stirred in acetonitrile/water (1/1, v/v). CuI (10 %) is added as a catalyst and triethylamine (20 %) is used as base. The reaction is carried out for 16 hours at room temperature. Yield: 53 %; ^{1}H-NMR (DMSO-d$_6$): δ = 7.74 (1H, d, ^{3}J(H,H) 8.8 Hz); 8.67 (1H, s), 7.19 (1H, d, ^{3}J(H,H) = 8.2 Hz), 6.88 (1H, s), 6.74 (1H, s), 6.41 (1H, d, ^{3}J(H,H) = 8.8 Hz), 5.68 (1H, t, ^{3}J(H,H) = 9.3 Hz), 5.57 (1H, t, ^{3}J(H,H) = 9.3 Hz), 5.49 (2H, s), 5.19 (1H, t, ^{3}J(H,H) = 9.3 Hz), 4.39 (1H, m), 4.11 (2H, m), 3.91 (4H, s), 3.28 (6H, s), 2.02 (3H, s), 2.00 (3H, s), 1.96 (3H, s), 1.78 (3H, s), 1.73 (6H, s); ^{13}C NMR (HMQC) δ
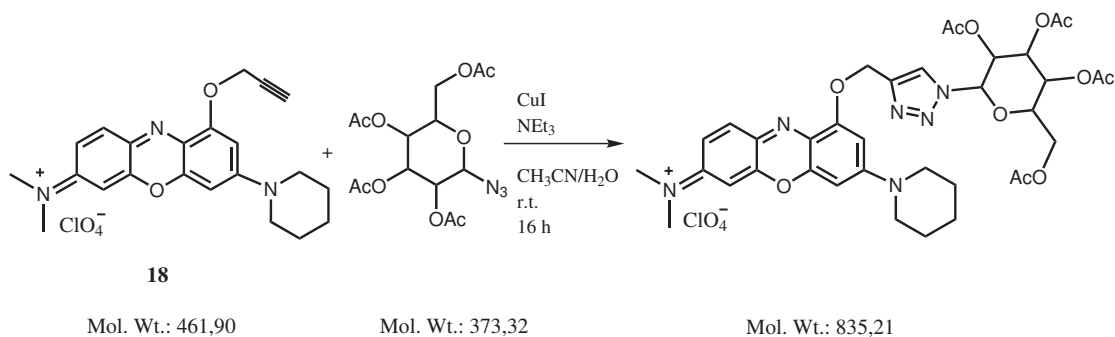
Figure 4.23: Click reaction of compound **18** with an azido sugar as a building block

= 132.9, 123.9, 115.1, 96.5, 95.3, 91.6, 83.3, 72.7, 71.4, 69.5, 66.9, 61.6, 61.1, 49.1, 40.3, 25.8, 23.0, 19.8, 19.7, 19.6, 19.2; HR-MS (ESI): [M^+] (calculated): 735.2984, [M^+] (found): 735.2981.

4.2.17 Synthesis of probe 21

2-[2-(4-Methoxy-phenylamino)-ethyl]-isoindole-1,3-dione (19)
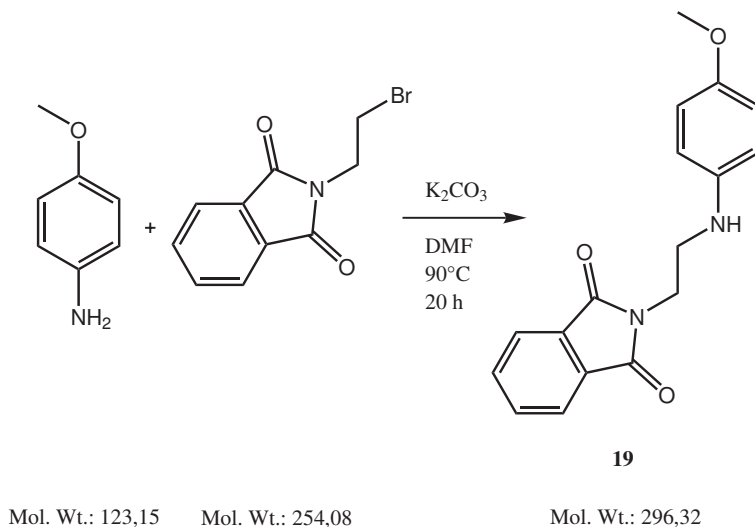
Figure 4.24: Preparation of compound **19**

2 g (0,016 mol) of p-anisidine, 4.13 g (0,016 mol) of N-(2-bromoethyl)phthalimide and 2.24 g (0,016 mol) of K_2CO_3 in 12 mL of DMF are heated at 90°C for 20 hours. The reaction mixture is poured into 300 mL of ice water. After two hours, the brown-white precipitate is filtered off, washed with cold water and dried

over CaCl$_2$ in vaccum. The crude product is recrystallized from ethanol to yield off-white crystalls. Yield 3.3 g (71 %); m.p.: 103-104°C; ^{1}H-NMR (CDCl$_3$): δ = 7.83-7.62 (m, 4H), 6.72 (d, 2H), 6.58 (d, 2H), 3.93 (t, 2H, ^{3}J = 6.17 Hz), 3.68 (s, 3H, ^{3}J = 6.17 Hz), 3,38 (t, 2H); ^{13}C-NMR (CDCl$_3$): δ = 168.65, 152.28, 141.37, 134.04, 132.02, 123.33, 114.9, 114.08, 55.8, 43.8, 37.62; elementary analysis (calaculated): C 68.91 %, H 5.44 %, N 9.45 % (found): C 68.92 %, H 5.46 %, N 9.25 %.

N-(4-Methoxy-phenyl)-ethane-1,2-diamine (20)
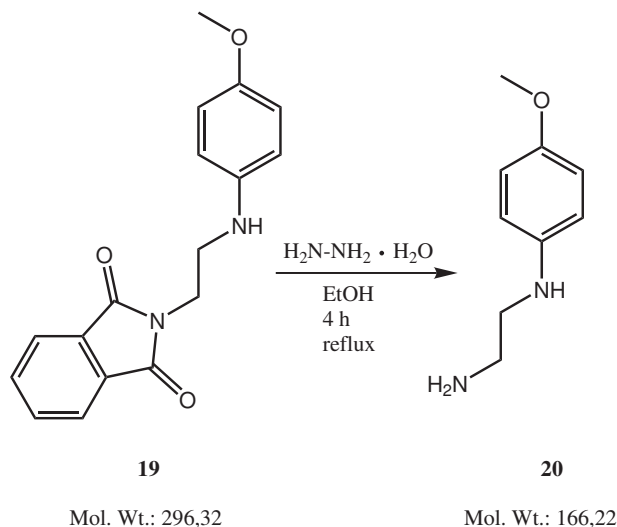
Figure 4.25: Preparation of compound **20**

Compound **19** (2 g, 0.0067 mol) is dissolved in 40 mL of boiling ethanol. 0.33 mL (0.0067 mol) of hydrazine monohydrate is added in one portion to the brown solution. The mixture is refluxed for 4 hours whereas a white solid precipitates. The mixture is cooled to room temperature and 10 mL of concentrated HCl (37 %) is added. After one hour the precipitate is filtered off. The filtrate is concentrated and the pH is adjusted to pH > 10 by aqueous NaOH. The solution is extracted five times with Et$_2$O. The combined extracts are dried over Na$_2$SO$_4$. After the solvent is removed, the product remains as a brown oil which crystallized in the refrigerator over night. It can be used without further purifications. Yield: 0.5 g (44 %); ^{1}H-NMR (CDCl$_3$): δ = 6.55-6.8 (m, 4H), 3.75 (s, 3H), 3.15 (t, 2H, ^{3}J = 5.76 Hz), 2,95 (t, 2H, ^{3}J = 5.76 Hz); ^{13}C-NMR (CDCl$_3$): δ = 152.18, 142.67, 114.93, 114.32, 55.84, 47.58, 41.31; HR-MS (EI$^-$-MS): [M$^{+\cdot}$] (calculated): 166.1106, [M$^{+\cdot}$] (found): 166.1102.

Synthesis of 4-N-(4-methoxyphenyl) ethylene diamine-N-caproic-acid-1,8-naphthalimide (21)

0.33 g (0.001 mol) of **3** (preparation see 4.2.4) and 0.32 g (0.002 mol) of **20** are dissolved in DMSO. 0.32 mL (0.002 mol) diisopropylethylamine is added as base. The mixture is stirred at 90°C for 18 h and is then poured into 50 mL of ice water. The precipitate is centrifuged and the tawny oil is collected. The oil is dissolved in DCM, washed two times with water and dried over Na_2SO_4. The solvent is evaporated to obtain another tawny oil which is purified by recrystallization in dichloromethane/diethylether yielding an ocker solid. Yield: 0.27 g (60 %); m.p.: 129-130°C; ^{1}H-NMR (acetone-d_6): δ = 8.6-8.25 (3xd, 3H), 7.6 (m, 1H), 6.82 (d, 1H), 6.76 (d, 2H, ^{3}J = 9.0565 Hz), 6.69 (d, 2H, ^{3}J = 9.0565 Hz,), 4.08 (t, 2H), 3.74-3.45 (1xs, 3H; 1xm, 4 H), 2.31 (t, 2H), 1.78-1.35 (m, 6H); ^{13}C-NMR (acetone-d_6): δ = 174.67, 164.85, 164.15, 152.85, 151.21, 143.68, 134.88, 131.38, 130.66, 128.43, 125.16, 123.63, 121.43, 115.6, 114.69, 110.26, 104.75, 55.86, 43.572,43.64, 40.17, 34.11, 28.66, 27.36, 25.44; IR (ATR): ν = 3377 cm^{-1}, 3140 cm^{-1}, 2935 cm^{-1}, 2854 cm^{-1}, 1704 cm^{-1}, 1673 cm^{-1}, 1638 cm^{-1}, 1548 cm^{-1}, 1518 cm^{-1}, 1478 cm^{-1}, 1428 cm^{-1}, 1389 cm^{-1}, 1353 cm^{-1}, 1313 cm^{-1}, 1228 cm^{-1}, 1176 cm^{-1}, 1123 cm^{-1}, 856 cm^{-1}, 814 cm^{-1} 776 cm^{-1}, 670 cm^{-1}; HR-MS (EI$^.$-MS): [M$^{+\cdot}$] (calculated): 475.2107, [M$^{+\cdot}$] (found): 475.2106.
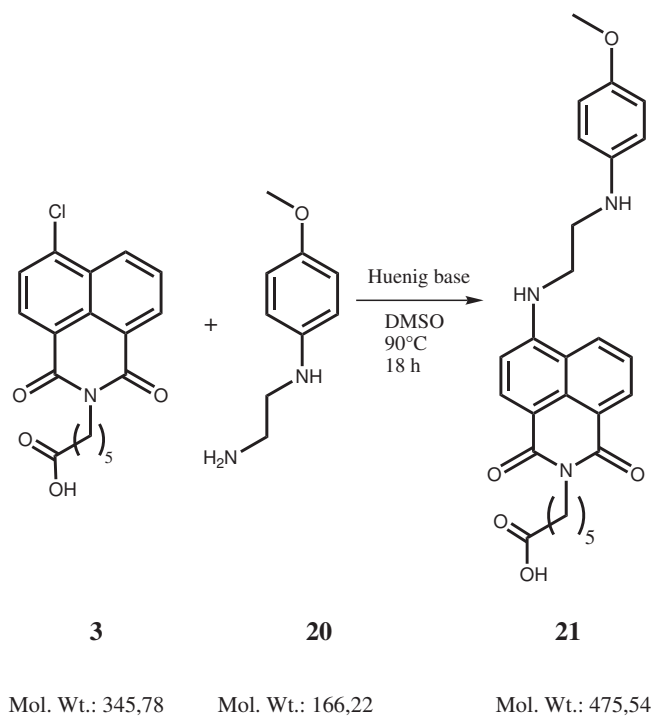
Figure 4.26: Preparation of compound **21**

4.2.18 Covalent attachment of probe 21 to cellulose

Activation of probe 21 as NHS-ester
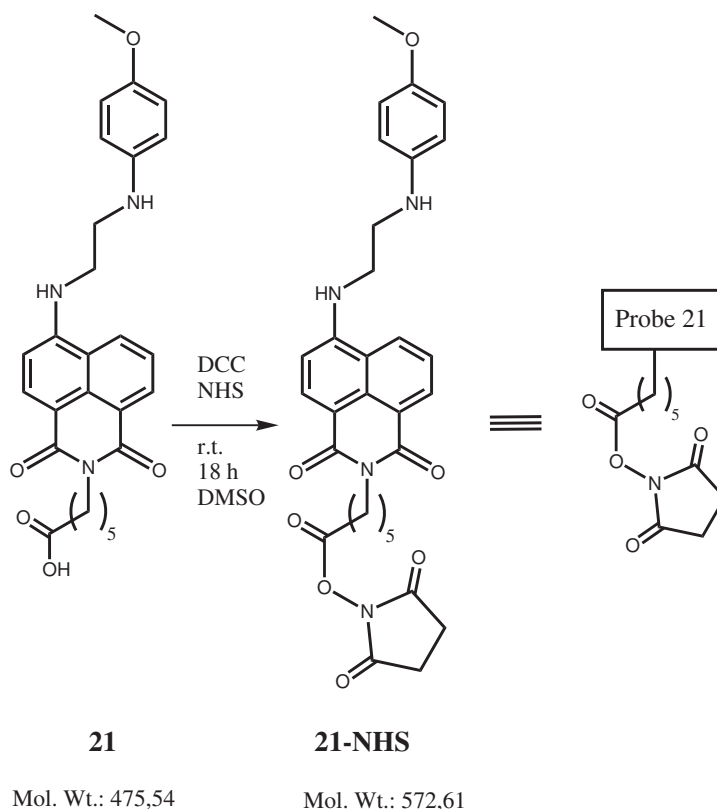
Figure 4.27: Activation of compound **21** to its NHS-ester

4 mg (8.4 μmol) of **21**, 2.6 mg (12.7 μmol) of DCC and 1.5 mg (12.7 μmol) of NHS are dissolved in 300 μL of dry DMSO. The reaction is carried out for 18 hours at room temperature and this solution is used without further purification for labeling experiments (see figure 4.27).

Labeling of O-(2-aminoethyl)-cellulose with probe 21-NHS

250 mg of O-(2-aminoethyl)-cellulose (0.3 eq. -NH$_2$/g) from Optosens (www.opto-sens.de) is suspended in bicarbonate buffer (50 mM, pH 8.3) in order to deproto-nate the primary amino groups. The polymer is collected by centrifugation (12000 rpm, 10 min.), the buffer solution is decanted and the polymer is suspended again in 1 mL of ethanol. 300 μL of the activated probe is added and the labeling is performed for 18 hours at room temperature (see figure 4.28). The labeled cellu-lose is again collected by centrifugation (12000 rpm, 10 min.) and washed with
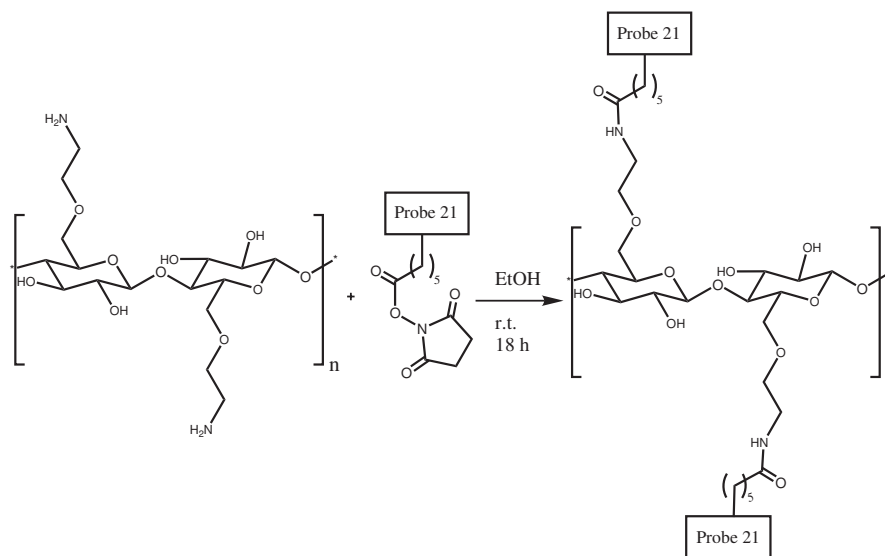
Figure 4.28: Labeling of O-(2-aminoethyl)-cellulose with compound **21-NHS**

ethanol (5-8 times) whereas a yellow colored polymer is retained. In parallel a blank sample is prepared by combining 250 mg of O-(2-aminoethyl)-cellulose with the non-activated probe **21** (4 mg/300μL) solved in DMSO. After the centrifugation/washing steps the blank sample exhibits almost no color whereas the amino-labeled particles are strongly colored.

4.2.19   Synthesis of probe 26

6-(6-Chloro-1,3-dioxo-1H,3H-benzo[de]-isoquinolin-2-yl)-hexanoic acid ethyl ester (22)

2 g (0.0056 mol) of **3** is suspended in 150 mL of ethanol. 2 mL of H_2SO_4 is added as catalyst. The reaction mixture is refluxed for 24 hours whereas the solution clarifies. The solvent is reduced to 10 mL and 50 mL of ethyl acetate is added. The mixture is washed two times with water and one time with brine. The organic layer is dried over Na_2SO_4. After the solvent is evaporated a yellow oil is retained which solidifies over night in the refrigerator. The crude product is purified by recrystallization in methanol. Product **22** (yellow crystals) is filtered off and washed with ice cold methanol (see figure 4.29). Yield: 1.8 g (85 %). m.p.: 73.5-74.5°C; ^{1}H-NMR (DMSO-d$_6$): δ = 8.53 (d, 1 H), 8.505 (d, 1 H), 8.35 (d, 1 H), 8.0- 7.95 (m, 2 H), 4.0 (m, 4 H); 2.29 (t, 2 H), 1.7 - 1.5 (m, 4 H), 1.4 - 1.25 (m, 2 H), 1.14 (t, 3 H); ^{13}C-NMR (DMSO-d$_6$): δ = 172.7, 162.79, 162.52, 137.29, 131.42, 131.16, 130.71, 129.85, 128.45, 128.26, 127.54, 122.55, 121.27, 59.54, 39.46, 33.2, 26.97, 25.75, 24.06, 13.98.
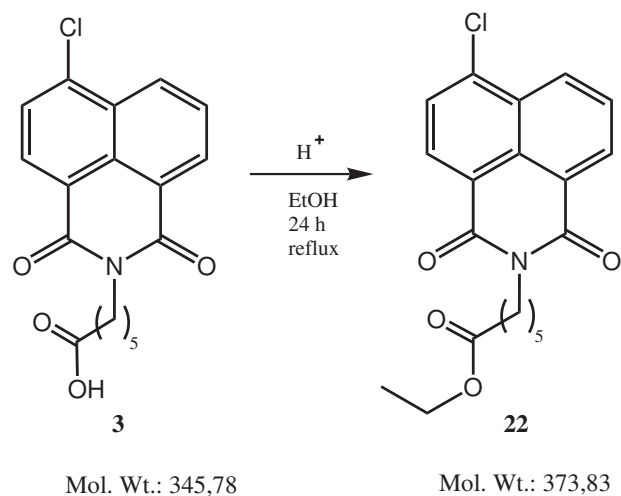
Figure 4.29: Preparation of compound **22**

6-[6-(2-Hydroxy-ethylamino)-1,3-dioxo-1H,3H-benzo[de]-isoquinolin -2-yl]-hexanoic acid-ethyl ester (23)
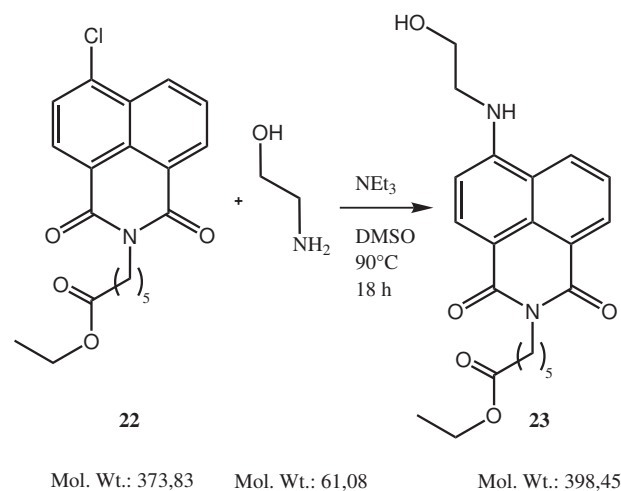
Figure 4.30: Preparation of compound **23**

0.9 g (2.4 mmol) of **22** is dissolved in 20 mL of DMSO. 0.3 mL (4.8 mmol) of monoethanolamine and 0.7 mL (4.8 mmol) of triethylamine are added. The slightly yellow solution darkens at once and the reaction is carried out for 18 hours at 90°C. The reaction mixture is poured into 150 mL of water and allowed to stand for three hours until the crude product precipitates. The crude product is filtered off and recrystallized in ethyl acetate. Product **23** (yellow crystals) is filtered off and washed with ice cold ethyl acetate (see figure 4.30). Yield: 0.5 g (52 %); m.p.:

115°C; ^{1}H-NMR (CDCl$_3$): δ = 8.42 (dd, 1 H, ^{3}J = 1.03 Hz, 7.34 Hz), 8.315 (d, 1 H, ^{3}J = 8.37 Hz), 8.05 (dd, 1 H, ^{3}J = 1.03 Hz, 8.37 Hz), 7.5 (m, 2 H), 6.63 (d, 1 H, ^{3}J = 8.51 Hz); 5.8 (s broad, 1 H), 4.09 (m, 6 H), 3.55 (t, 2 H, ^{3}J = 5.2 Hz), 2.69 (s, 1 H), 2.31 (t, 2 H, ^{3}J = 7.4 Hz), 1.82 - 1.6 (m, 4 H), 1.51 - 1.38 (m, 2 H), 1.23 (t, 3H, ^{3}J = 7.13 Hz); ^{13}C-NMR (CDCl$_3$): δ = 173.92, 164.53, 164.12, 149.49, 134.28, 131.10, 129.53, 126.01, 124.68, 122.74, 120.27, 110.29, 104.41, 60.43, 60.29, 45.45, 39.96, 34.27, 27.82, 26.67, 24.71, 14.24; ; elementary analysis (calaculated): C 66.32 %, H 6.58 %, N 7.03 % (found): C 66.33 %, H 6.48 %, N 6.96 %.

6-[6-(2-Chloroethylamino)-1,3-dioxo-1H,3H-benzo[de]isoquinolin-2-yl]-hexanoic acid ethyl ester (24)
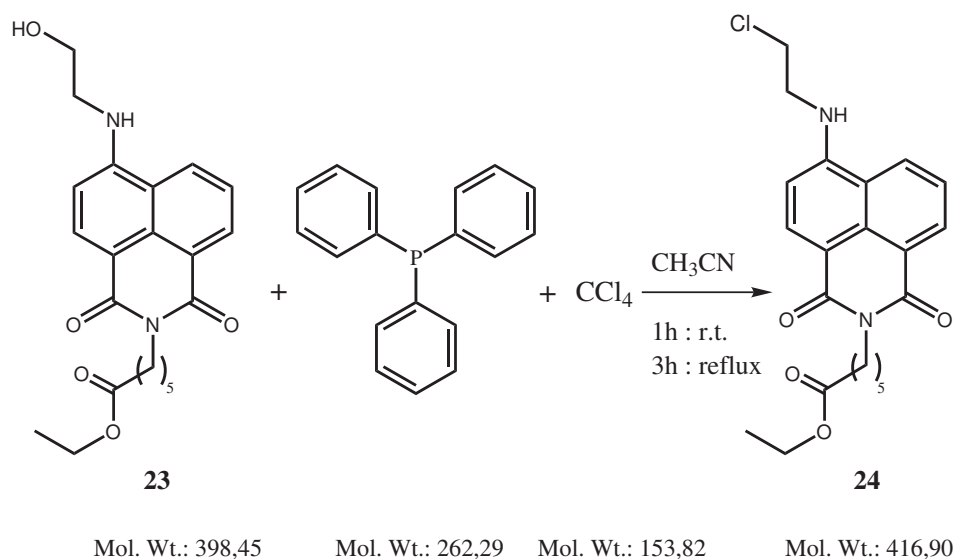
Figure 4.31: Preparation of compound **24**

0.6 g (1.5 mmol) of **23** and 0.55 g (2.1 mmol) of triphenylphosphine are suspended in 25 mL of dry acetonitrile. 0.38 mL (3.9 mmol) of CCl$_4$ is added. The reaction mixture is first stirred 1 hour at room temperature and then refluxed for 3 hours. The magnetic stirrer is removed and the produced crystallized over night at room temperature. Alternatively, the solution can be kept in the refrigerator over night. The product (yellow tinsel) is filtered off and washed with ice cold acetonitrile (see figure 4.31). Yield: 0.3 g (50 %); m.p.: 152°C; ^{1}H-NMR (CDCl$_3$): δ = 8.58 (dd, 1 H, ^{3}J = 1.03 Hz, 7.34 Hz), 8.45 (d, 1 H, ^{3}J = 8.37 Hz), 8.12 (dd, 1H, ^{3}J = 1.03 Hz, 8.51 Hz), 7.65 (m, 1 H), 6.73 (d, 1 H, ^{3}J = 8.37 Hz), 5.64 (t, 1 H, ^{3}J = 5.42 Hz); 4.18 - 4.06 (m, 4 H), 3.91 (t, 2 H, ^{3}J = 5.28 Hz), 3.8 (q, 2H, ^{3}J = 5.28 Hz), 2.31 (t, 2 H, ^{3}J = 7.34 Hz), 1.8 - 1.64 (m, 4 H), 1.51 - 1.39 (m, 2 H), 1.23 (t,

3 H, ^{3}J $=$ 7.13 Hz); ^{13}C-NMR (CDCl$_3$): $\delta =$ 173.77, 164.53, 164.02, 148.43, 134.1, 131.29, 129.73, 125.84, 125.18, 122.02, 120.56, 111.59, 104.56, 60.21, 44.82, 42.69, 39.98, 34.29, 27.83, 26.68, 24.75, 14.24; elementary analysis (calaculated): C 63.38 %, H 6.04 %, N 6.72 % (found): C 63.38 %, H 5.90 %, N 6.53 %.

4-Trimethylsilanyloxy-phenylamine (25)
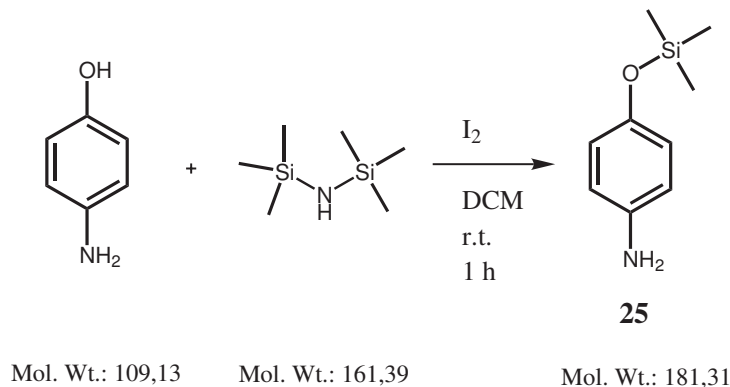
Figure 4.32: Preparation of compound **25**

The synthesis is performed according to literature [149, 150]. 1.1 g (10 mmol) of p-aminophenol and 12 mg (0.1 mmol) of I$_2$ are suspended in 40 mL of DCM. 0.48 mL (8 mmol) of 1,1,1,3,3,3-hexamethyldisilazane in 10 mL of DCM is added dropwise within 5 minutes. After one hour 3 g Na$_2$S$_2$O$_3$ is added in small portions and the mixture is stirred for another 30 minutes. The crude product is filtered over a small column (silica gel 60, CH$_2$Cl$_2$) and washed twice with 40 mL of CH$_2$Cl$_2$. The product **25** is retained as a brown oil (see figure 4.32). Yield 0.9 g (49 %); R$_f$ (silica gel 60; ethyl acetate): 0.69; ^{1}H-NMR (CDCl$_3$): $\delta =$ 6.61 (d, 2 H, ^{3}J $=$ 8.92 Hz), 6.51 (d, 2 H, ^{3}J $=$ 8.92 Hz), 3.41 (s, 2H), 0.19 (s, 9 H).

6-{6-[2-(4-Hydroxy-phenylamino)-ethylamino]-1,3-dioxo-1H,3H-benzo [de]-isoquinolin-2-yl}-hexanoic acid ethyl ester (26)

153 mg (0.36 mmol) of **24** and 130 mg (0.72 mmol) of 4-trimethyl-silanyloxy-phenylamine **25** are solved in ethyl acetat. KI is added in catalytic quantities and the reaction mixture is refluxed for 24 hours. The solvent is evaporated and the crude product is purified by coloum chromatography using silica gel 60 as stationary phase and ethyl acetate as eluent. The protecting group is lost during the reaction/purification and the phenolic form of the probe is obtained (see figure 4.33). Yield 10 mg (6 %, yellow solid); ^{1}H-NMR (acetone-d$_6$): $\delta =$ 8.57 (d, 1 H), 8.5 (dd, 1 H), 8.36 (d, 1 H), 7.66 (m, 1 H), 7.13 (s, 1 H), 6.9 (d, 1 H), 6.78 (d,
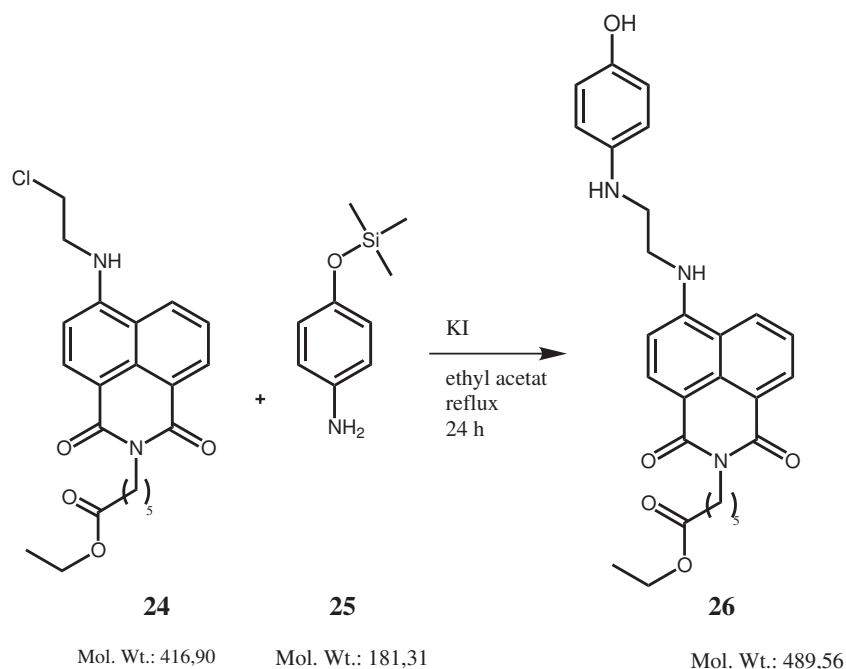
Figure 4.33: Preparation of compound **26**

2 H), 6.74 (d, 2 H), 4.05 (m, 4 H), 3.72 (q, 2 H), 3.51 (t, 2 H), 2.31 (t, 2 H), 1.75 - 1.6 (m, 4 H), 1.5 -1 .35 (m, 2 H), 1.18 (t, 3 H); ES-MS: m/z (MH$^+$, calculated) = 490.23, (MH$^+$, found) = 490.1.

4.2.20 Experimental procedures for H_2O_2 calibration curve

The procedures were contrived and performed by Martin Link as well as by Dominik Grögel.

Preparation of probe 21 stock solutions

Stock solution of 21a:

The methoxy derivative (1.92 mg, 0.004 mmol) is dissolved in 1 mL DMSO to give stock solution 1 ($c_{stock-1}$ = 4 mM). 250 μL of **stock-1** are diluted with 750 μL phosphate buffer (pH 8, 10 mM) to yield **stock-21a** ($c_{stock-21a}$ = 1 mM).

Stock solution of 21b:

The methoxy derivative (1.92 mg, 0.004 mmol) is dissolved in 1 mL DMSO to give stock solution 1 ($c_{stock-1}$ = 4 mM). 250 μL of **stock-1** are diluted with 1750 μL phosphate buffer (pH 8, 10 mM) to yield **stock-21b** ($c_{stock-21b}$ = 500 μM).

Preparation of probe 26 stock solutions

The phenol derivative (1.95 mg, 0.004 mmol) is dissolved in 1 mL DMSO to yield stock solution 2 ($c_{stock-2}$ = 4 mM). 248 μL of **stock-2** are diluted with 1752 μL phosphate buffer (pH 7 or 8, 10 mM) to obtain **stock-26** ($c_{stock-26}$ = 500 μM).

Preparation of H_2O_2 stock solutions

1 mL stock solutions of hydrogen peroxide in phosphate buffer (pH 7 or 8, 10 mM) are prepared as follows:

1. $c(H_2O_2)_{st}$ = 1000 mM: 102 μL H_2O_2 (30%) are diluted with 898 μL phosphate buffer

2. $c(H_2O_2)_{st}$ = 100 mM: 10.2 μL H_2O_2 (30%) are diluted with 990 μL phosphate buffer

3. $c(H_2O_2)_{st}$ = 10 mM: 10 μL of H_2O_2 (**1**) are diluted with 990 μL phosphate buffer

4. $c(H_2O_2)_{st}$ = 1 mM: 10 μL of H_2O_2 (**2**) are diluted with 990 μL phosphate buffer

Experimental procedure

All measurements are carried out on the AB 2 fluorimeter by the following parameters:

- λ_{exc} = 450 nm; Bandpassfilter 16 nm

- λ_{em} = 530 nm; Bandpassfilter 16 nm

- temperature = 25°C

- c(probe 21a) = 10 μM

- c(probe 21b) = 5 μM

- c(probe 26) = 5 μM

- total volume: 1000 μL in quarz cuvette (cv)

First, the probe (**21** or **26**) is dissolved in phosphate buffer (pH 7 or 8, 10 mM) and an emission spectra is measured conducted as blank sample/baseline (t = 0 min). Afterwards the experiment is started by adding 10 μL of the corresponding H_2O_2 solutions **1-7**.

1. $c(H_2O_2)_{cv} = 1$ mM: 10 μL (stock **21a/b** or **26**) + 10 μL H_2O_2 (**2**) + 980 μL phosphate buffer

2. $c(H_2O_2)_{cv} = 500$ μM: 10 μL (stock **21a/b** or **26**) + 5 μL H_2O_2 (**2**) + 985 μL phosphate buffer

3. $c(H_2O_2)_{cv} = 250$ μM: 10 μL (stock **21a/b** or **26**) + 2.5 μL H_2O_2 (**2**) + 987 μL phosphate buffer

4. $c(H_2O_2)_{cv} = 100$ μM: 10 μL (stock **21a/b** or **26**) + 10 μL H_2O_2 (**3**) + 985 μL phosphate buffer

5. $c(H_2O_2)_{cv} = 50$ μM: 10 μL (stock **21a/b** or **26**) + 5 μL H_2O_2 (**3**) + 985 μL phosphate buffer

6. $c(H_2O_2)_{cv} = 20$ μM: 10 μL (stock **21a/b** or **26**) + 20 μL H_2O_2 (**4**) + 970 μL phosphate buffer

7. $c(H_2O_2)_{cv} = 10$ μM: 10 μL (stock **21a/b** or **26**) + 10 μL H_2O_2 (**4**) + 980 μL phosphate buffer

Chapter 5

Summary

5.1 Summary in English

The first part of this thesis describes the synthesis, the spectroscopic properties and the application of several labels. These labels can be devided into two groups. On the one hand there are labels (**2** and **5**) operating in the visible part of the electromagnetic spectrum (VIS-labels). They are based on the 1,8-naphthalimide as an important and highly photostable yellow daylight fluorophore which bears the advantages of photoexcitation by blue or purple diode lasers. These light sources have become very attractive because of their small size, longevity, and low power consumption. The labels are functionalized with a C-6 linker carrying a carboxy-group which is in-situ activated (via its NHS-ester) to give the amino-reactive labels **2** and **5**. The ability of the VIS-labels are proven in various tagging experiments ranging from labeling biological analytes (amino acids, bovine serum albumin) to inorganic material (amino-modified silica nanoparticles). Furthermore, the application of label **2** and **5** concerning the most common separation techniques e.g. CE, MCE, SEC, TLC and HPLC are demonstrated in various experiments.

On the other hand there are labels (**9**, **14a/b**, **16** and **18**) operating in the far-visible to near infrared part of the spectrum (NIR-labels). These compounds are very attractive due to the reduction of interferences caused by background fluorescence and straylight as well as the excitation by small laser diodes as inexpensive, stable and easily affordable light sources. Furthermore, radiation of this wavelength penetrates biological material easily which is an advantageous feature when working with cells and tissues. All NIR-labels presented here are derived from a purple (comparable to Nile Red) or from a blue (comparable to Nile Blue) phenoxazine as fluorophore. They are functionalized with either a C-6 linker carrying a carboxy group in order to get an amino-reactive label (after activation as NHS-ester) or with an alkyne moiety creating a clickable fluorophore. The broad

application of these labels is illustrated both by tagging various important analytes e.g. peptides, proteins, sugars and silica nanoparticles and by their utilization in different separation techniques including MCE, TLC and SEC.

The second part of this thesis deals with the preparation and application of two novel probes (**21** and **26**) for sensing hydrogen peroxide based on the PET-effect. These probes are derived from the 1,8-napththalimide as highly photo- and chemostable yellow daylight fluorophore in accordance with the VIS-labels **2** and **5**. A p-anisidine (probe **21**) or a p-aminophenol moiety (probe **26**) serves as receptor for hydrogen peroxide. The experiments involve the behavior of the probe in the prescence of the analyte (time and intensity dependance of the fluorescence signal) as well as the generation of a calibration curve for hydrogen peroxide. In the end probe **21** is covalently attached to a polymeric support to show its future application in a sensor device.

5.2 Summary in German

Der erste Teil dieser Dissertation beschäftigt sich mit der Synthese, den spektroskopischen Eigenschaften und mit der Anwendung verschiedener fluoreszenten Marker. Diese Verbindungen sind wiederum in zwei Gruppen unterteilt. Auf der einen Seite die Marker **2** und **5**, deren Anwendungsbereiche im sichtbaren Teil des elektromagnetischen Spektrums liegen und welche vom 1,8-Naphthalimid als Fluorophor abgeleitet sind (VIS-Marker). Die Vorteile dieses wichtigen Fluorophors sind zum einen die hohe Photo- und Chemostabilität und zum anderen die Möglichkeit der Anregung mit blauen oder violetten Laserdioden. Diese Lichtqellen sind kompakt, stabil und kostengünstig. Beide Marker werden mit einem C-6 Linker, welcher eine Carbonsäuregruppe trägt, funktionalisiert. Diese Säuregruppe kann nun in-situ als NHS-Ester aktiviert werden, wodurch die aminoreaktiven Marker **2** und **5** erhalten werden. Die praktische Anwendung dieser beiden VIS-Marker wird in einer Vielzahl von Experimenten unter Beweis gestellt. Die Markierungen reichen von biologischen Analyten wie Aminosäuren und Proteinen (BSA) bis hin zu anorganischem Material in Form von aminomodifizierten Silicananopartikeln. Darüber hinaus kommen die Verbindungen **2** und **5** und deren Konjugate in Trenntechniken wie CE, MCE, SEC, DC und HPLC zum Einsatz, was ihren großen Anwendungsbereich unterstreicht.

Die zweite Gruppe der Marker stellen jene funktionalisierten Verbindungen dar, deren optische Eigenschaften im langwellig sichtbaren Bereich bis hin zum nahen Infrarotbereich des elektromagnetischen Spektrums liegen (NIR-Marker). Der Vorteil dieser Marker (**9**, **14a/b**, **16** und **18**) liegt zum einen in der Verminderung von Interferenzen, welche durch Hintergrundfluoreszenz und Streulicht bedingt werden, und zum anderen in der Eigenschaft, dass das langwelligere

Anregungslicht tiefer als kurzwelligere Strahlung in biologisches Material einzudringen vermag. Dies ist vor allem bei der Arbeit mit Gewebe und Zellen von großer Bedeutung. Letzten Endes können auch diese Fluorophore von Laserdioden mit den oben beschriebenen Vorteilen angeregt werden. Alle NIR-Marker basieren entweder auf einem violetten Phenoxazin (vergleichbar mit Nilrot) oder einem blauen Phenoxazin (vergleichbar mit Nilblau). Diese Fluorophore werden entweder mit einem C-6 Linker, welcher eine Carbonsäuregruppe trägt, funktionalisiert oder sie besitzen eine Alkingruppe. Somit erhält man einen klassischen aminoreaktiven Marker aber auch Verbindungen, welche mit Azidgruppen sogenannte "Clickreaktionen" beschreiben können. Der breite Anwendungsbereich wird durch verschiedenste Markierungsexperimente mit Aminosäuren, Peptiden, Proteinen, Zuckern und Partikeln (μm bis nm) veranschaulicht. Auch kommen hier in Analogie zu den VIS-Markern verschiedene Trenntechniken wie MCE, TLC und SEC erfolgreich zum Einsatz.

Der zweite Teil der Promotionsarbeit beschreibt die Synthese und die Anwendung zweier Sonden (**21** und **26**) welche auf dem Photoelektronentransfer (PET-Effekt) zur Detektion von Wasserstoffperoxid basieren. Wie schon die VIS-Marker **2** und **5** leiten sich diese Sonden vom 1,8-Naphthalimid als wichtigem photo- und chemostabilen Fluorophor ab. Als Rezeptor für Wasserstoffperoxid wird zum einen ein p-Anisidinrest (**21**) und zum anderen ein p-Aminophenolrest (**26**) verwendet. Die durchgeführten Experimente umfassen sowohl das Verhalten des Fluoreszenzsignals in Bezug auf den Anstieg der Intensität und dessen zeitliche Entwicklung bei der Reaktion mit dem Analyten als auch die Aufstellung einer Kalibrationskurve für unterschiedliche Wasserstoffperoxidkonzentrationen. Zum Schluss erfolgt noch die kovalente Anbindung der Sonde **21** an einen polymeren Träger mit Hinblick auf die mögliche Entwicklung eines Sensors.

Chapter 6

Curriculum vitae

Persönliches
Martin Link
geboren April 1981 in Regensburg

Promotion
seit Dezember 2006 an der Universität Regensburg
Ende April 2010
Thema: Synthese und Anwendung neuer fluoreszenter Farbstoffe und Sonden für biologische Anwendungen

Hochschulbildung
2001-2006
an der Universität Regensburg
Chemiestudium
Studienschwerpunkt: Analytische Chemie
Diplomarbeit in analytischer Chemie

Schulbildung
1992-2001 Gymnasium in Parsberg (Lkr. Neumarkt), Abitur
1987-1992 Volksschule in Laaber (Lkr. Regensburg)

Chapter 7

Publications and Presentations

Diploma Thesis

"Amino-reactive fluorescent markers with either high brightness or bathochromic deepening of colour", Institute of Analytical Chemistry, Chemo- and Biosensors, University of Regensburg, October 2006

Journal Papers

1. Mader, H., Li, XH., Saleh, S., Link, M., Kele, P., Wolfbeis, O. S., *Fluorescent silica nanoparticles*, Ann. N.Y. Acad. Sci. **1130** (2008) 218.

2. Link, M., Schulze, P., Belder, D., Wolfbeis, O. S., *New diode laser-excitable green fluorescent label and its application to detection of bovine serum albumin via microchip electrophoresis*, Microchim Acta **166** (2009) 183.

3. Kele, P., Li. X., Link, M., Nagy, K., Herner, A., Lorincz, K., Béni, S., Wolfbeis, O. S., *Clickable fluorophores for biological labeling-with or without copper*, Org. Biomol. Chem. **7** (2009) 3486.

4. Mader, H. S., Link, M., Achatz, D. E., Uhlmann, K., Li, X., Wolfbeis, O. S., *Surface-Modified upconverting microparticles and nanoparticles for use in click chemistries*, Chem. Eur. J., 2010, in press.

5. Achatz, E., Heiligtag, F. J., Li, X., Link, M., Wolfbeis, O. S., *Azido-Modified silica nanoparticles for use in click chemistries*, Langmuir. in revision.

6. Schulze, P., Link, M., Schulze, M., Thuermann, S., Wolfbeis, O. S., Belder, D., *A new weakly basic fluorescent label for use in isoelectric focusing and chip electrophoresis.* Electrophoresis, in revision (2010).

7. Link, M., Li, X., Kleim, J., Wolfbeis, O. S., *Novel Method for Introducing Maleinimido Groups into Thiol-Reactive Labels*, Eur. J. Org. Chem., submitted Feb. 2010 (MS ejoc.201000175).

8. Wang, X., Meier, R. J., Link, M., Wolfbeis, O. S., *Photographing Oxygen Distribution*, to be submitted March 2010.

9. Link, M., Achatz, D. E., Wolfbeis, O. S., *New Amino Reactive Phenoxazine Based Fluorescent Labels*, in prep.

10. Link, M., Grögel, D., Wolfbeis, O. S., *New fluorescent PET-probes for H_2O_2 sensing*, in prep.

Poster Presentations

1. M. Link, O. S. Wolfbeis *"A "Piggyback" Fluorescent Protein Marker."* 10th Conference on Methods and Applications of Fluorescence: Spectroscopy, Imaging and Probes (MAF), September 9-12, 2007, Salzburg, Austria

2. M. Link, O. S. Wolfbeis *"Phenoxazinone Derivative for Use as Fluorescent Protein Label"* 8th Summer meeting of the "Graduate College" of the University of Regensburg, July 15-18, 2008, Kostenz, Germany

3. M. Link, J. Kleim, O. S. Wolfbeis *"New Purple and Blue Phenoxazines for Use as Fluorescent Labels for Amines and in Click Conjugation."* 11th Conference on Methods and Applications of Fluorescence: Spectroscopy, Imaging and Probes (MAF), September 6-9, 2009, Budapest, Hungary

Oral Presentation

M. Link *"Phenoxazinone Derivative for Use as Fluorescent Protein Label"* 8th Summer meeting of the "Graduate College" of the University of Regensburg, July 15-18, 2008, Kostenz, Germany

References

[1] Oswald, B. et al., Bioconjugate Chem. **10** (1999) 925Ũ931.

[2] Stich, M. I. J., Schaeferling, M., and Wolfbeis, O. S., Adv. Mater. **21** (2009) 2216.

[3] Wang, X. et al., Anal. Chem. **81** (2009) 7885.

[4] Skoog, D. A. and Leary, J. J., *Instrumentelle Analytik*, Springer, 1996.

[5] Zollinger, H., *Color Chemistry: Syntheses, Properties and Applications of Organic Dyes and Pigments*, volume 3, Wiley-VCH, Zuerich, 2003.

[6] Gros, C. and Labouesse, B., European J. Biocem. **7** (1969) 463.

[7] Kallmayer, H. J. and Schwarz, P., Pharmazie **40** (1989) 119.

[8] Maeda, H., Ishida, N., Kawauchi, H., and Tuzimura, K., J. Biochem. **65** (1969) 777.

[9] Wischke, C. and Borchert, H. H., Pharmazie **61** (2006) 770.

[10] Ogawa, T., Aoyagi, S., Miyasaka, T., and Sakai, K., Sensors **9** (2009) 8271.

[11] Weidgans, B. M., Krause, C., Klimant, I., and Wolfbeis, O. S., Analyst **129** (2004) 645.

[12] Weissleder, R., Nat. Biotechnol. **19** (2001) 316.

[13] Vasylevska, G. S., Borisov, S. M., Krause, C., and Wolfbeis, O. S., Chem. Mater. **18** (2006) 4609.

[14] Nagy, K. et al., Tetrahedron **64** (2008) 6191.

[15] Stich, M., *Preparation and Calibration of Pressure Sensitive and Temperature Sensitive Paints for Fluorescence Lifetime Imaging Applications*, PhD thesis, University of Regensburg, 2009.

[16] Hoefelschweiger, B. K., Duerkop, A., and Wolfbeis, O. S., Anal. Biochem. **344** (2005) 122.

[17] McLane, J. A., Alcohol **7** (1990) 103.

[18] Hermanson, G. T., *Bioconjugate Techniques*, volume 1, Academic Press, San Diego and New York, 1996.

[19] Bolton, A. E. and Hunter, W. M., Biochem. J. **133** (1973) 529.

[20] Ledoan, T., Auger, R., Benjahad, A., and Tenu, J. P., Nucleosides Nucleotides **18** (1999) 277.

[21] Srinivasan, V., Pamula, V. K., and Fair, R. B., Lab Chip **4** (2004) 310.

[22] Link, M., Amino-reactive fluorecent markers with either hight brightness or bathochromic deepening of color, Master's thesis, University of Regensburg, 2006.

[23] Hoefelschweiger, B. K., *The Pyrylium Dye: A new class of biolabels*, PhD thesis, University of Regensburg, 2005.

[24] Valeur, B., *Molecular Fluorescence, Principle and Applications*, Wiley-VHC, Weinheim, 2002.

[25] Ulrich, G., Ziessel, R., and Harriman, A., Angw. Chem. Int. Ed. **47** (2008) 1184.

[26] Gribbon, P., Drug Discovery Today (DDT) **8** (2003).

[27] Gründler, P., *Chemische Sensoren*, Springer Verlag, 2003.

[28] Cho, H. K. et al., Polymer **50** (2009) 2357.

[29] Singh, M. K., Phys Chem Chem Phys **11** (2009) 7225.

[30] Volke, D. and Hoffmann, R., Electrophoresis **29** (2008) 4516.

[31] Wang, D. et al., J. Org. Chem. **74** (2009) 7675.

[32] Terpetschnig, E., B. Szmacinski, A. O., and Lakowicz, J. R., Anal. Biochem. **217** (1994) 197.

[33] Brinkley, M., Bioconjugate Chem. **3** (1992) 2.

[34] Kolb, H., Finn, M., and Sharpless, K., Angew. Chem. Int. Ed. **40** (2001) 2004.

[35] Hawker, H. C., Finn, M. G., and Sharpless, K. B., Angw. Chem. Int. Ed. **60** (2007) 381.

[36] Lutz, J. and Schlaad, H., Polymer **49** (2008) 817.

[37] Achatz, D. E., Fluorescent silica nanoparticles for click labeling of proteins, Master's thesis, University of Regensburg, 2008.

[38] Lutz, J.-F., Angew. Chem. Int. Ed. **47** (2008) 2182.

[39] Rostovtsev, V. V., Green, L. G., Fokin, V. V., and Sharpless, K. B., Angw. Chem. Int. Ed. **114** (2002) 2708.

[40] Kele, P., Mezoe, G., Achatz, D., and Wolfbeis, O. S., Angew. Chem. Int. Ed. **48** (2009) 344.

[41] Kele, P. et al., Org. Biomol. Chem. **7** (2009) 3486.

[42] Baskin, J. M. et al., Proc. Natl. Acad. Sci. USA **104** (2007) 16793.

[43] Licchelli, M. et al., Dalton Trans. (2003) 4537.

[44] Liu, J. et al., J. Mater. Chem. **19** (2009) 7753.

[45] Stewart, W. W., J. Am. Chem. Soc. **103** (1981) 7615.

[46] Li, Z.-Z. et al., Sensors and Actuators B **114** (2006) 308.

[47] Chang, S., Utecht, R., and Lewis, D. E., Dyes and Pigments **43** (1999) 83.

[48] Stewart, W. W., Nature **292** (1981) 17.

[49] Alexiou, M. S. and Tyman, J. H. P., J. Chem. Res., Synopses **4** (2000) 208.

[50] Ghorbanian, S., Tyman, J. H., and Tychopoulos, V. J., Chem. Technol. Biotechnol. **75** (2000) 1127.

[51] Southwick, P. L., Hahn, K. M., Perry, P. L., Wagner, A. S. W. M., and Waggoner, A. S., J. Fluoresc. **5** (1995) 231.

[52] Suman, S., Singhal, R., Sharma, A., Malthotra, B., and Pundir, C., Sensors and Actuators B **107** (2005) 768.

[53] Sezgintuerk, M. K. and Dinckaya, E., Biosensors & Bioelectronics **23** (2008) 1799.

[54] Fuh, M. R. S., Burgess, L. W., Hirschfeld, T., and Christian, G. D.,
     Analyst **112** (1987) 1159.

[55] Naumer, H. and Heller, W, *Untersuchungsmethoden in der Chemie*,
     Thieme, NY, 1997.

[56] Wetzl, B. et al., J. Chromatography B **792** (2003) 83.

[57] Sotootero, R., Mendezalvarez, E., Galanvalientb, J., Aguilarveiga, E., and
     Sierramarcuno, G., Biomed. Chromatogr. **8** (1994) 114.

[58] Schulze, P. et al., Electrophoresis submitted Jan. 2010.

[59] Deheney, T. P., Department of Obstetrics Gynaecology and Department of
     Pharmacologie (1981).

[60] Nelson, D. L. and Cox, M. M., *Lehninger Biochemie*, Springer, 2001.

[61] Hardman, R., Environ. Health Perspect. **114** (2006) 165.

[62] Hauck, T. S., Anderson, R. E., Fischer, H. C., Newbigging, S., and Chang,
     W. C. W., Small **6** (2010) 138.

[63] Senarath-Yapa, M. D. et al., Langmuir **23** (2007) 12624.

[64] Mader, H. et al., Ann. N. Y. Acad. Science **1130** (2008) 218.

[65] Schulze, P. and Belder, D., Anal. Bioanal. Chem. **393** (2009) 515.

[66] Link, M., Schulze, P., Belder, D., and Wolfbeis, O. S., Microchim Acta **166**
     (2009) 183.

[67] Belder, D. and Schomburg, G., J. Chromatogr. A **666** (1994) 351.

[68] Chen, Y., Koehler, B., and Wehrmann, R., DE 19505941 A1 (1996).

[69] Roth, M., Fontoura, B., Wei, S., and Satterly, N., US 2009170840 A1
     20090702 (2009).

[70] Bevers, H. A. J. M., Wijntje, R., and de Haan, A. B., Spectroscopy **21**
     (2006) 52.

[71] Jambor, A. and Molnar-Perl, I., J. Chromatogr. A **1216** (2009) 3064.

[72] Wang, X., Meier, R. J., Link, M., and Wolfbeis, O. S., Angw. Chem. Int.
     Ed. submitted Feb. 2010.

[73] Cao, H., Chang, V., Hernandez, R., and Heagy, M., J. Org. Chem. **70** (2005) 4929.

[74] Patrick, L. G. F. and Whiting, A., Dyes and Pigments **55** (2002) 123.

[75] Grabchev, I., Moneva, I., Bojinov, V., and Guittonneauc, S., J. Mater. Chem. **10** (2000) 1291.

[76] Brown, M. B., Edmonds, T. E., Miller, J. N., Riley, D. P., and Searev, N. J., Analyst **118** (1993) 407.

[77] Umenzawa, K., Matsui, A., Nakamura, Y., Citterio, D., and Suzuki, K., Chem. Eur. J. **15** (2009) 1096.

[78] Yao, J. H., Chi, C., Wu, J., and Loh, K.-P., Chem. Eur. J. **15** (2009) 9299.

[79] Umezawa, K., Citterio, D., and Suzuki, K., Anal. Science **24** (2008) 213.

[80] Song, X., Kassaye, D. S., and Foley, J. W., J. Fluoresc. **18** (2008) 513.

[81] Kang, J. S., Lakowicz, J. R., and G., P., Arch. Pharmacol. Res. **25** (2002) 143.

[82] Chen, Q. et al., Analyst **124** (1999) 901.

[83] Abu-Absi, S. F., Friend, J. R., and Hansen, L. K. and. Hu, W., Spheroids, Exp. Cell Res. **274** (2002) 56.

[84] Sanchez-Martinez, M. L., Aguilar-Caballos, M. P., Eremin, S. A., and Gomez-Hens, A., Anal. Bioanal. Chem. **386** (2006) 1489.

[85] Sens, R. and Drexhage, K.-H., Journal of Luminescence **24/25** (1981) 709.

[86] Hartmann, H., Chimia **48** (1994) 512.

[87] Tung, C. H., Biopolymeres **76** (2004) 391.

[88] Simmonds, A. C. et al., U. S. Patent US006166202A (2000).

[89] Gokan, N. et al., Biochemical Pharmacology **70** (2005) 676.

[90] Mank, R., Kala, H., and Strubb, M., Pharmazie **43** (1988) 692.

[91] Kotoucek, M., Martinek, M., and Ruzika, E. M., Monatsh. Chem. **96** (1965) 1433.

[92] Kanitz, A. and Hartmann, H., Eur. J. Chem. (1999) 923.

[93] Pirrung, M., *Molecular diversity and combinatory chemistry; Principles and applications*, Elsevier, Oxford u.a., 2004.

[94] Chen, S., Li, X., and Ma, H., ChemBioChem **10** (2009) 1200.

[95] Sackett, D. L. and Wolff, J., Analytical Biochemistry **167** (1987) 228.

[96] Hazra, P., Chkrabarty, D., Chakraborty, A., and Sarkar, N., Chem. Phys. Letters **388** (2004) 150.

[97] Greaves, M. and Shuster, S., J. Physiol. **193(2)** (1967) 255.

[98] Stöber, W., Fink, A., and Bohn, E., J. Colloid Interface Sci. **26** (1968) 62.

[99] Schmidt, M. P. and Sues, O., Ger. Pat. (1934) 639,125.

[100] Das, K., Jain, B., and Patel, H. S., Spectrochimica Acta Part A **60** (2004) 2059.

[101] Dutta, A. K., Kamada, K., and Ohta, K., Journal of Photochemistry and Photobiology A: Chemistry **93** (1996) 57.

[102] Wolfbeis, O. S., Angew. Chem. Int. Ed. **46** (2007) 2980.

[103] Dondoni, A., Chem. Asian J. **2** (2007) 700.

[104] Auzel, F., Chem. Rev. **104** (2004) 139.

[105] Mader, H. S. et al., Chem. Eur. J., 2010, in press.

[106] Davis, M. M. and Hetzer, H. B., Anal. Chem. **38** (1966) 451.

[107] Fowler, D. F. and Greenspan, P., Histochem. Cytochem. **33** (1985) 833.

[108] Briggs, M. S. J. et al., J. Chem. Soc., Perkin Trans. 1 (1997) 1051.

[109] Breadmore, M. C., Henderson, R. D., Fakhari, A. R., Macka, M., and Haddad, P. R., Electrophoresis **2** (2007) 1252.

[110] Herrmann, R., Josel, H.-P., Drexhage, K.-H., and Marx, N.-J., Eur. Pat. Appl. EP 747447 A2 (1996).

[111] Kleim, J., Synthese und Charakterisierung von thiolreaktiven langwelligen Markern mittels Click-Reaktion, Master's thesis, University of Regensburg, 2009.

[112] Link, M., Li, X., Kleim, J., and Wolfbeis, O. S., Eur. J. Org. Chem. submitted Feb. 2010.

[113] de Silva, A. P. et al., Chem. Rev. **97** (1997) 1515.

[114] Bryan, A. J., de Silva, A. P., Rupasighe, R. A. D., and Sandanayake, K. R. A., Biosensors **4** (1989) 169.

[115] Minkin, V. I., Dubonosov, A. D., Bren, V. A., and Tsukanov, A. V., Arkivoc (2008) 90.

[116] Gan, J., Chen, K., Chang, C.-P., and Tian, H., Dyes and Pigments **57** (2003) 21.

[117] de Silva, A. P., Gunnlaugsson, T., and Rice, T. E., Analyst **121** (1996) 1759.

[118] de Silva, A. P. et al., Angew. Chem. Int. Ed. Engl. **34** (1995) 1728.

[119] Soh, N. et al., Bioorg. Med. Chem. **13** (2005) 1131.

[120] de Silva, A. P., Moody, T. S., and Wright, G. D., Analyst **134** (2009) 2385.

[121] Wang, Y.-C. and Morawetz, H., J. Am. Chem. Soc. **98** (1976) 3611.

[122] Tusa, J. K. and He, H., J. Mater. Chem. **15** (2005) 2640.

[123] Kele, P., Orbulescu, J., Calhoun, T., Gawley, R., and Leblanc, R., Tetrahedron Lett. **43** (2002) 4413.

[124] Stamler, J. S., Singel, D. J., and Loscalzo, J., J. Science **158** (1992) 1898.

[125] Schmidt, R. F., *Physiologie des Menschen*, Springer, 2007, 957.

[126] Martin, W. J., Am. Rev. Respir. Dis. **130** (1984) 209.

[127] Mohazzab, H. K., Kaminski, P. M., Fayngersh, R. P., and Wolin, M. S., Am. J. Physiol. Heart Circ. Physiol. **270** (1995) H1044.

[128] Okimoto, Y., Watanabe, A., Niki, E., Yamashita, T., and Noguchi, N., FEBS Letters **474** (2000) 137.

[129] Xu, K. et al., Chem. Commun. (2005) 5974.

[130] Soh, N., Anal. Bioanal. Chem. **386** (2006) 532.

[131] Veale, E. B. and Gunnlaugsson, T., J. Org. Chem. **73** (2008) 8073.

[132] Sheng, X. and Wei, L. and Kong-Chang, C., Chin. J. Chem. **25** (2007) 778.

[133] Hanaoka, K., Muramatsu, Y., Urano, Y., Terai, T., and Nagno, T., Chem. Eur. J. **16** (2010) 568.

[134] Simon, P., Farsang, G., and Amatore, C., Journal of Electroanalytical Chemistry **435** (1997) 165.

[135] Nagl, S., Stich, M. I. J., Schaeferling, M., and Wolfbeis, O. S., Anal. Bioanal. Chem. **393** (2009) 1199.

[136] Weidgans, B. M., Diode Laser Compatibel Fluorescent Markers of Bioanalytical Applications, Master's thesis, University of Regensburg, 2001.

[137] Belder, D., Deege, A., Maas, M., and Ludwig, M., Electrophoresis **23** (2002) 2355.

[138] Hong, J. S. and Rabinowitz, J. C., J. Biolo. Chem. **245** (1970) 4982.

[139] Kasprzak, A. A., Papas, E. J., and Steenkamp, D. J., Biochem. J. **211** (1983) 535.

[140] Otto, M., *Analytische Chemie*, volume 2, Wiley-VHC, 2000.

[141] Lakowitz, J. R., *Principles of Fluorescence Spectroskopy*, Kluwer Academic/Plenum Publisher, New York, 2 edition, 1999.

[142] Demas, J. N. and Crosby, G. A., J. Phys. Chem. **75** (1971) 991.

[143] Tyman, J. et al., Syn. Comm. **19** (1989) 179.

[144] Bojinov, V. and Grabchev, I., Dyes and Pigments **51** (2001) 57.

[145] Saha, S. and Samanta, A., J. Phys. Chem. A **106** (2002) 4763.

[146] Ke, C. et al., Heterocycles **76** (2008) 155.

[147] Bickley, J., Bonar-Law, R., MacGrath, T., Singh, N., and Steiner, A., New. J. Chem. **28** (2004) 425.

[148] Wetzl, B. K., Yarmoluk, S. M., Craig, D. B., and Wolfbeis, O. S., Angew. Chem. Int. Ed. **43** (2004) 5400.

[149] Ito, H., Watanabe, A., and Sawamura, M., Org. Lett. **7** (2005) 1869.

[150] Wuts, P. G. M. and Greene, T. W., *Greene's Protective Groups in Organic Synthesis (Fourth Edition)*, John Wiley & Sons, Inc., 2006.

Erklärung

Hiermit versichere ich, dass ich die vorliegende Arbeit selbst verfasst und keine anderen als die angegebenen Quellen und Hilfsmittel verwendet habe.

Regensburg, 15. März 2010

Martin Link